December 2019

Application and Parameterization of a Semi-Analytical/Numerical Method for Modeling Matrix Diffusion Effects in Groundwater Chemical Transport

Wesley Prater
Clemson University, wesprater11@gmail.com

APPLICATION AND PARAMETERIZATION OF A SEMI-ANALYTICAL/NUMERICAL METHOD FOR MODELING MATRIX DIFFUSION EFFECTS IN GROUNDWATER CHEMICAL TRANSPORT

A Thesis
Presented to
the Graduate School of
Clemson University

In Partial Fulfillment
of the Requirements for the Degree
Master of Science
Hydrogeology

---

by
Wesley Todd Prater
December 2019

Accepted by:
Dr. Ronald Falta, Committee Chair
Dr. Lawrence Murdoch
Dr. James Henderson

ABSTRACT

The back diffusion of dissolved chemicals from low permeability zones to aquifers can cause contaminant plumes to persist long after remediation (Chapman and Parker, 2005). Because of the complicated nature of some field sites, the effect of back diffusion on plume persistence can sometimes be ambiguous. A novel approach for simulating matrix diffusion effects was previously adapted from geothermal reservoir modeling, which combines numerical and analytical methods by discretizing only the high permeability parts of the aquifer and treating the matrix diffusion flux into the high permeability gridblocks as a concentration dependent source/sink term (Falta and Wang, 2017; Muskus and Falta, 2018). This semi-analytical/numerical method, as a result, is not as computationally intensive as conventional matrix diffusion modeling methods.

The objective of this research is to better understand the parameterizations that affect the back diffusion signal in a chemical transport model, which is accomplished by applying the semi-analytical/numerical modeling method to theoretical scenarios that are representative of field conditions. This research aims to develop a better intuition for back diffusion effects that can be applied to future field studies.

From this study, it was concluded that the observation of the most significant back diffusion effects in any aquifer system is dependent on monitoring well location relative to the highest concentrations within the aquifer and the low permeability/high permeability interfaces. The initial source concentration is critical for determining the magnitude at which back diffusion affects aquifer concentrations, which in some cases can be below the MCL. The low *k* zone degradation rate was found to be a key parameter

for determining the magnitude of plume persistence caused by back diffusion. Diffusive mass flow was shown to be governed by porosity and the geometric parameterization for embedded low *k* material or fractures. Lastly, partial source zone remediation that results in a residual source mass can cause plume persistence that looks similar to the effect of back diffusion, and the relative contributions of a residual source mass and back diffusion to overall plume persistence are determined by the amount of source mass removed, the amount of low *k* material or fractures in the aquifer system, the location in the aquifer relative to the source zone, and the low *k* zone parameterization.

Finally, a field site was assessed where the gained insights from this study were used to determine the potential risk for back diffusion at the site and to develop a model to evaluate any observed plume persistence for back diffusion.

ACKNOWLEDGMENTS

First and foremost, I would like to thank my advisor, Dr. Ron Falta, for welcoming me as his student. My meetings with him have been invaluable, and I am grateful not only for his around-the-clock guidance on this project but also for his assistance in helping me identify future endeavors and find opportunities for post-graduate school life.

I would also like to thank Dr. Larry Murdoch and Dr. James Henderson for being members of my committee. To Dr. Murdoch, I thank for his indirect contribution to this project by equipping me with a robust hydrogeological toolset for tackling any problem in the sciences and beyond. I would like to acknowledge Dr. Henderson for his contribution to this project by providing the field data from the DuPont Kinston Plant that was used in the case study.

TABLE OF CONTENTS

Page

TITLE PAGE i

ABSTRACT ii

ACKNOWLEDGMENTS iv

LIST OF TABLES ix

LIST OF FIGURES x

CHAPTER

1. INTRODUCTION 1

    1.1 Matrix Diffusion 3

    1.2 Semi-Analytical Method 8

2. RESEARCH OBJECTIVES 11

3. SEMI-ANALYTICAL SIMULATION OF MATRIX DIFFUSION IN POROUS MEDIA CASES WITH A CONSTANT SOURCE 12

    3.1 Methods 12

    3.2 Scenario 1: Homogenous sand aquifer with an underlying clay aquitard 14

        3.2.1 Results 15

    3.3 Monitoring Well Location 19

    3.4 Effect of the Initial Source Concentration 22

    3.5 Low *k* Zone Parameterization 25

        3.5.1 Degradation Rate 25

        3.5.2 Retardation Factor 27

Table of Contents (Continued)

Page

3.6 Scenario 2: Heterogenous sand aquifer with an underlying clay aquitard 29

3.6.1 Results 33

3.7 Conclusions 41

4. SEMI-ANALYTICAL SIMULATION OF MATRIX DIFFUSION IN POROUS MEDIA CASES WITH A DECAYING SOURCE 44

4.1 Methods 44

4.2 Scenario 1: Homogenous sand aquifer with an underlying clay aquitard 47

4.2.1 Results 47

4.2.2 Partial Source Zone Remediation 50

4.3 Scenario 2: Heterogenous sand aquifer with an underlying clay aquitard 56

4.3.1 Partial Source Zone Remediation 57

4.4 Conclusions 61

5. SEMI-ANALYTICAL SIMULATION OF MATRIX DIFFUSION IN FRACTURED MEDIA CASES 63

5.1 Methods 63

5.2 Results 66

5.2.1 Partial Source Zone Remediation 71

5.3 Conclusions 75

Table of Contents (Continued)

Page

6. CASE STUDY 77

6.1 Site Background and Remediation Activities 77

6.2 Match to Previous Analytical Model 80

6.3 Back Diffusion Risk Assessment 86

6.4 Model Parameterization 89

6.5 Matrix Diffusion Model Results 91

6.6 Discussion 96

6.7 Conclusions 97

7. FINAL CONCLUSIONS 99

REFERENCES 101

LIST OF TABLES

Page

Table 1. Input parameters used in base model for porous media cases. 13

Table 2. Geometric parameters used in embedded low *k* case with a diffusion length of 1 m and a total gridblock volume of 50 m^2 33

Table 3. Geometric parameters used in embedded low *k* case with a diffusion length of 0.1 m and a total gridblock volume of 50 m^2 33

Table 4. Input parameters used in base model for fractured rock cases 65

Table 5. Input parameters used to match the numerical model to the analytical model from Liang et al. (2011) 85

Table 6. Geometric matrix diffusion parameters and low *k* zone parameters used in the MD model for the Kinston Plant field site 90

LIST OF FIGURES

Page

Figure 1. Cross-sectional view of conceptual model for a theoretical scenario of a homogenous sand aquifer with an underlying clay aquitard.....13

Figure 2. Comparison of TCE concentrations at different observation wells for No MD and MD models.....16

Figure 3. Comparison of REMChlor-MD TCE concentration contours in *xy* plane (at lowest gridblock). A-D: No MD contour plots. A) t=30 yrs; B) t=60 yrs; C) t=90 yrs; D) t=120 yrs. E-H: MD contour plots. E) t=30 yrs; F) t=60 yrs; G) t=90 yrs; H) t=120 yrs 18

Figure 4. Comparison of REMChlor-MD TCE concentration contours in *xz* plane (at first gridblock from center). A-D: No MD contour plots. A) t=30 yrs; B) t=60 yrs; C) t=90 yrs; D) t=120 yrs. E-F: MD contour plots. E) t=30 yrs; F) t=60 yrs; G) t=90 yrs; H) t=120 yrs 19

Figure 5. Comparison of TCE concentrations at the same observation well location (x=100 m, y=2.5 m) with different well screen elevations for a MD model.....20

Figure 6. Comparison of TCE concentrations across the plume width at x=100 m with a screen interval at 0-2 m for a MD model 21

Figure 7. Comparison of TCE concentrations at two observation wells for MD and No MD models with different initial source concentrations. A) C_i = 100,00 times the MCL; B) 10,000 times the MCL; C) 1,000 times the MCL; and D) 100 times the MCL 24

Figure 8. Comparison of TCE concentrations at different observation wells for models with varying decay rates in the underlying aquitard.....27

Figure 9. Comparison of TCE concentrations at different observation wells for models with varying retardation factor values in the underlying aquitard.....28

List of Figures (Continued) Page

Figure 10. Cross-sectional view of conceptual model for a theoretical scenario of a heterogenous sand aquifer with an underlying clay aquitard....31

Figure 11. Comparison of scaled TCE concentrations from MD and No MD models at different observation wells for varying amounts of interbedded low *k* material and a diffusion length of 1 m....34

Figure 12. Comparison of scaled TCE concentrations from MD and No MD models at different observation wells for varying amounts of interbedded low *k* material and a diffusion length of 0.1 m....37

Figure 13. Comparison of REMChlor-MD TCE concentration contours in *xy* plane (at lowest gridblock) for MD models with embedded low *k* material and a diffusion length of 1 m. A) V_f=75% at t=30 yrs; B) V_f=75% at t=90 yrs; C) V_f=25% at t=30 yrs; and D) V_f=25% at t=90 yrs.....40

Figure 14. Comparison of REMChlor-MD TCE concentration contours in *xz* plane (at first gridblock from center) for MD models with embedded low *k* material and a diffusion length of 1 m. A) V_f=75% at t=30 yrs; B) V_f=75% at t=90 yrs; C) V_f=25% at t=30 yrs; and D) V_f=25% at t=90 yrs....40

Figure 15. Comparison of REMChlor-MD TCE concentration contours in *xy* plane (at lowest gridblock) for MD models with embedded low *k* material and a diffusion length of 0.1 m. A) V_f=75% at t=30 yrs; B) V_f=75% at t=90 yrs; C) V_f=25% at t=30 yrs; and D) V_f=25% at t=90....41

Figure 16. Comparison of REMChlor-MD TCE concentration contours in *xz* plane (at first gridblock from center) for MD models with embedded low *k* material and a diffusion length of 0.1 m. A) V_f=75% at t=30 yrs; B) V_f=75% at t=90 yrs; C) V_f=25% at t=30 yrs; and D) V_f=25% at t=90 yrs....41

List of Figures (Continued) Page

Figure 17. Comparison of scaled TCE concentrations from MD and No MD models at observation wells for different source zone decay rates (dissolution)..... 48

Figure 18. Comparison of scaled TCE concentrations at observation wells from MD and No MD models with 99% source zone remediation and varying source zone decay rates (dissolution) 51

Figure 19. Comparison of scaled TCE concentrations at observation wells from MD and No MD models with 90% source zone remediation and varying source zone decay rates (dissolution) 53

Figure 20. Comparison of REMChlor-MD TCE concentration contours in *xy* plane (at lowest gridblock) for No MD and MD models with a decaying source and 90% source zone remediation. A-D: No MD contour plots. A) t=30 yrs; B) t=60 yrs; C) t=90 yrs; D) t=120 yrs. E-H: MD contour plots. E) t=30 yrs; F) t=60 yrs; G) t=90 yrs; H) t=120 yrs..... 55

Figure 21. Comparison of REMChlor-MD TCE concentration contours in *xz* plane (at first gridblock from center) for No MD and MD models with a decaying source and 90% source zone remediation. A-D: No MD contour plots. A) t=30 yrs; B) t=60 yrs; C) t=90 yrs; D) t=120 yrs. E-H: MD contour plots. E) t=30 yrs; F) t=60 yrs; G) t=90 yrs; H) t=120 yrs..... 55

Figure 22. Comparison of scaled TCE concentrations at observation wells from No MD and MD models with 99% source zone remediation 57

Figure 23. Comparison of scaled TCE concentrations at observation wells from No MD and MD models with 90% source zone remediation 59

Figure 24. Comparison of scaled TCE concentrations at observation wells from No MD and MD models with 80% source zone remediation 60

List of Figures (Continued) Page

Figure 25. Cross-sectional view of conceptual model for a fractured rock system. Fractures are shown in the *xy* plane, but they can be in any direction assuming they are all parallel 66

Figure 26. Comparison of scaled TCE concentrations from MD and No MD models at different observation wells for cases with fractured granite, sandstone, and shale that have a constant source. 67

Figure 27. Comparison of scaled TCE concentrations from MD and No MD models at different observation wells for cases with fractured granite, sandstone, and shale that have a decaying source. 68

Figure 28. Comparison of scaled TCE concentrations from MD and No MD models at different observation wells for cases with fractured granite, sandstone, and shale that have a decaying source and low *k* zone decay rate of 0.03 yr^{-1}. 71

Figure 29. Comparison of scaled TCE concentrations from MD and No MD models at different observation wells for cases with fractured granite, sandstone, and shale that have a 90% source zone remediation 72

Figure 30. Comparison of scaled TCE concentrations from MD and No MD models at different observation wells for cases with fractured granite, sandstone, and shale that have a 90% source zone remediation and a low *k* zone decay rate of 0.03 yr^{-1} 75

Figure 31. Site map of Kinston plant with monitoring wells (reproduced with permission from Liang, 2009, personal communication, September 26, 2019) 78

Figure 32. Comparison of the analytical solution from REMChlor and the numerical solution from REMChlor-MD at the plume center line at t=90 years 86

List of Figures (Continued) Page

Figure 33. Comparison of TCE concentrations between modeled results and field data for MW-30A (source zone). 92

Figure 34. Comparison of TCE concentrations between modeled results and field data for MW-47 (source zone) 92

Figure 35. Comparison of TCE concentrations between modeled results and field data for MW-58 (downgradient of source, before PRB) 93

Figure 36. Comparison of TCE concentrations between modeled results and field data for MW-29 (downgradient of PRB) 94

Figure 37. Comparison of TCE concentrations between modeled results and field data for MW-35 (downgradient of PRB) 95

Figure 38. Comparison of TCE concentrations between modeled results and field data for MW-37 (downgradient of PRB) 95

1. INTRODUCTION

Groundwater is the largest source of accessible fresh water in the world, and therefore, it is also the main source of drinking water. (Fetter, 2014). In the United States alone, over half the population is dependent on groundwater for domestic use, and groundwater usage has been increasing over the last decade while surface water use has been declining. (Dieter et al., 2018). Because groundwater is crucial to the health and development of a society, the quality of groundwater is of utmost importance, and consequently, contamination poses a serious threat.

The most common chemicals found in groundwater that have health threatening properties are organic contaminants, with the most common contaminants being industrial solvents and aromatic hydrocarbons from petroleum products. (Mackay and Cherry, 1989). Groundwater contamination is often attributed to leakage, spillage, or disposal of nonaqueous-phase liquids (NAPLs) into the ground (Mackay and Cherry, 1989; Pankow and Cherry, 1996).

NAPLs are divided into two categories based upon their relative densities to water. Light NAPLs (LNAPLs) have a density less than water and as a result will float (e.g. gasoline). Dense NAPLs (DNAPLs) have a density greater than water and will sink (e.g. trichloroethylene). (Fetter, 2014).

Contaminants in the subsurface can be distributed among different phases, which presents various challenges for remediation. Once a NAPL has been spilled into the environment, the liquid will mostly travel down toward the water table due to density-driven flow. Within the subsurface, a NAPL may dissolve into pore water, volatilize into

air within pore spaces, or persist as a residual liquid trapped within pores. Additionally, lateral movement is possible due to spreading caused by capillary forces, vapor phase migration, and subsurface heterogeneities. After a contaminant has traveled through the vadose zone, it reaches the water table, where density differences govern NAPL behavior. LNAPLs will float at the water table and will mostly flow downgradient while DNAPLs will penetrate the water table and enter the saturated zone, where some dissolution of the DNAPL and subsequent transport of the dissolved contaminant occurs. This creates a plume that flows mostly downgradient in the horizontal direction. DNAPL that does not dissolve is able to move vertically toward the base of the aquifer. Low permeability layers (such as clay lenses) may promote lateral spreading and pooling of the DNAPL mass, where the residual fluid is then trapped by capillary forces and distributed as ganglia. These discontinuous DNAPL pools that form on top of low permeability lenses also dissolve into the groundwater, thereby acting as highly concentrated secondary source zones of contamination that contribute to the existing plume. (Mackay and Cherry, 1989; Pankow and Cherry, 1996).

In the 1980s, one of the first methods that was used to address the restoration of contaminated sites was pump-and-treat systems (Pankow and Cherry, 1996). Although this method can hydraulically contain a plume, DNAPL source zones will persist with no apparent reduction in long-term concentrations, and plume concentrations often bounce back up after pumping has stopped. By the end of the decade, the pump-and-treat system was determined to be an inefficient method for aquifer remediation, and the complexity of the aquifer restoration problem was becoming more acknowledged due the presence of

low permeability zones (Travis and Doty, 1990). Only a few years before peak deployment of the pump-and-treat system, the first journal article that identified matrix diffusion as a contaminant transport process was published in 1975 (Foster, 1975; Hadley and Newell, 2014). In the following years, multiple projects began exploring matrix diffusion as a chemical transport process (Goodall and Quigley 1977; Gillham et al. 1984; Sudicky et al. 1985). By the late 80's, the scientific community had recognized that low permeability zones could act as contaminant sources and sinks, and it was presented as an explanation for why pump-and-treat methods were not working (MacKay and Cherry, 1989). However, alongside this explanation, MacKay and Cherry also recognized NAPLs as playing an important role in remediation conceptual models, and matrix diffusion eventually took the backseat to the "Age of In-Situ Remediation" as NAPLs dominated most of the remediation discussion and research in the ensuing years (Hadley and Newell, 2014). It was not until the 2000s when remediation technologies were still unable to achieve aquifer restoration goals that matrix diffusion began to gain traction again as a possible explanation (Liu and Ball, 2002; Chapman and Parker, 2005; Falta, 2005; Parker et al., 2008; Sale et al., 2008).

1.1. Matrix Diffusion

Matrix diffusion is the chemical transport process of transferring solute mass between the main groundwater conduits and the surrounding low permeability zones as a result of a concentration gradient. When transport is from high to low permeability zones, the process is referred to as forward diffusion, which occurs during a "loading period" as contaminants reach the aquifer. During forward diffusion, low permeability material acts

as a contaminant sink. After the contaminant source has been removed or isolated and contaminant concentrations in the aquifer are reduced, the concentration gradient can reverse, resulting in transport that occurs from low to high permeability zones. This process is referred to as back diffusion, and the low permeability material now acts as a contaminant source. (Liu and Ball, 2002; Chapman and Parker, 2005; Falta, 2005; Parker et al., 2008; Sale et al., 2008; Rasa et al., 2011)

Due to back diffusion of contaminants out of low permeability material, plumes can persist long after remediation efforts have taken place. (Chapman and Parker, 2005; Parker et al., 2008; Sale et al., 2008; Rasa et al., 201; Seyedabbasi et al., 2012). Therefore, in order to improve remediation strategies, it is critical to be able to model matrix diffusion and better predict its impact. Although analytical solutions to model matrix diffusion are available (e.g. Tang et al., 1981; Sudicky and Frind, 1982; Liu and Ball, 2002; Sale et al., 2008; Seyedabbasi et al., 2012; Yang et al., 2015), these solutions are restricted to idealized cases with simple geometries. Numerical methods have been successful in simulating transient matrix diffusion effects (e.g. Chapman and Parker, 2005; Parker et al., 2008; Rasa et al., 2011; Chapman et al., 2012; Chapman and Parker, 2013); however, in order to simulate the diffusive fluxes at the high permeability/low permeability interfaces, very fine discretization is required, which can be computationally intensive (Chapman et al., 2012; Falta and Wang, 2017).

Despite the challenges associated with modeling matrix diffusion, many research projects have continued to focus their efforts on studying back diffusion as a contaminant source. One of the first projects that analyzed matrix diffusion at a field-scale was

conducted in 1997 at the Dover Air Force Base in Delaware, where the analysis of soil cores from the site revealed contamination that extended into an underlying aquitard. (Ball et al., 1997). By using independent estimates of sorption and diffusion properties in the aquitard, mathematical modeling was used to make inferences about the history of concentrations in the overlying aquifer and to predict future aquitard concentrations based on hypothesized conditions after remediation. A return to the Dover site in 2002 yielded a study that used soil core samples over time to validate analytical models that could predict concentration profiles within a natural aquitard. (Liu and Ball, 2002). A few years later, another field-scale study was conducted at an industrial site in Connecticut where a zone of TCE was isolated at the bottom of a sand aquifer overlying a clayey silt aquitard (Chapman and Parker, 2005). Groundwater monitoring at the site showed a persistent TCE plume downgradient of the DNAPL zone 6 years after the source zone was isolated by a sheet piling enclosure. Numerical simulations indicate that the plume tailing, a term used to describe the asymptotic nature of observed concentrations in a monitoring well over time, can be fully explained by back diffusion. Additionally, it was concluded that back diffusion in the aquifer would sustain TCE concentrations above the maximum contaminant level (MCL) of 5 μg/L for centuries. Another field study was carried out at a contaminated site in Florida by Parker and Chapman (2008) where the contaminant source was hydraulically isolated, and groundwater was monitored downgradient. This study concluded that back diffusion from one or a few thin clayey beds (<0.2 m to 0.5 m) in a sand aquifer was the most plausible theory that explained plume persistence above MCLs for several years to decades. Additionally, a fine grid

numerical model was used to the model the site, and matrix diffusion was shown to fully account for the observed plume persistence.

Other studies have focused on laboratory scale experiments. In 2008, Sale et al. performed a set of idealized experiments using sand tanks to explore how reductions in contaminant loading to plumes affect downgradient water quality. It was concluded that the longevity of contaminants in plumes is a function of both the source at the plume head and the downgradient contaminant storage-release processes. To better characterize the experimental data for this study, analytical solutions were developed, and the results were found to be satisfactory (Sale et al., 2008). Chapman et al. (2012) explored the validity of various numerical models (HydroGeoSphere, FEFLOW, MODFLOW/MT3DMS) by simulating scenarios involving back diffusion, and close matches to experimental data from a lab sandbox study were found when using high resolution modes.

Ensuing research projects have continued efforts to study matrix diffusion by evaluating back diffusion risk and the factors that contribute to longer-term plume persistence. Rasa et al. (2011) used 2D numerical simulations to model a field site at the Vandenberg Air Force Base and found good matches to field data. This study concluded that although back diffusion causes aquifer contaminants to persist longer, degradation reactions will limit long-term persistence of contaminants in the aquifer, which results in less plume persistence compared to diffusion processes alone. Seyedbbasi et al. (2012) addressed the question of the relative contribution of DNAPL dissolution and matrix diffusion to the long-term persistence of source zones by developing a hypothetical

DNAPL source zone architecture. In this study, several analytical models were used to characterize source zone attenuation curves, and the results showed that matrix diffusion might play a bigger role in the persistence of contamination sources than DNPAL dissolution alone, depending on the contaminant's solubility. In that same year, Brown et al. (2012) also investigated the influence of DNAPL source architecture on back diffusion risk, but the focus was shifted toward plume zones. The study used a 1D analytical model where source zone dissolution was represented by a power law source depletion model, and it was found that the greatest risk of back diffusion occurs from a constant source strength function. Chapman and Parker (2013), using a 2D domain, showed the ability of popular numerical models to capture the matrix diffusion process when adequately discretized spatially and temporally by comparing the simulations to analytical solutions and experimental data. Additionally, the study demonstrated the effects of mass storage and release for "type site" conditions by developing hypothetical simulations that were aimed to represent real site conditions. From this portion of the study, the simulations showed that higher sorption increases the storage capacity in the low permeability zones, which can increase back diffusion rates. Furthermore, it was found that because degradation in low permeability zones effectively removes contaminant mass, even low decay rates can significantly reduce the impact of back diffusion (Chapman and Parker, 2013).

More recently, Yang et al. (2016) evaluated three transient source depletion models (step-change, linear, and exponential) for the effects of back diffusion using a series of lab experiments in a 2D well-controlled flow chamber. One-dimensional

analytical solutions were used to match experimental data and describe the dynamic aquitard-aquifer diffusive transfer. Additionally, for these scenarios, the plume evolution was divided into three distinct stages based on relative importance of dissolution and back diffusion. In 2017, Yang et al. continued to build upon this work and analyzed aquitard concentration profiles from different field sites in order to identify signature shapes in the profiles that could be uniquely attributed to stages in the three-stage classification system.

1.2. Semi-Analytical Method

The aforementioned studies have all used modeling to varying degrees to characterize matrix diffusion. However, the analytical solutions have been constrained to simple geometries and idealized cases, and the numerical simulations have required very fine spatial and temporal discretization that constrain modeling efforts to one or two dimensional domains. A different modeling approach, however, combines the analytical and the numerical modeling methods. This hybrid method was first developed in petroleum reservoir engineering to model transient heat conduction in reservoirs bounded by impermeable caprocks (Vinsome and Westerveld, 1980) and in fractured reservoirs (Pruess and Wu, 1988, 1993). Vinsome and Westerveld (1980) understood that the heat conduction process in confining units is mainly 1-dimensional, and therefore, the temperature profile in the confining beds could be represented with a 1D trial function that is updated at every time step. This method discretizes only the high permeability parts of the reservoir in the numerical model while the heat conductive flux is treated as a temperature dependent source/sink term that is calculated analytically in the gridblocks at

the low permeability/high permeability interfaces at every time step（Vinsome and Westerveld, 1980; Pruess and Wu, 1988; Pruess and Wu, 1993）. By simulating the conductive response in the confining units, the need to discretize the low permeability zones is eliminated, and the computational effort is greatly reduced (Muskus and Falta, 2018).

Because the heat conduction equations and the matrix diffusion equations are analogous, the semi-analytical method was adapted to matrix diffusion processes with the addition of a first order decay term (Bear et al., 1994; Falta and Wang, 2017; Muskus and Falta, 2018).

Falta and Wang (2017) used the semi-analytical method to model matrix diffusion for a two-layer aquifer system consisting of an aquifer and an aquitard of infinite thickness, and the accuracy of the model was verified with analytical solutions. Muskus and Falta (2018) expanded upon the method used in Falta and Wang (2017) by allowing for coupled parent-daughter decay reactions with multiple species that each have independent retardation factors, decay rates, and yield coefficients in both the low and high permeability materials and by extending the model to simulate embedded low k zones. This generalization of the semi-analytical method allows for its implementation in many more scenarios, and the study verified this expansion by showing favorable fits with analytical solutions and experimental data for both heterogenous and fractured systems. (Muskus and Falta, 2018).

Because of the challenging and often complicated nature of field sites, the application of matrix diffusion models can be difficult and the effects of back diffusion

can be ambiguous. For example, if the presence of low permeability material at a field site is coupled with unsuccessful remediation realized by plume persistence, it can be hypothesized that back diffusion is responsible. While back diffusion may to be blame, it is difficult to quantify back diffusion unless low permeability soil core is analyzed, a practice that has not historically been a site investigation standard (Ball et al., 1997). Site managers often operate only from the perspective of monitoring well data, where plume persistence is realized when aquifer concentrations fail decrease after remediation has occurred. However, it would be misguided to attribute plume persistence only to back diffusion without any soil core data. Additionally, plume persistence may not always be obvious, especially in cases when field data extends over small time periods or has a lot of noise. In reality, there is more than one process that can result in plume persistence, and as a result, the back diffusion signal needs to be better characterized.

Therefore, it is the purpose of this project to apply the matrix diffusion semi-analytical model to theoretical scenarios with conditions that are representative of field sites and to a field case study in order to better understand the parameterizations that result in strong back diffusion signals in a chemical transport model. It is the desire that from this study, a better intuition can be developed for assessing back diffusion risk at field sites.

2. RESEARCH OBJECTIVES

The main goal of this study is to better understand the parameterizations that affect the back diffusion signal in a chemical transport model. The specific objectives are:

- Apply the semi-analytical method for modeling matrix diffusion to theoretical scenarios that are representative of field conditions for a homogenous aquifer with an underlying aquitard, a heterogenous aquifer with an underlying aquitard, and fractured systems
- Compare models with and without matrix diffusion to assess parameter effects on matrix diffusion
- Better understand how monitoring well location and design affects observation of the back diffusion signal
- Better understand how the parameterization for the low *k* zone affects back diffusion
- Better understand how source zone remediation affects back diffusion
- Apply gained insights to a more complicated field case study

3. SEMI-ANALYTICAL SIMULATION OF MATRIX DIFFUSION IN POROUS MEDIA CASES WITH A CONSTANT SOURCE

3.1 Methods

The semi-analytical method was implemented using REMChlor-MD, which is a Visual Basic program in Excel® (Falta et al., 2018). A common base model was developed as the foundation for each scenario. The porous media base model is 1200 meters long in the x-direction (direction of groundwater flow) with a cell size of 5 m, 400 m in the y-direction with a cell size of 5 m, and 20 m in the z-direction with a cell size of 2 m. Tricholorethylene (TCE) without any daughter products is the chemical contaminant used in this analysis. The source is 40 m wide, 4 m thick, and located at the bottom of the model. The source, transport, and natural attenuation parameters used in the base model are shown in Table 1.

The effect of matrix diffusion on the chemical transport model was explored using monitoring wells across the plume length at the first gridblock from the centerline (y=2.5 m). A well screen length of 2 m was used because it is the smallest scale possible given the base model discretization. A small scale is necessary to increase the sensitivity of the matrix diffusion signal when diffusion is occurring in an adjacent aquitard. The well screens were located at the bottom of the model (z=0 - 2 m). The geometry between the source location, well screen interval, and transmissive zone/low permeability zone interface may be critical to observing the back diffusion signal, and the configuration used for the first scenario is shown in Figure 1.

Table 1: Input parameters used in base model for porous media cases.

Source, Transport, and Natural Attenuation Parameters Used in Base Model		
Parameter	**High K Zone**	**Low K Zone**
Initial Source Concentration, C_0 (mg/L)	1,100	-
Initial Source Mass, M_0 (kg)	75,000	-
Source width, w (m)	40	-
Source depth, d (m)	4	-
Darcy velocity, V_d (m/yr)	5	-
Hydraulic Conductivity (cm/s)	3.16×10^{-2}	-
Porosity, ϕ	0.25	0.47
Retardation factor, R	3	3
Tortuosity, τ	0.56	0.32
Longitudinal dispersivity (m)	1	-
Transverse dispersivity (m)	1	-
Vertical dispersivity (m)	0.01	-
Source decay rate (yr^{-1})	0	-
Power function exponent, Γ	0	-
TCE plume natural degradation rate, λ (yr^{-1})	0.3	0.3
Molecular Diffusion Coefficient (cm^2/s)	9.10×10^{-6}	9.10×10^{-6}

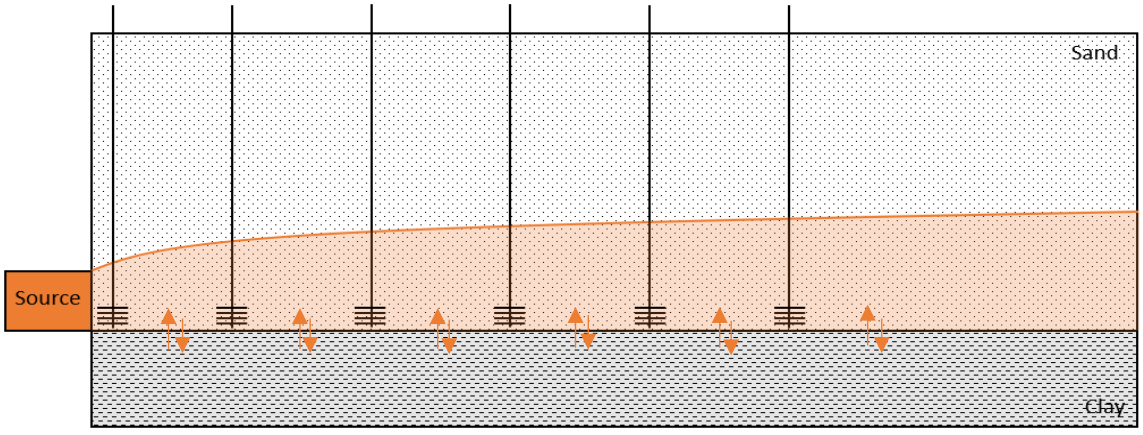

Figure 1: Cross-sectional view of conceptual model for a theoretical scenario of a homogenous sand aquifer with an underlying clay aquitard.

The back diffusion signal was assessed by comparing models with matrix diffusion to models without matrix diffusion at different observation wells, which will be denoted from here on as MD and No MD models. Removing matrix diffusion from a model can be achieved by manually removing the low permeability material through the REMChlor-MD interface or by simply making the porosity of the low permeability zone equal to a near-zero number, thereby eliminating the diffusive flux. The latter option was used for this study, and for the No MD models, the porosity of the low *k* material was set equal to $1x10^{-20}$.

3.2 Scenario 1: Homogenous sand aquifer with an underlying clay aquitard

For the first scenario, a homogenous sand aquifer with an underlying clay aquitard was assessed (Figure 1). To begin, the porous media scenarios were evaluated with a constant source and 100% source mass removal after 30 years. The step-function resulting from a constant source and complete source removal will cause an instantaneous reversal in the concentration gradient of the chemical constituent. The gradient reversal triggers back diffusion, and the resulting signal should be visually identifiable. Previous work has shown that back diffusion risk is greatest when the source is constant (Brown et al., 2012; Yang et al., 2016). Although aquifer concentrations in real source zones decrease at more gradual rate (Rao and Jawitz, 2003), it is important to be able to characterize back diffusion under idealized conditions before exploring more complicated scenarios.

To further magnify the matrix diffusion signal, the models were first assessed using an initial source concentration equal to the solubility of TCE. A previous field

study of a site in Connecticut showed a strong effect from back diffusion into a sand aquifer from an underlying aquitard, and the soil cores that were analyzed showed concentrations in the range of TCE solubility (Chapman & Parker, 2005). Lastly, it is initially being assumed that degradation and sorption in the transmissive and low permeability zones are the same.

3.2.1. Results

In Figure 2, four observation wells located along the plume centerline at x=2.5, 100, 250, and 500 m show TCE concentrations over a period of 150 years for MD and No MD models. With an initial source concentration of 1,100 mg/L, significant differences result between the two models. In the first two monitoring wells, concentrations in the MD models take approximately 30 more years to decline to concentrations below the MCL than the No MD models. The No MD models show a steady, exponential decline after source removal while the MD models show a deviation from the initial rate and then proceed to decline at a slower rate. This pattern, although not asymptotic as described by previous studies (Chapman & Parker, 2005), can still be described as "plume tailing" because concentrations are sustained in the aquifer at higher levels than expected. This difference between the two models, indicated by the tailing in the MD models, can be characterized as the back diffusion signal. The back diffusion signal is additionally seen at observation wells located at x=250 m and 500 m, but the tailing observed at the more downgradient locations is not as pronounced. At x=500 m, there are only small differences observed between the two models.

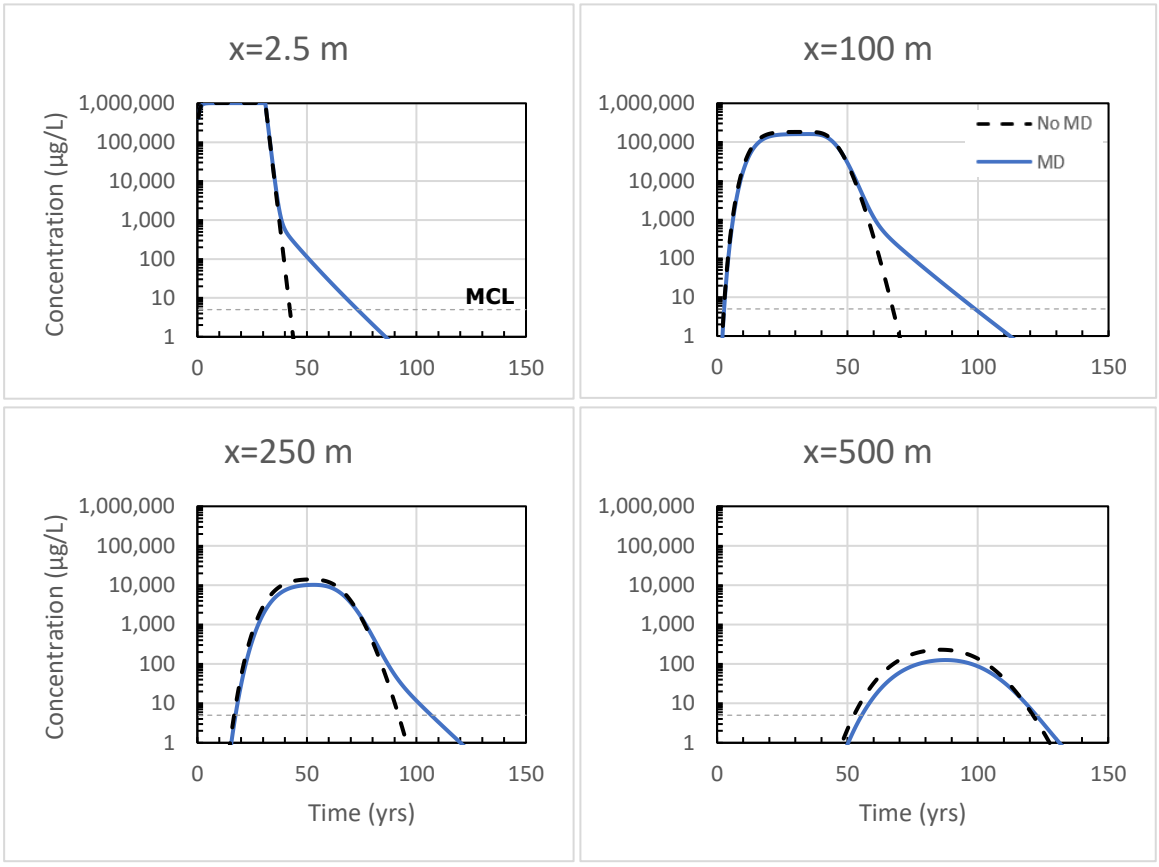

Figure 2: Comparison of TCE concentrations at different observation wells for No MD and MD models.

In Figures 3 and 4, the TCE concentration distribution from the REMChlor-MD output file was input to Surfer® (Golden Software, 2017) to create 2-D concentration contour maps. Vertical and horizontal slices were made at different time frames in order to compare the resulting plumes from the MD and No MD models. In Figure 3, the TCE plume is shown in plan view at four different time frames. At 30 years, the time when source removal occurs, the No MD and MD plumes look nearly identical. At 60 years, however, the No MD plume is completely detached and isolated from the source while

the MD plume is still showing a connectedness to the source location. As time continues, the No MD plume continues to travel downgradient. The MD plume continues to travel downgradient as well, but at 90 years, it is still attached to the source location, and a narrow tail develops on the upgradient portion of the plume. Finally, at 120 years, the upgradient tail is below a concentration of 1 μg/L, and the MD plume is shown isolated from the source. It should be noted that the described "tail" in the MD contour plots is a feature of the plume shape and is different from the "plume tailing" observed from monitoring well data, although both are caused by back diffusion.

The cross-section view shown in Figure 4 reiterates the differences previously observed between the two models while also providing more insight into the matrix diffusion signal with depth. At 30 years, the matrix diffusion process can already be detected from the contours. In the No MD model, the contours of the plume travel downgradient and terminate perpendicular to the bottom boundary of the model. In the MD model, the contours follow the same pattern but kink back toward the upgradient direction at the bottom, which shows forward diffusion occurring at the leading edge of the plume. This subtle difference in the behavior of the contours is indicative of matrix diffusion occurring at the aquifer/aquitard interface. In cross-section view, it is also evident that the upgradient part of the aquitard that is closest to the source is where the strongest effect from back diffusion is observed. Back diffusion may be occurring at more downgradient aquitard locations; however, because the No MD and the MD plumes do not differ significantly, back diffusion is likely only occurring at very low concentrations.

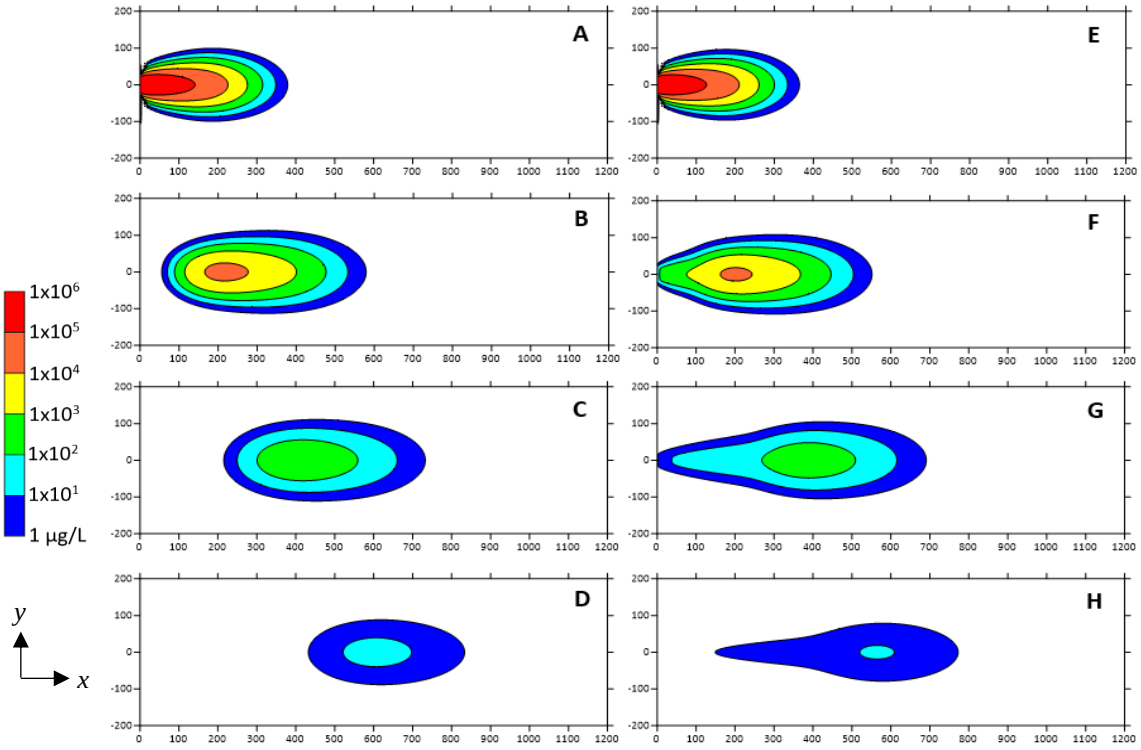

Figure 3: Comparison of REMChlor-MD TCE concentration contours in *xy* plane (at lowest gridblock). A-D: No MD contour plots. A) t=30 yrs; B) t=60 yrs; C) t=90 yrs; D) t=120 yrs. E-H: MD contour plots. E) t=30 yrs; F) t=60 yrs; G) t=90 yrs; H) t=120 yrs.

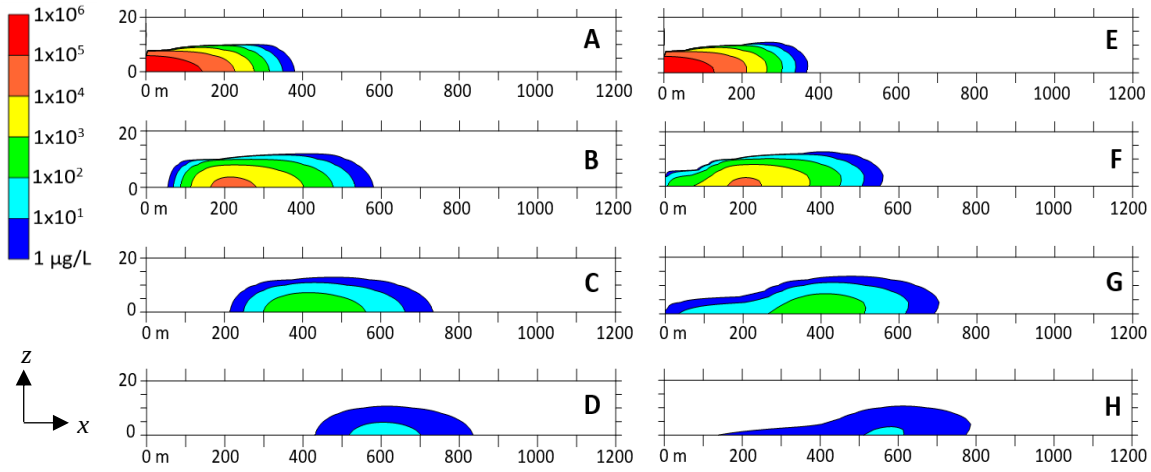

Figure 4: Comparison of REMChlor-MD TCE concentration contours in *xz* plane (at first gridblock from center). A-D: No MD contour plots. A) t=30 yrs; B) t=60 yrs; C) t=90 yrs; D) t=120 yrs. E-F: MD contour plots. E) t=30 yrs; F) t=60 yrs; G) t=90 yrs; H) t=120 yrs.

3.3 Monitoring Well Location

Parker et al. (2008) observed that the position of monitoring wells in relation to back diffusion zones strongly impacts the perception of the degree of remediation success, specifically in regard to well screen depth. It is intuitive that in order to observe the effects of back diffusion within an aquifer, a monitoring well should be placed near a back diffusion source. However, monitoring wells are not always designed for the specific purpose of observing back diffusion, and their location at any given field site might vary. Therefore, it should be better understood how the back diffusion signal is affected by monitoring well location.

Using the previous MD model with an observation well located at x =100 m and y =2.5 m, the well screen interval was varied with depth (Figure 5). The 2 m screen located at the bottom of the model (0 - 2 m) shows the strongest back diffusion signal,

which is expected because it is the well screen closest to the clay aquitard. As the well screen intervals are moved up in the aquifer and away from the aquitard, the plume tailing effect lessens, and the back diffusion signal dampens. For the well screened from 8 – 10 m, little to no tailing is observed.

In Figure 6, the MD model with an observation well located at x =100 m and screened from 0 to 2 m is explored across the width of the plume at 15 m increments. At the 2.5, 17.5, and 32.5 gridblocks in the y-direction moving away from the centerline, significant plume tailing is observed, and the effect of back diffusion is significant. At y =47.5 m, the back diffusion signal begins to lessen, and at y = 62.5 m, little to no tailing is observed.

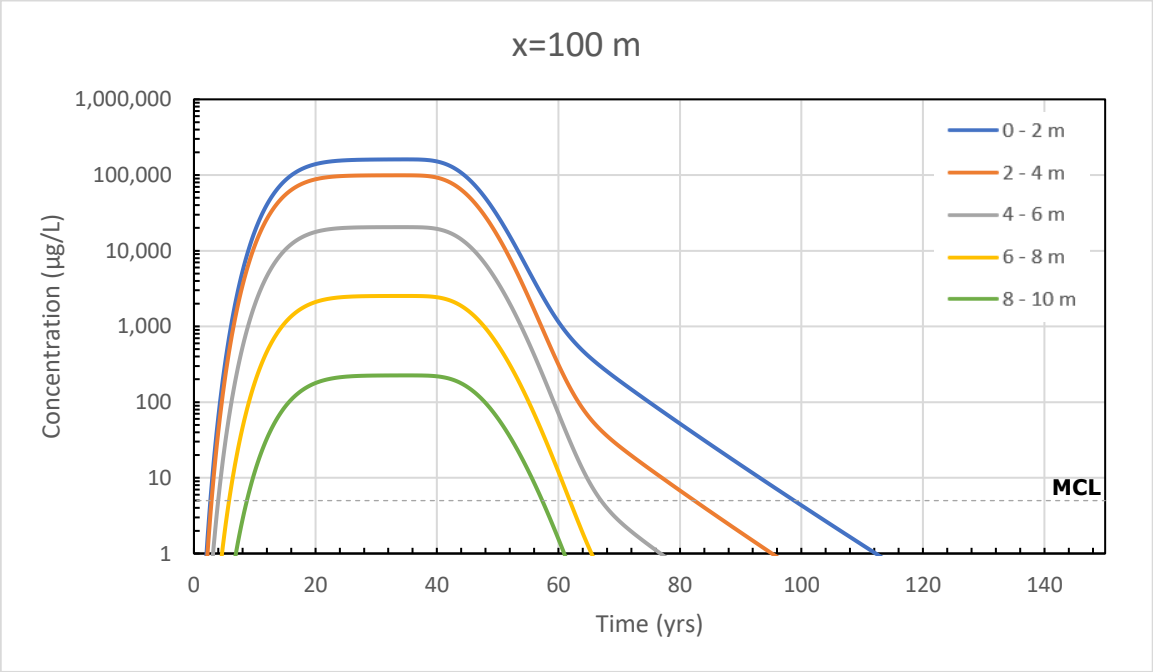

Figure 5: Comparison of TCE concentrations at the same observation well location (x=100 m, y=2.5 m) with different well screen elevations for a MD model.

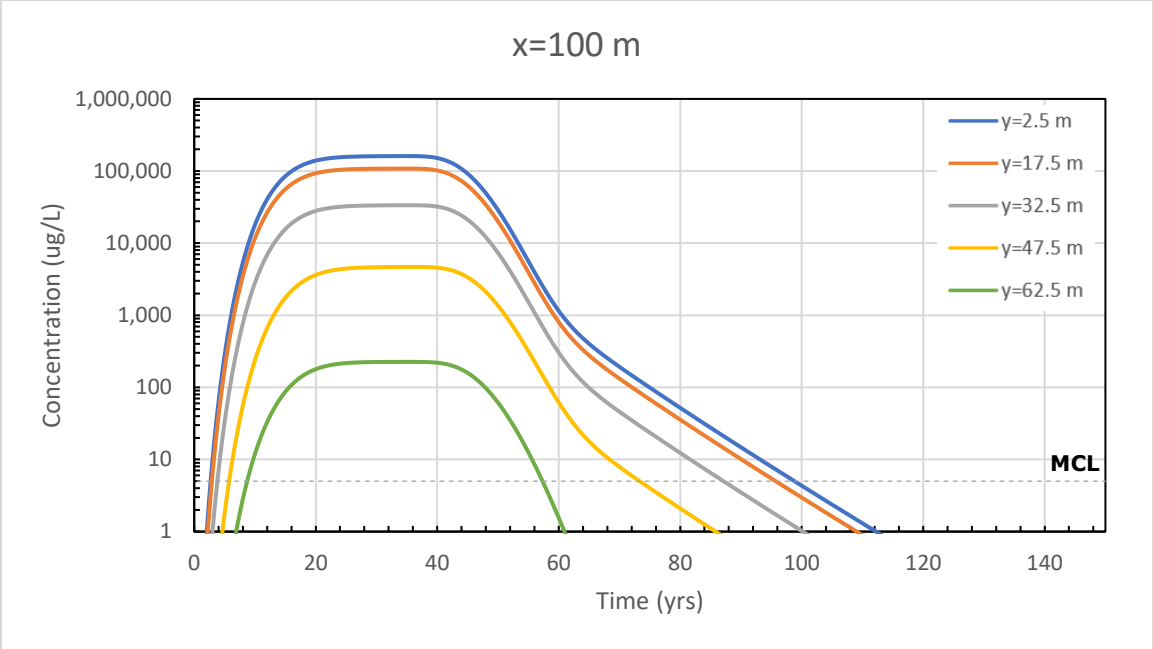

Figure 6: Comparison of TCE concentrations across the plume width at x=100 m with a screen interval at 0 - 2 m for a MD model.

In the previous section, Figure 2 demonstrated that for the first porous media scenario, the back diffusion signal weakens at locations farther downgradient from the source, most notably seen at x=500 m. Figure 6 shows that the diffusion signal weakens moving away from the centerline of the plume, and Figure 5 shows that it weakens moving away from the aquitard in the z-direction. Therefore, based on the simple scenario of an underlying clay aquitard, the observation of the back diffusion signal is 1) strongest nearest the diffusion source, i.e. the aquitard, and 2) strongest where concentrations in the aquifer are highest, i.e. near the source and near the center of the plume. At locations near the edges of the plume, aquifer concentrations are much lower, and as a result, contaminants at lower concentrations diffuse into and out of the aquitard.

Back diffusion is still occurring, but it is likely occurring at concentrations near or below the MCL. These insights on well positioning for back diffusion observation can be applied to any field site configuration and should be considered when designing and installing monitoring wells at field sites that have a back diffusion risk.

3.4 Effect of the Initial Source Concentration

The previous model comparison aimed to identify and characterize the back diffusion signal under known conditions that are primed for strong back diffusion responses using the upper limit of aqueous TCE concentration as the source and ideal monitoring well placement. However, although it is possible to have contaminated sites with source concentrations near or at solubility, the reality is that source concentrations will vary by several magnitudes from site to site. Therefore, it is pertinent to understand how observation of the back diffusion signal is affected by the magnitude of the source concentration. For the previous case, the solubility of TCE is 220,000 times greater than the 5 μg/L MCL. With this in mind, the matrix diffusion signal was evaluated as a function of the ratio of the source concentration to the MCL.

Figure 7 shows comparisons of MD and No MD models with differing initial source concentrations for monitoring wells located 2.5 m and 100 m downgradient of the source. Each graph spans six orders of magnitude of TCE concentration and the MCL is marked by a red line. For a source concentration that is 100,000 times the MCL, the results are comparable to the previous models with a source concentration equal to the solubility of TCE, and contaminants take around 30 additional years to decline to concentrations below the MCL in the well at x=2.5 m compared to the No MD case. For

a source concentration that is 10,000 times the MCL, the effect of back diffusion is visually the same; however, above the MCL, the difference in the models is less, and it takes about 10 additional years for concentrations to decline to remediation standards at x=2.5 m. When the initial concentration is 1,000 times the MCL or below, the MD and No MD models are practically identical above the MCL for both monitoring wells. Below the MCL, it is evident that back diffusion is occurring; however, it only occurs at very low concentrations.

Therefore, the observation of the back diffusion signal is dependent on the source concentration. If source concentrations are relatively low, remediation efforts can clean up an aquifer to concentrations below the MCL with negligible effects from back diffusion. For the conditions simulated in this example, a rule of thumb might be that for contaminant concentrations that are 1,000 times the MCL or lower, back diffusion can be considered a negligible chemical transport process and will not affect remediation timelines. However, this model is a simple case for back diffusion, and due to the high degradation in the aquitard, the effects of back diffusion might be an underestimate relative to sites with lower degradation rates. Also, the addition of low permeability material to the aquifer might increase the effect of back diffusion. Nevertheless, the initial source concentration should be factored into every back diffusion risk analysis for contaminated sites.

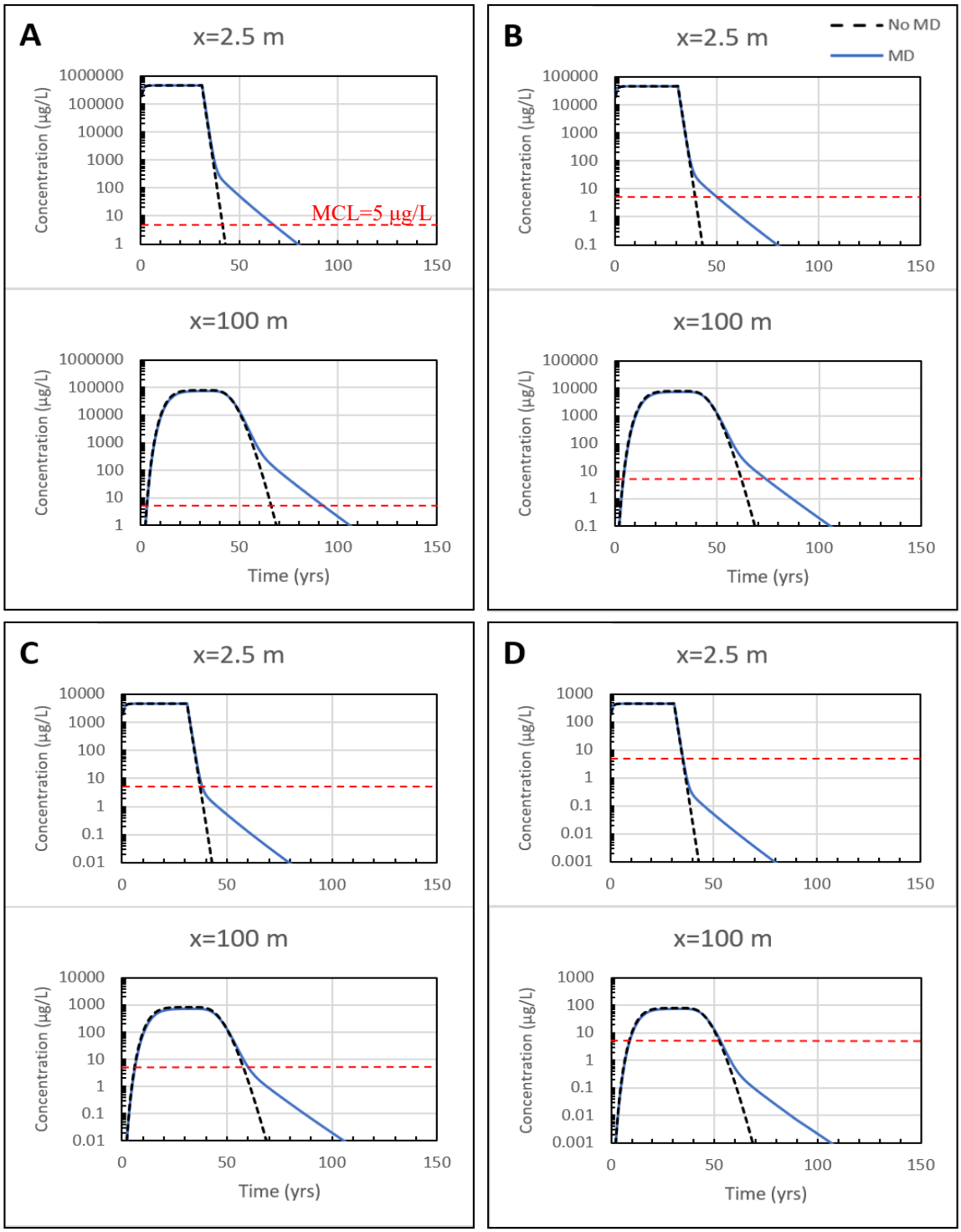

Figure 7: Comparison of TCE concentrations at two observation wells for MD and No MD models with different initial source concentrations. A) C_i = 100,00 times the MCL; B) 10,000 times the MCL; C) 1,000 times the MCL; and D) 100 times the MCL.

3.5 Low *k* Zone Parameterization

3.5.1. Degradation Rate

Contaminant transport in low *k* zones is controlled by diffusion and sorption (Lima et al., 2013), and contaminant degradation within these zones determines the longevity of the contaminant mass. Because degradation in low *k* zones effectively removes contaminant mass, even low decay rates can significantly reduce the impact of back diffusion (Chapman and Parker, 2013).

Decay rates in the low permeability zones relative to transmissive zones are a subject of ongoing investigation. Factors that favor low *k* degradation are long retention times and favorable reducing conditions and factors that limit low *k* degradation are pore throat exclusion, which restricts both the migration of microbes and the influx of nutrients (Lima et al., 2013). In unconsolidated aquitards, pore throats can be smaller than 2 nm (Reszat and Hendry, 2009), which can exclude the migration of most microbes, which are on the order of 1 μm in diameter (Lima and Sleep, 2007).

Studies have shown that low permeability/high permeability interfaces can act as reactive zones, where the aquitard serves as a source of fatty acids, organic matter, electron donors, and electron acceptors, all of which promote microbial growth on both sides of the interface (Krumholz et al. 1997; McMahon, 2001; Van Stempvoort et al. 2009). Despite the restriction of microbial mobility due to pore throat exclusion, a few field studies have suggested the presence of microbial communities deeper within the matrix of low *k* zones, and evidence of dechlorinating microorganisms have been observed within low permeability zones in the 10's of centimeters or more from the

interface, although microbial numbers and growth rates were relatively low (Scheutz et al. 2010; Takeuchi et al. 2011; Lima et al. 2012).

Because decay rates will vary from site to site, it is important to gain some better intuition about the extent that degradation can impact the back diffusion signal. Figure 8 shows a case with a homogenous sand aquifer and an underlying clay aquitard over a time frame of 250 years. The low *k* zone degradation rate was varied while the degradation rate in the transmissive zone was held constant (λ=0.3 yr^{-1}), and the effect of back diffusion was evaluated. As the decay rate in the aquitard decreases and the half-life of TCE increases, the observed plume tailing due to back diffusion increases. When the decay rate of 0.3 yr^{-1} is decreased by half to 0.15 yr^{-1}, back diffusion results in 3-4 additional decades of plume tailing in the monitoring wells closer to the source. As the decay rate approaches zero, the plume tailing approaches an asymptotic behavior that shows aquifer concentrations being sustained above the MCL for many decades and even centuries. This shows that high source concentrations can be preserved in low permeability material sinks if degradation is minimal, and as result, back diffusion can cause remediation timelines to increase significantly.

Therefore, degradation rates in low *k* zones should be treated as a key parameter when modeling matrix diffusion. Successful predictions of back diffusion effects at field sites are dependent on accurate characterization of degradation in the low *k* zones. Many of the cases in this study use degradation rates that the same for both the transmissive and low *k* zones, and therefore, should be considered as conservative predictions for back diffusion effects.

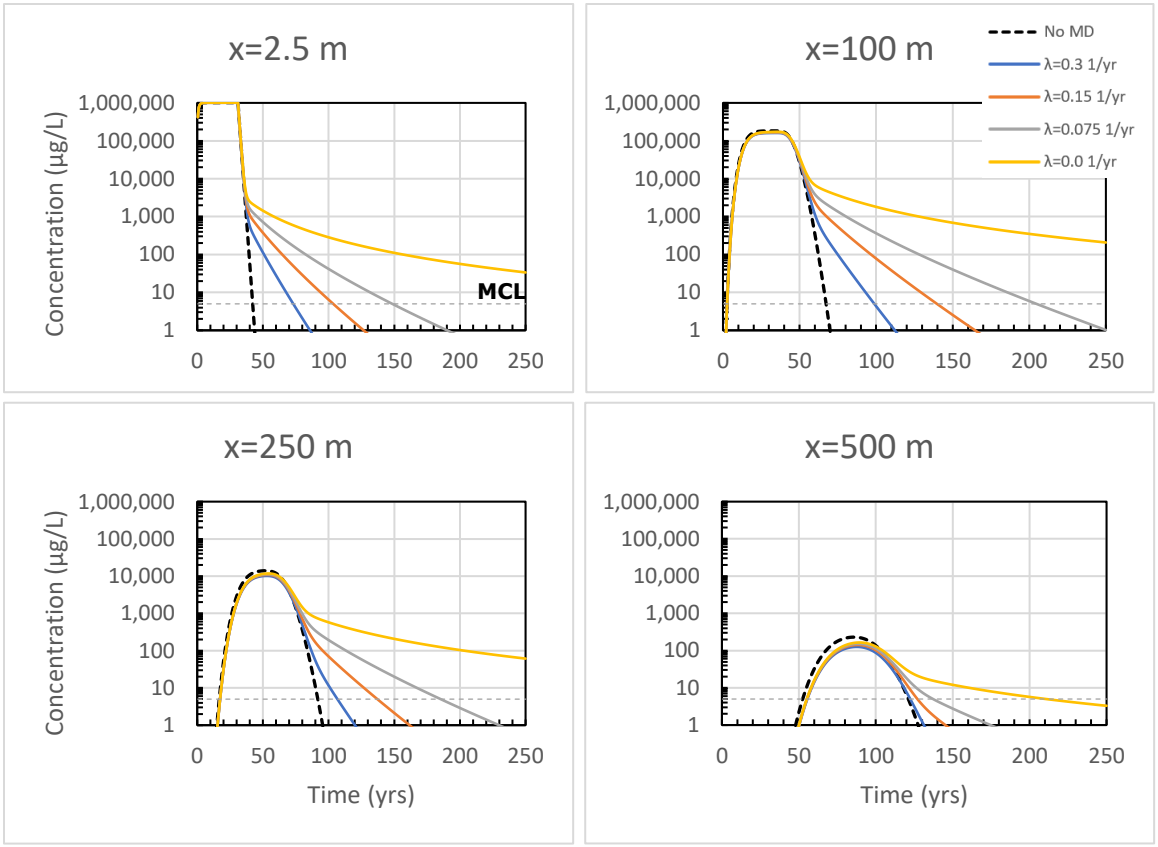

Figure 8: Comparison of TCE concentrations at different observation wells for models with varying decay rates in the underlying aquitard

3.5.2. Retardation Factor

The retardation factor describes the amount of sorption of contaminants to solids in the subsurface and is the ratio of the dissolved plus sorbed contaminant mass to the dissolved contaminant mass in the aqueous phase in a unit volume of aquifer or aquitard (Farhat et al., 2018). Some researchers suggest that retardation factors may be higher in the low *k* zones relative to the transmissive zones, which is supported by the presence of clay minerals which have been shown to have a larger sorption capacity than primary

minerals, and the presence of more organic material, which can lead to more sorption by organic solvents such as TCE (Jing et al., 2010).

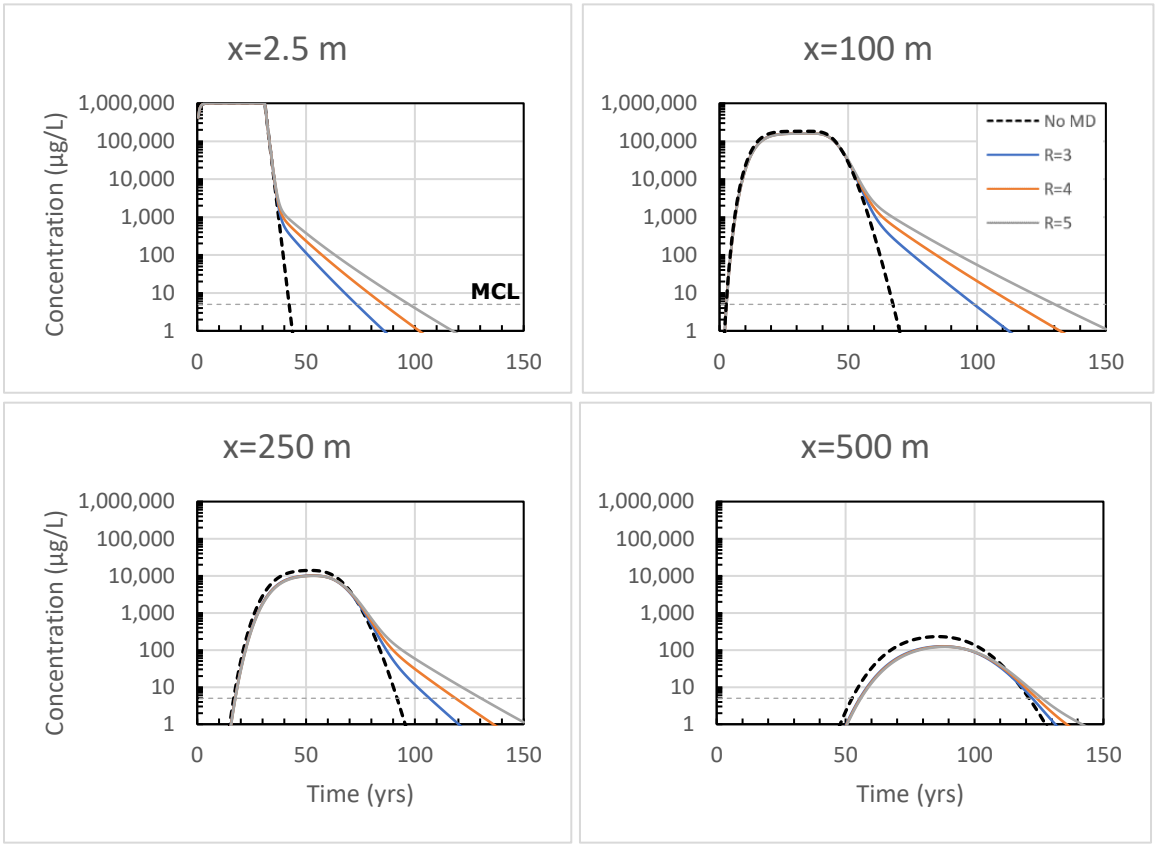

Figure 9: Comparison of TCE concentrations at different observation wells for models with varying retardation factor values in the underlying aquitard.

Figure 9 demonstrates the effect of higher sorption in the low *k* zone on back diffusion by varying the retardation factor. In the transmissive zone, the retardation factor is held constant and equal to 3. It is evident from the observation wells that plume tailing increases as the retardation factor increases. In all the wells minus the most downgradient

well, each increase in the retardation factor by one in the low *k* zone results in back diffusion that causes about 1-2 decades of additional plume tailing compared to the model where the retardation factor is the same in both the low *k* and transmissive zones.

It may seem counterintuitive that a higher retardation factor in the low *k* zone results in a larger back diffusion effect because more sorption will immobilize more contaminants; however, this process is not irreversible, and back diffusion will likely re-mobilize the sorbed contaminants. Additionally, a higher retardation factor will result in more contaminant mass being stored in the low *k* zones, and as a result, the back diffusion of those contaminants becomes relatively larger as the retardation factor increases.

All in all, the retardation factor in the low *k* zone should be considered when modeling matrix diffusion because it can result in back diffusion effects that range on the order of decades. The retardation factor can be used a fine-tuning parameter to calibrate models to field data if the sorption at a field site is not investigated.

3.6 Scenario 2: Heterogenous sand aquifer with an underlying clay aquitard

Following Muskus and Falta (2018), there are two main geometrical configurations for low permeability material. The first configuration is for a case with a semi-infinite aquitard that is adjacent to a high permeability aquifer. For this case, the aquifer is treated normally in the numerical formulation, and the matrix diffusion flux only occurs in the gridblocks that are adjacent to the low permeability material. This case was explored in the previous sections by using a homogenous sand aquifer and an underlying clay aquitard. The second configuration is the case of embedded low

permeability material or a fractured system. For this case, the volume fraction of the high and low permeability material in each gridblock must be specified, and the volume fraction is dependent on low permeability material geometry (Muskus and Falta, 2018). If a gridblock contains low permeability material, then the transmissive zone volume fraction (V_f) is less than 1.

The fully implicit numerical formulation of the transport equation used with the semi-analytical method incorporates matrix diffusion as a concentration-dependent source/sink term where in this term, the matrix diffusion flux is multiplied by the interfacial matrix diffusion area for the matrix diffusion mass flow rate (Muskus and Falta, 2018). The interfacial matrix diffusion area (A_{md}) and the characteristic average maximum diffusion length (L), defined as the average maximum depth or distance of diffusion into low permeability material, are also determined by the low permeability material geometry. Therefore, the semi-analytical method uses 3 geometric parameters when considering low permeability material within an aquifer. By considering that the volume of low permeability material in a gridblock should be equal to the product of the matrix diffusion area and the characteristic average maximum diffusion length, then the 3 geometric parameters can be related to one another using Equation 1, where for a total gridblock volume of V_i (Muskus and Falta, 2018),

$$V_i(1 - V_f) = A_{md}L \tag{1}$$

Therefore, in order to evaluate the back diffusion signal in cases where there is low permeability material embedded within an aquifer, these geometric parameters regarding matrix diffusion must be evaluated as well.

The next porous media scenario builds upon the previous model. Instead of a homogenous sand aquifer, a heterogeneous sand aquifer was assessed by adding embedded clay lenses to the aquifer in addition to the underlying aquitard. By adding clay lenses, more high permeability/low permeability interfaces are created where matrix diffusion can occur as shown in the conceptual model in Figure 10, and thereby possibly causing a stronger back diffusion signal than the underlying clay aquitard alone.

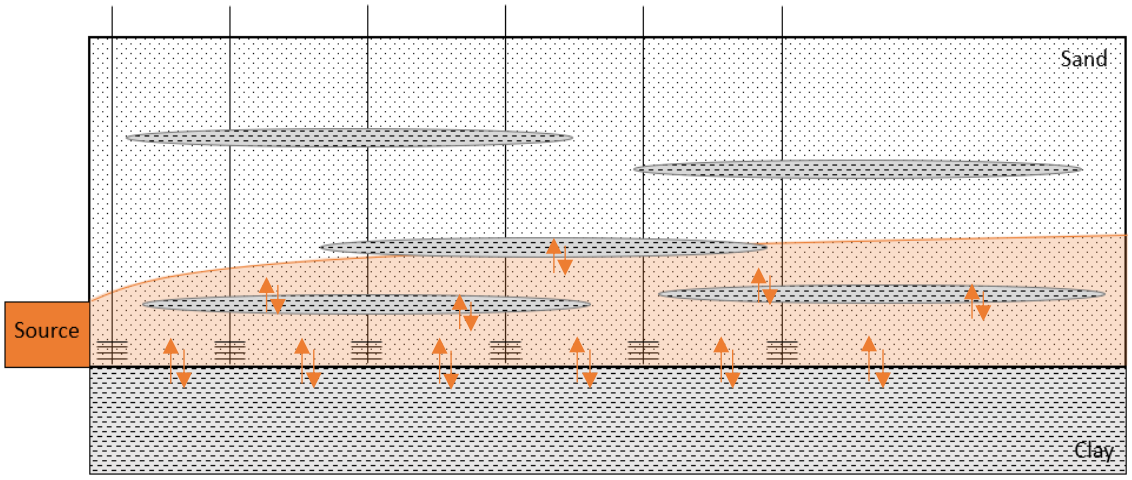

Figure 10: Cross-sectional view of conceptual model for a theoretical scenario of a heterogenous sand aquifer with an underlying clay aquitard.

Because of the geometric parameterization for embedded low *k* material, this analysis was divided into two cases: 1) a case with a diffusion length of 1 m and a smaller diffusion area and 2) a case with a diffusion length of 0.1 m and a larger diffusion area. The interfacial diffusion area is dependent on the amount of low permeability material in each gridblock, as show in Equation 1, and therefore will vary. The two cases for this scenario can be thought of as analogous to a field site with thick clay lenses (~2 m) and a field site with thin clay lenses (~0.2 m), respectively.

Both cases were evaluated for the effect of matrix diffusion on transport models with transmissive zone volume fractions of 25, 50, and 75%. The effect of matrix diffusion was again explored using monitoring wells across the plume length at the first gridblock from the centerline (y=2.5 m) with 2 m screen lengths located at the bottom of the model in the gridblock nearest the aquitard. Because each gridblock is treated as having the same amount of embedded low *k* material, the maximum back diffusion signal will still be in gridblocks nearest the aquitard.

The source, transport, and natural attenuation parameters used in the base model all remain the same (Table 1), and the only change is the addition of embedded low permeability material to the aquifer. The geometric parameters used in these cases are shown in Tables 2 and 3. The transmissive zone Darcy velocity was held constant throughout this analysis, and the total average Darcy velocity varied based on transmissive zone volume fraction.

Table 2: Geometric parameters used in embedded low *k* case with a diffusion length of 1 m and a total gridblock volume of 50 m^2.

Geometric Parameters for L=1 m			
V_f (%)	25	50	75
A_{md} (m^2)	37.5	25	12.5

Table 3: Geometric parameters used in embedded low *k* case with a diffusion length of 0.1 m and a total gridblock volume of 50 m^2.

Geometric Parameters for L=0.1 m			
V_f (%)	25	50	75
A_{md} (m^2)	375	250	125

3.6.1. Results

In Figure 11, four observation wells show TCE concentrations scaled to the initial concentration of 1,100 mg/L over a period of 150 years for a case where the diffusion length is 1 m for the embedded low permeability material. Because the transmissive zone Darcy velocity is held constant, the No MD models for each volume fraction are the same at each well. From the models, it is evident that as the volume of low permeability material within the aquifer increases, the difference between the MD models and the No MD models increases, and more plume tailing is observed. At x=2.5 m, the monitoring well shows that the addition of embedded low *k* material to the aquifer results in about

39, 45, and 54 more years for concentrations to decline below the MCL (C/C_o =4.5x10^{-6}) for transmissive zone volume fractions of 75, 50, and 25%, respectively. This is ~10-25 more years of plume persistence than from the aquitard alone. At x=50 m, plume persistence is observed to be even longer, but moving downgradient past 50 m, the observed tailing starts to lessen.

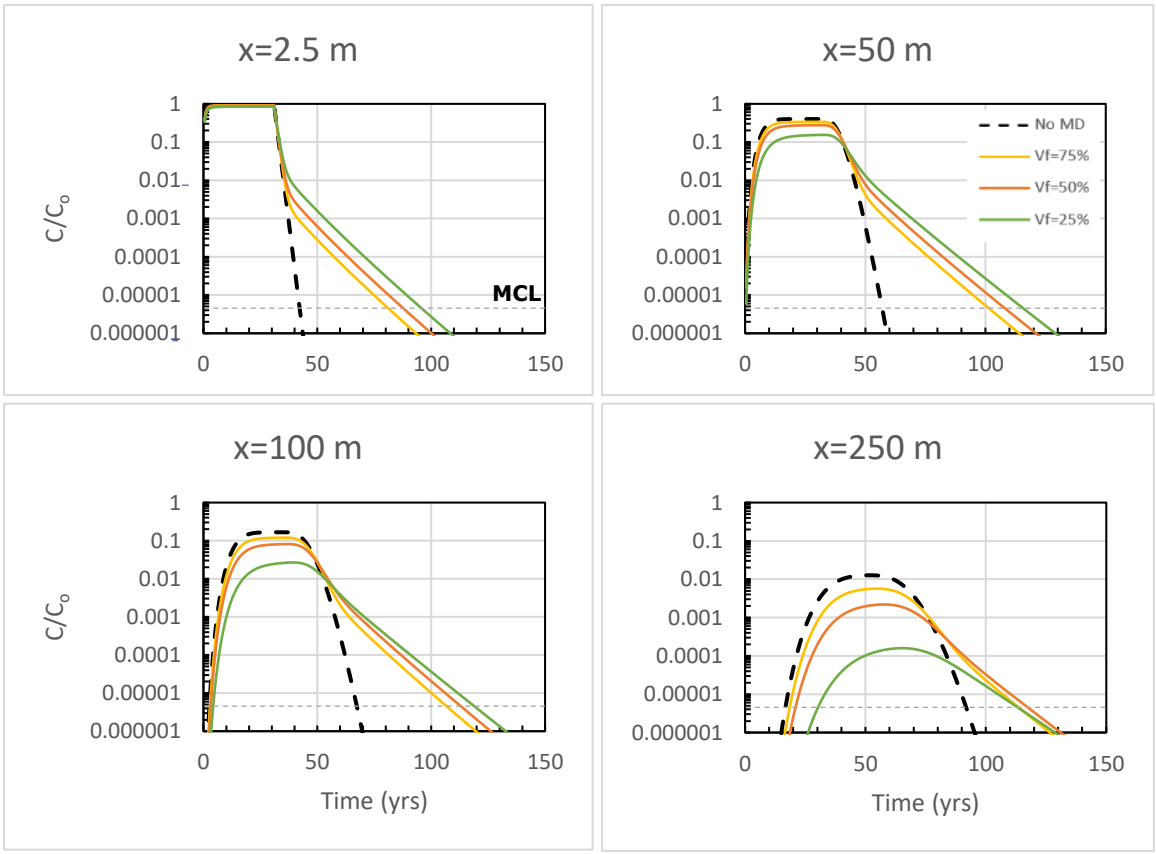

Figure 11: Comparison of scaled TCE concentrations from MD and No MD models at different observation wells for varying amounts of interbedded low *k* material and a diffusion length of 1 m.

As demonstrated before, the initial source concentration affects the magnitude at which the back diffusion signal is observed. The initiation of plume tailing can be marked by the concentration at which a MD model first diverges past a No MD model, and for this study, this point is being defined as 1 year of tailing. In Figure 11, for V_f=25%, the start of plume tailing occurs when C/C_o=0.01 at x=2.5 m, 0.03 at x=50 m, and 0.009 at x=100 m. These ratios provide insight about the magnitude at which back diffusion occurs. This is achieved by dividing the MCL by the concentration ratio at which plume tailing begins, and therefore, $MCL/(C/C_o)$ will yield the upper limit for the source concentration where back diffusion only occurs at or below the MCL.

For example, in the first three monitoring wells for V_f =25%, plume tailing begins on average at C/C_o=0.02, and therefore, for sites with an initial source concentration of 250 μg/L (50 times the MCL) or lower, back diffusion will only occur at concentrations below the MCL. For V_f =75%, the plume tailing begins when C/C_o=0.002, 0.008, and 0.006 for monitoring wells at x=2.5, 50, and 100 m, respectively. Therefore, on average, back diffusion is not significant for this volume fraction when the initial concentration is 1000 μg/L (200 times the MCL) or lower.

Moving to the furthest downgradient well at x=250 m, however, plume tailing occurs at concentration ratios that are magnitudes lower for each volume fraction relative to the upgradient wells. Because the effect of back diffusion is dependent on well location and the amount of embedded low permeability material, it is difficult to determine a general rule of thumb for assessing back diffusion risk for a heterogenous aquifer with a diffusion length of 1 m and the parameters used. Nevertheless, in

comparison to the homogenous aquifer case, an initial source concentration that is 1,000 times the MCL will likely result in significant back diffusion effects that would impact remediation timelines, especially at locations near the source. For back diffusion to possibly be considered negligible, the initial source concentration would need to be in the magnitude of 10 times the MCL for sites with large volumes of embedded low *k* material and 100 times the MCL for sites with smaller volumes.

The second case in the heterogenous aquifer scenario, where L = 0.1 m, is shown in Figure 12. At x=2.5 m, the monitoring well shows that the addition of low *k* material to the aquifer results in about 33, 36, and 44 more years for concentrations to decline below the MCL for transmissive zone volume fractions of 75, 50, and 25%, respectively. In general, a diffusion length of 0.1 m results in less plume tailing than a length of 1 m. However, there is an exception. For a case with V_f=25% and L=0.1 m, significant plume tailing is observed in monitoring wells x=50 m and x=100 m that extends further than any model with L=1 m. Although concentrations are not as high, this case can sustain concentrations above the MCL for decades in wells near the center of the plume, and therefore, presents a very strong risk for back diffusion.

In comparison to the L=1 m case, three significant differences can be observed that give insight into how the geometry of the embedded low permeability material affects the back diffusion signal. First, plume tailing is evident very soon after source removal when L=0.1 m, which is most obvious in the monitoring well at x=2.5 m. For the shorter diffusion length, the diffusion area is relatively larger, resulting in a diffusive mass flow that is faster. Additionally, since the contaminant does not travel very

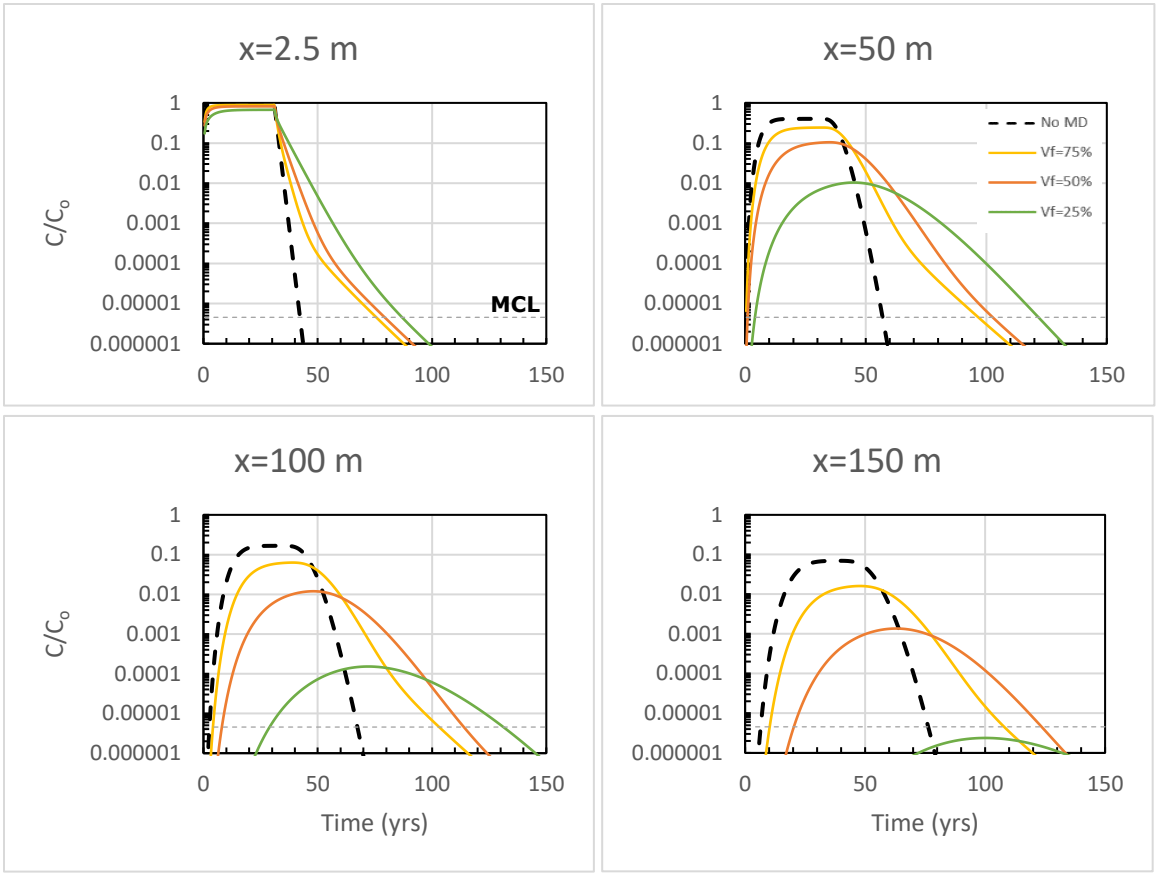

Figure 12: Comparison of scaled TCE concentrations from MD and No MD models at different observation wells for varying amounts of interbedded low *k* material and a diffusion length of 0.1 m.

far into the low permeability material, the mass in the low permeability zones is depleted more quickly for the shorter diffusion length. This depletion could cause multiple concentration gradient reversals over the lifetime of a plume. In Figure 12, the MD models at x=2.5 m show rates of decline that vary over time after source removal. This might be indicative of the dynamic interplay occurring at the high permeability/low permeability interfaces for the shorter diffusion length. For the longer diffusion length, the interfacial area between the high permeability and low permeability zones is smaller,

and therefore, there are less places for diffusion to occur. This results in a slower diffusive mass flow Because the initial concentration gradient reversal occurs at the same time for each case, the difference in the back diffusion signal is a result of the differing diffusive mass flows caused by the geometric parameterizations.

The second difference between the diffusion lengths is that for L=0.1 m, the diffusion signal is first observed at an earlier time, and as a result, it occurs at relatively higher concentrations. At the first monitoring well at x=2.5 m in Figure 12, the MD model with V_f =25% starts to tail out at C/C_o=0.3, and the MD model with V_f =75% tails out at C/C_o=0.05. This suggests that back diffusion will only be insignificant at near source locations for initial source concentrations less than 17 μg/L (3.4 times MCL) and 100 μg/L (20 times MCL), respectively. For V_f =75%, the concentration ratio for plume tailing initiation fluctuates over about 1 magnitude across the plume length. However, for V_f =25%, the start of plume tailing drops by many magnitudes moving downgradient. Therefore, for near source locations, the back diffusion signal occurs about 1 magnitude lower than the case with L=1 m, and as a result, only a very low initial source concentration in the magnitude of the MCL for V_f=25% and in the magnitude of 10 times the MCL for V_f=75% could result in negligible back diffusion effects. Moving downgradient, the observation of the back diffusion signal is highly dependent on well location and the amount of embedded low permeability material in the aquifer, and therefore the source concentration at which back diffusion occurs below the MCL will vary greatly.

Lastly, the third difference is that for L=0.1 m, the contaminant plume is shorter in length, and as a result, concentrations are generally lower in magnitude relative to models with a longer diffusion at length locations 50 m downgradient of the source and beyond. Figure 12 shows that at x=50 m, the three MD models are at lower concentrations than the No MD model before source removal, which is likely due to increased rates of forward diffusion and a decreased transmissive zone volume fraction. At x=150 m, the model with V_f =25% shows a plume that persists for decades, however, the plume is only sustained at concentrations that are about 1 millionth of the initial source concentration. For an initial source concentration at solubility, this only a few μg/L.

The contour plots in plan view in Figure 13 show the contrast in the plume shapes for the different transmissive zone volume fractions of 75% and 25% for L= 1 m and Figure 15 shows the same for L=0.1 m. As determined before, the lower volume fractions result in shorter plume lengths, which can be explained by decreased amounts of mass leaving the source, which is proportional to the volume fraction, and increased forward diffusion rates. Both processes result in less contaminant mass in the transmissive zone. A lower diffusion length also results in a shorter plume length, which is likely a result of the faster diffusive mass flow that causes more mass to be pulled out of the transmissive zone. Figures 14 and 16 show TCE contours in cross-section for the different diffusion lengths. At the bottom of the aquifer, the interplay between the aquitard and the aquifer is still noticeable by the kink in the contours. However, the addition of embedded low permeability material causes a small change in the plume shapes by decreasing the signal

from the aquitard, which is indicated by the upstream plume tail. This "tail" is not part of the main bulk of the plume and is a result of higher back diffusion fluxes from the aquitard near the source zone. The embedded low *k* material, which acts as a secondary source from within the plume, causes the upstream plume tail to be less noticeable, and the tail decreases with increasing embedded material.

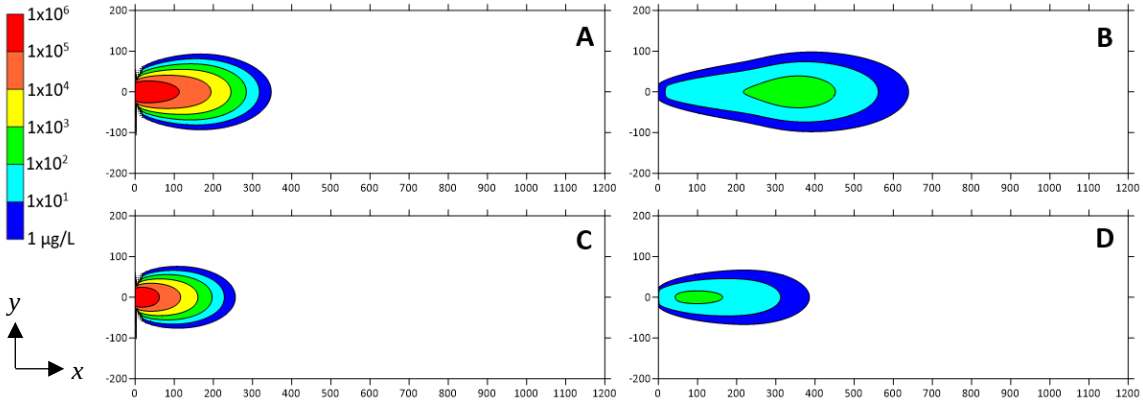

Figure 13: Comparison of REMChlor-MD TCE concentration contours in *xy* plane (at lowest gridblock) for MD models with embedded low *k* material and a diffusion length of 1 m. A) V_f=75% at t=30 yrs; B) V_f=75% at t=90 yrs; C) V_f=25% at t=30 yrs; and D) V_f=25% at t=90 yrs.

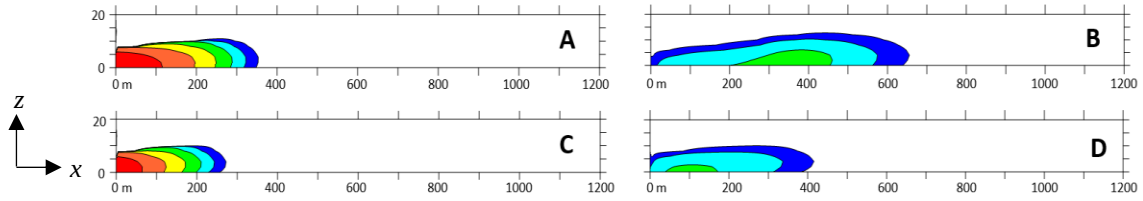

Figure 14: Comparison of REMChlor-MD TCE concentration contours in *xz* plane (at first gridblock from center) for MD models with embedded low *k* material and a diffusion length of 1 m. A) V_f=75% at t=30 yrs; B) V_f=75% at t=90 yrs; C) V_f=25% at t=30 yrs; and D) V_f=25% at t=90 yrs.

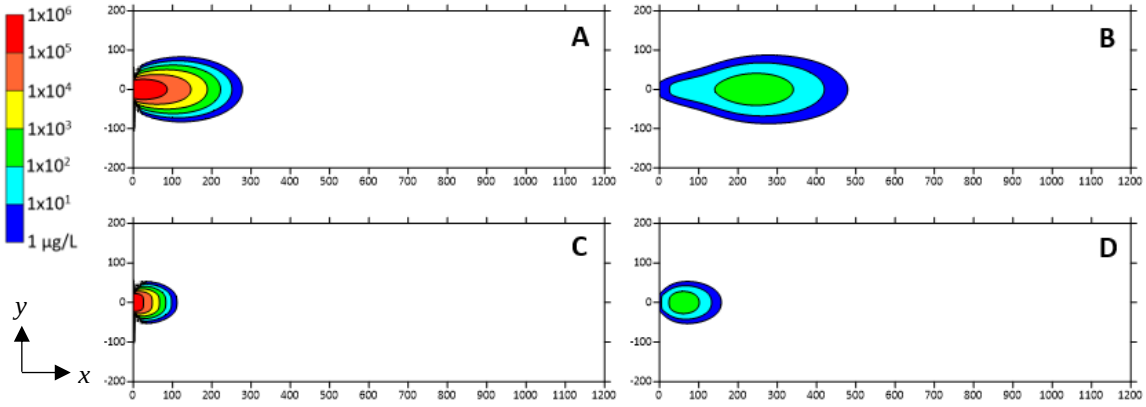

Figure 15: Comparison of REMChlor-MD TCE concentration contours in *xy* plane (at lowest gridblock) for MD models with embedded low *k* material and a diffusion length of 0.1 m. A) V_f=75% at t=30 yrs; B) V_f=75% at t=90 yrs; C) V_f=25% at t=30 yrs; and D) V_f=25% at t=90 yrs.

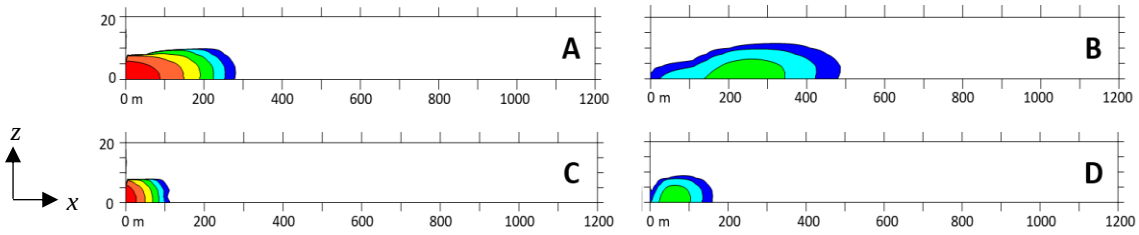

Figure 16: Comparison of REMChlor-MD TCE concentration contours in *xz* plane (at first gridblock from center) for MD models with embedded low *k* material and a diffusion length of 0.1 m. A) V_f=75% at t=30 yrs; B) V_f=75% at t=90 yrs; C) V_f=25% at t=30 yrs; and D) V_f=25% at t=90 yrs.

3.7 Conclusions

In this chapter, the back diffusion signal was first characterized through the analysis of a theoretical case with a homogenous sand aquifer and an underlying aquitard. The effect of back diffusion was shown by the comparison of MD and No MD models,

and the signal was identified by “plume tailing” in the MD model, which is observed when a model sustains aquifer concentrations above the MCL longer than a model without matrix diffusion.

Next, the observation of the back diffusion signal was shown to be dependent on observation well location. To observe the strongest back diffusion signal in any system, a monitoring well should be installed and screened near the back diffusion source and near the highest concentrations in the plume (i.e. near the initial source zone and near the plume centerline).

For a system with a constant source, the observation of the back diffusion signal was shown to be dependent on the initial source concentration. For the case of a homogenous sand aquifer with an underlying clay aquitard and with the parameters used, an initial concentration that is 1,000 times the MCL will result in back diffusion that occurs at magnitudes below the MCL. Above the MCL, the MD and No MD models will be identical.

The low *k* zone parameterization was evaluated, and it was found that the decay rate is a key parameter for determining the longevity of plume persistence and will determine whether aquifer concentrations will be sustained above the MCL for either a few years or for many centuries due to back diffusion. If the retardation factor in the low *k* zone is increased by one or two values, back diffusion increases and will result in additional plume tailing in the magnitude of decades.

For the theoretical case of a heterogenous sand aquifer with an underlying aquifer and with the parameters used, the source concentration at which the back diffusion is

observable above the MCL is 1 to 3 orders of magnitude lower than the homogenous case; however, this value varies greatly by the observation well location, the amount of embedded low *k* material, and the parameterization that characterizes the low *k* material geometry. For locations close to the source, a few generalizations can be made. For an aquifer with a lower volume of interbedded clay material, back diffusion would occur at or below the MCL with initial source concentrations in the magnitude of 100 times the MCL for a longer diffusion length and with initial source concentrations in the magnitude of 10 times for a shorter diffusion length. For an aquifer with a higher volume of interbedded clay material, back diffusion would occur at or below the MCL with initial source concentrations in the magnitude of 10's of times the MCL for a long diffusion length. For a short diffusion length, back diffusion will almost always occur above the MCL near the source.

Lastly, the geometric parameterization for low *k* material affects the behavior of back diffusion. A shorter diffusion length results in larger diffusive mass flows, which creates a stronger back diffusion response at early times after source removal. Because of the larger diffusive mass flow, more contaminant mass leaves the transmissive zone and the plume does not travel as far downgradient. A longer diffusion length results in a slower diffusive mass flows and a more gradual back diffusion response, which is comparable to the effect of back diffusion from a thick aquitard.

4. SEMI-ANALYTICAL SIMULATION OF MATRIX DIFFUSION IN POROUS MEDIA CASES WITH A DECAYING SOURCE

4.1 Methods

A description of the relationship between the source mass and the contaminant discharge that follows was taken from (Falta et al. 2007a). The contaminant discharge from a source zone is equal to the product of the flowrate of water passing through the source zone and the average concentration of contaminant in that water. A mass balance on the source results in:

$$\frac{dM}{dt} = -Q(t)C_s(t) - \lambda_s M \tag{2}$$

where Q(t) is the flowrate, C_s(t) is the time-dependent source dissolved concentration (flow averaged), λ_s is the source decay rate by processes other than dissolution, and M is the mass remaining in the source zone with time. This source mass/source discharge relationship can be roughly approximated by a simple power function (Rao and Jawitz, 2003; Parker and Park, 2004; Zhu and Sykes, 2004; Falta et al., 2005).

$$\frac{C_s(t)}{C_0} = \left(\frac{M(t)}{M_0}\right)^{\Gamma} \tag{3}$$

One case that can occur for Equation 2 is when Γ=1 and λ_s =0, thereby making the differential equation linear and allowing for integration to get a simple exponential decay solution (Newell et al., 1996; Parker and Park, 2004; Zhu and Sykes, 2004):

$$M(t) = M_0 e^{-(\frac{QC_0}{M_0})t} \quad (4)$$

and

$$C_s(t) = C_0 e^{-(\frac{QC_0}{M_0})t} \quad (5)$$

As a result of dissolution, both the source mass and the source discharge will decline exponentially with time when Γ=1. The apparent source decay rate due to dissolution is QC_o/M_o, resulting in a half-life of $0.693M_o/(QC_o)$ (Newell and Adamson, 2005).

For each theoretical porous media scenario evaluated so far, the source behavior has been characterized as Γ=0, and therefore, the source discharge (concentration) is constant until the source is fully depleted, either by dissolution or remediation. However, this is an idealized approximation of source zone dissolution. Laboratory and field studies have shown that aquifer concentrations in real source zones decrease gradually instead of instantaneously (Rao and Jawitz, 2003). Therefore, it is more realistic to use a source the declines over time to better simulate the more gradual decline of contaminant concentrations in an aquifer.

Past work has shown that many sites will have a source function exponent greater than zero, with younger sites having a Γ<1 and older sites having a Γ>1 (Falta et al., 2007a). For this analysis, the effect of back diffusion will be evaluated using a source with exponential decay due to dissolution (Γ=1). When using a source function of Γ=1,

the source is never completely depleted, and the source discharge is always greater than zero. This could have a significant impact on not only the timing of concentration gradient reversals but also the occurrence of any gradient reversals. Previous studies have shown that as Γ increases, the risk of back diffusion decreases (Brown, 2012, Yang et al., 2016).

A few studies have explored the relative contributions of source zone dissolution and matrix diffusion to source zone and plume persistence (Seyedabbasi et al., 2012; Yang et al., 2016); however, these studies focused more on the dissolution dynamics and did not explore in detail the effects of remediation on back diffusion. In 2012, Brown et al. demonstrated how the timing of remediation by means of partial source mass reduction impacts the long-term risk of back diffusion by using one dimensional analytical solutions to characterize the concentration profiles in an aquitard. This study found that the earlier remediation occurs, the greater the reduction in aquifer concentrations, and as a result, the long-term risk of back diffusion reduces. However, this study neglected dispersion and degradation in the aquifer and degradation in the aquitard.

The semi-analytical method for modeling matrix diffusion provides the opportunity to further explore how source zone remediation affects back diffusion. For a source mass that is constant, any amount of source removal results in a decrease in the constant source discharge, which is known as a "step function" model. This only affects the magnitude of the concentrations in the model and decreases that amount of time it takes for source depletion to occur. A decaying source mass, however, with remediation

that results in less than 100% source mass removal may have a significant impact on the concentration gradients that drive back diffusion as the remaining source mass continues to feed the plume. In most cases, it is impossible to completely remove the source mass at a contaminated site and often, a source mass removal of 90% is a more achievable remediation goal.

4.2 Scenario 1: Homogenous sand aquifer with an underlying clay aquitard

For this study, the original base model for the porous media scenarios was used (Table 1). The theoretical scenario of a homogenous sand aquifer with an underlying clay aquitard was assessed first. The source strength function was changed from $\Gamma=0$ to $\Gamma=1$, and the source mass removal was explored. The apparent source decay rate due to dissolution was also varied during this analysis. For the purpose of making comparisons with previous models with a constant source, the initial source concentration and the flowrate were held constant, and only the initial source mass was varied. A source mass of 75,000 kg was used for cases with no source decay, and source masses of 12,700 kg, and 7,500 kg were used for source decay rates of 0.06 yr^{-1} and 0.12 yr^{-1}, respectively.

4.2.1. Results

Figure 17 shows four observation wells with scaled TCE concentrations for MD and No MD models with three different rates of source decay due to dissolution. The source is completely removed after a loading period of 30 years. In the first monitoring well at x=2.5 m, back diffusion results in 31 additional years for concentrations to decline below the MCL for the model with no source decay. For a source decay of 0.06 yr^{-1}, back diffusion results in 22 years of plume tailing, and for a decay of 0.12 yr^{-1}, it results in 15

years. At x=100 m, the same pattern is observed, with back diffusion resulting in an additional 31, 24, and 18 more years for concentrations to decline below the MCL for models with source zone decay rates of 0 yr^{-1}, 0.06 yr^{-1}, and 0.12 yr^{-1}, respectively. Therefore, it is evident that back diffusion decreases with a decaying source in comparison to a constant source, which can be explained by the relative decrease in overall aquifer concentrations.

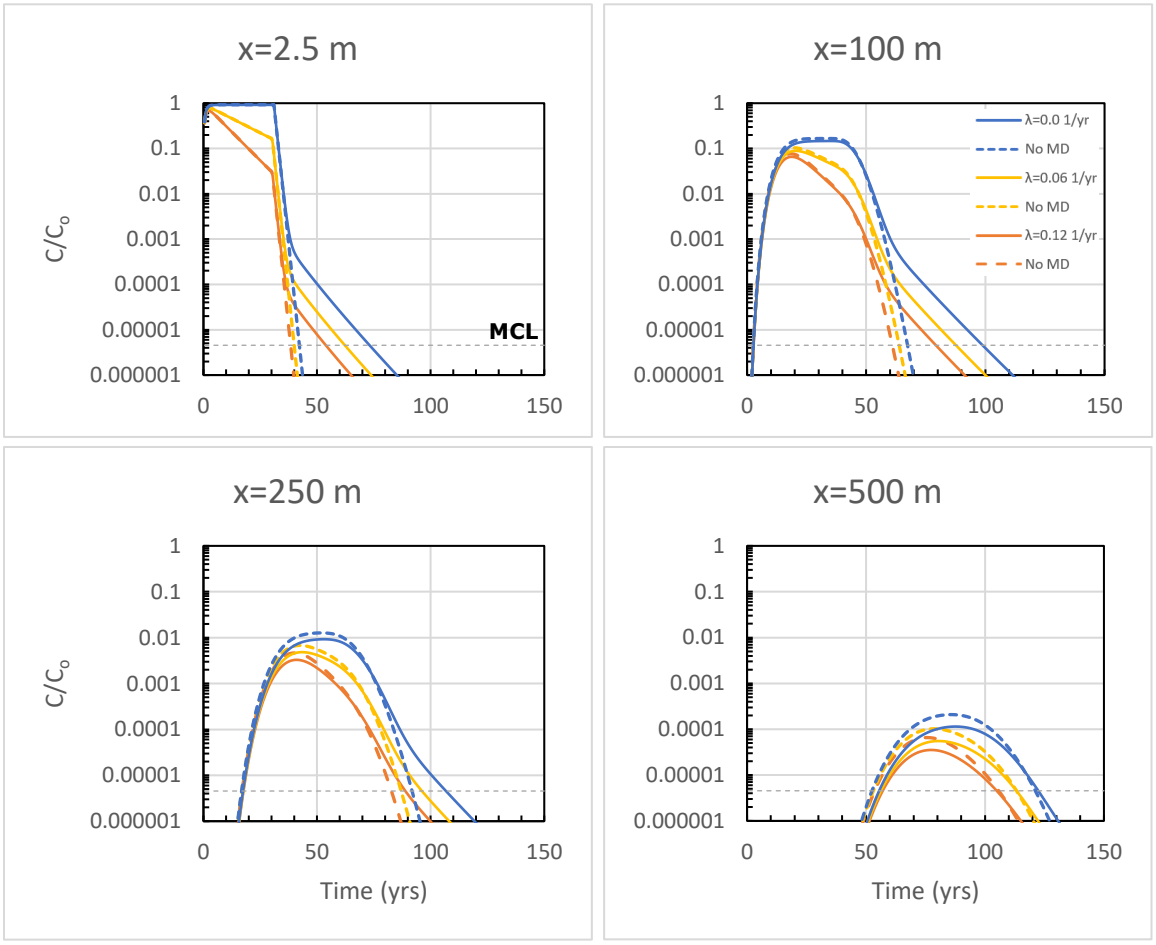

Figure 17: Comparison of scaled TCE concentrations from MD and No MD models at observation wells for different source zone decay rates (dissolution).

It has already been shown that a large source concentration is critical for observing back diffusion above the MCL for cases with a constant source. Although the source concentration determines the upper limit of aquifer concentrations, for cases with $\Gamma=1$, the dynamics of source dissolution cause the effect of the source concentration on back diffusion to be more ambiguous. Equation 4 showed how the initial source concentration, the initial source mass, and the groundwater flowrate are related to determine the source zone decay rate due to dissolution. Therefore, as C_o decreases, the dissolution rate decreases as well. The effect of the source zone decay rate on back diffusion is shown in Figure 17. The case with the lower decay rate of 0.06 yr^{-1} results in a source that sustains higher concentrations in the plume in comparison to the case with the higher decay rate of 0.12 yr^{-1}. Because of this, when source zone removal occurs and back diffusion begins, the resulting plume tailing occurs at higher concentrations relative to the case with the higher decay rate.

Therefore, contrary to the cases when $\Gamma=0$, higher initial source concentrations might actually result in less of an effect from back diffusion due to a resulting lower decay rate by dissolution. However, it would be inaccurate to make this assumption solely on the initial source concentration alone. Instead, the source decay rate, as determined by the site conditions, should be used in conjunction with C_o to evaluate potential back diffusion risks above the MCL. The initial source concentration determines the upper limit of aquifer concentrations while the source decay rate will determine how long those concentrations will be sustained in the aquifer. As the source decay rate decreases and approaches zero as shown in Figure 17, the effects of back diffusion will

increase and become comparable to the effects observed in models with a constant source.

4.2.2. Partial Source Zone Remediation

Figure 18 shows a comparison of MD and No MD models with 99% source mass removal after 30 years for a case with Γ=0 and a case with Γ=1. For the decaying source case, the decay rate due to dissolution is 0.12 yr^{-1}. In all four monitoring wells, the plume tailing in the constant source models is nearly identical to the case when 100% of the source mass is removed. With a starting source mass of 75,000 kg, the 1% mass remaining after 30 years depletes shortly after remediation as a result of dissolution. The decaying source models, however, show differing results.

At x=2.5 m, the monitoring well shows only minimal differences between the MD and No MD models (Figure 18). The MD model shows TCE at slightly higher concentrations than in the No MD model after source mass removal; however, no significant differences are observed between the two models and the remediation timeline for both is the same. In the wells at x=100 and 250 m, back diffusion is observed, and it adds about 13 years and 5 years, respectively, to the remediation timeline. At x=100 m, the difference between the MD and No MD models is about 5 years less than the plume tailing observed in the MD model with complete source removal (Figure 17). At x=250 m, however, the plume tailing is about the same for both cases. Therefore, remediation that results in 99% source mass removal has an effect on the back diffusion signal that varies with location with respect to the source.

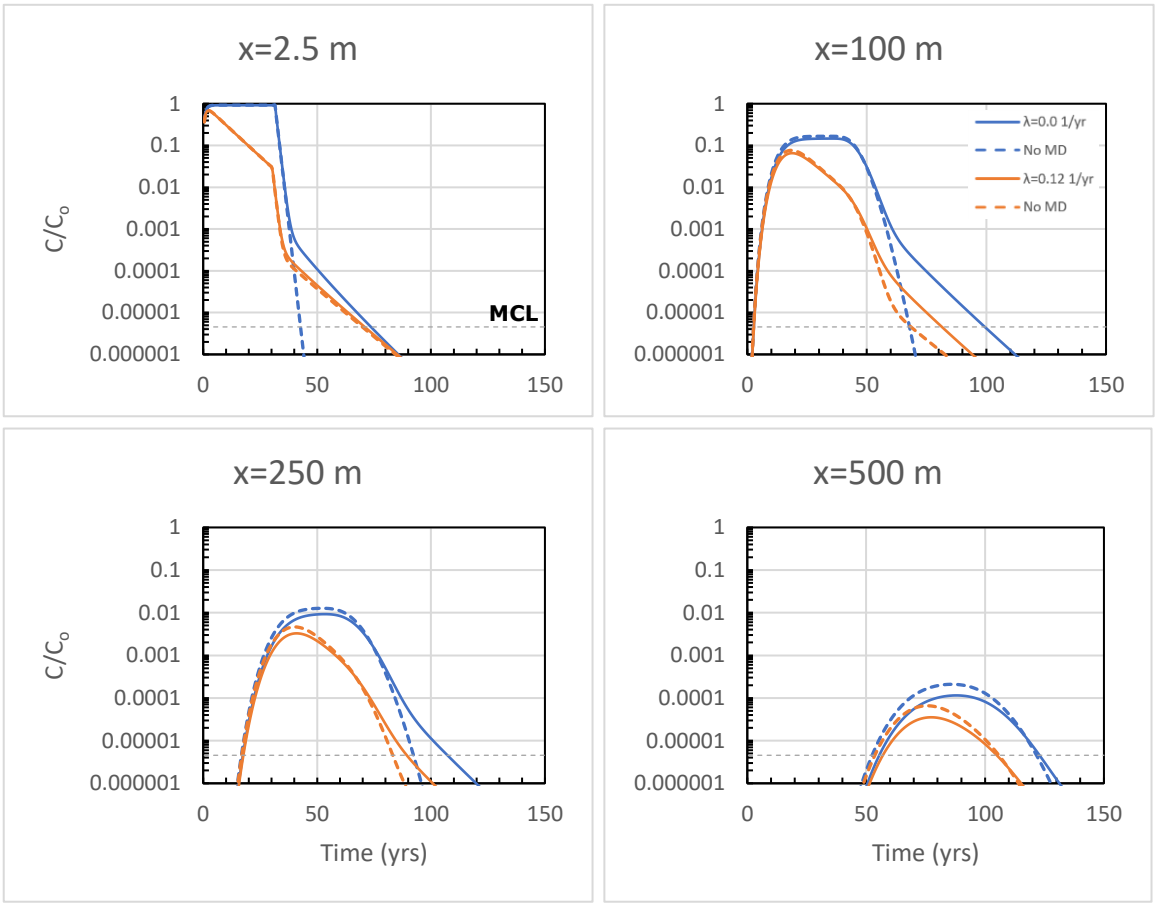

Figure 18: Comparison of scaled TCE concentrations at observation wells from MD and No MD models with 99% source zone remediation and varying source zone decay rates (dissolution).

Remediation that results in 99% source mass removal is still an optimistic remediation goal, and therefore, cases with 90% source mass removal were evaluated in Figure 19 for both constant and decaying source models. For the constant source case, the source removal of 90% results in source depletion that take a few years longer than 99% removal; however, the overall amount of plume persistence in the MD models is comparable to what was observed for the 99% source mass removal case (Figure 18). For the decaying source case, minimal plume tailing is observed across the plume length. At

x=2.5 m, no differences between the MD and No MD models is observed. Further downgradient, it takes two additional years for concentrations to decline below the MCL at x=100 m and 5 more years at x=250 m, and no tailing is observed in the monitoring at x=500 m.

Therefore, for cases with source mass removals less than 100% and the parameters used, the highest risk for back diffusion is not near the source but instead further downgradient. For the monitoring wells in this experiment, back diffusion was observed to be greatest in a well 100 m downgradient for a 99% source mass removal and 250 m downgradient for a 90% removal. There are two possible explanations for why back diffusion is less significant near the source. First, because complete source depletion never occurs when the source is characterized by $\Gamma=1$, the source continues to feed the plume, albeit at low concentrations, for the entire duration of the model timeframe. At early times when concentrations are still high, the remaining source mass affects the concentration gradients that drive back diffusion.

Second, as the source continues to feed the plume overtime, TCE degrades in both the aquifer and the aquitard at the same rate. The combination of the delay in a concentration gradient reversal and the overall declination of concentrations in both the aquifer and aquitard cause back diffusion to be insignificant near the source. At locations downgradient of the source, back diffusion is observed because the plume is not in direct contact with the remaining source, and as a result, aquifer concentrations are able to degrade to low enough concentrations that a gradient reversal occurs, thereby triggering back diffusion.

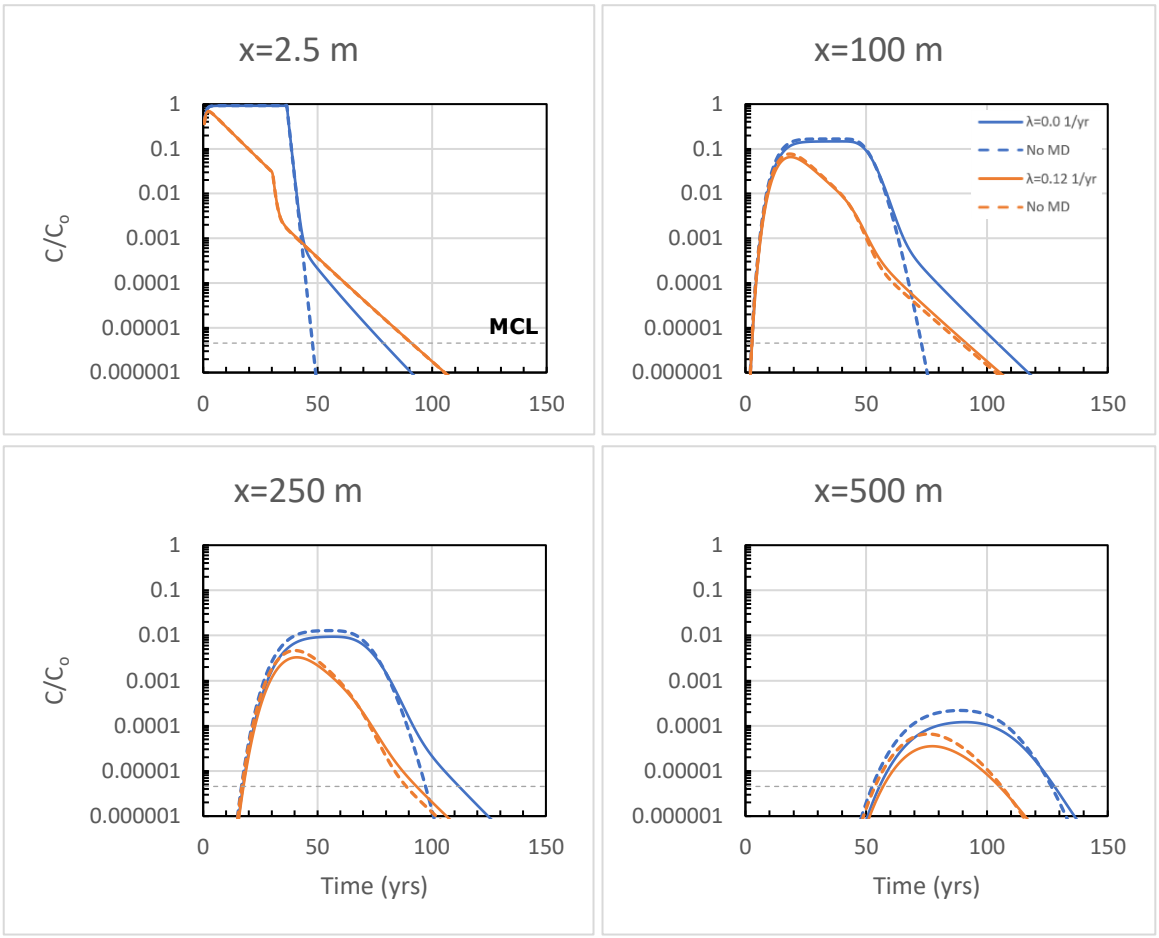

Figure 19: Comparison of scaled TCE concentrations at observation wells from MD and No MD models with 90% source zone remediation and varying source zone decay rates (dissolution).

Figure 20 show contour plots in plan view for MD and No MD models for the case of Γ=1 and 90% source mass removal. One important observation to take away from the contour plots in plan view is that the upgradient ends of the plumes for both the MD and No MD models closely resemble each other. This upgradient tail was seen previously as a result of back diffusion from an aquitard in Figures 3 and 4 for the case of a homogeneous aquifer with an underlying aquitard with a constant source. The plume's

connectedness to the source, whether it is to the initial source or to the secondary source of the aquitard due to back diffusion, shows that the plume is still being fed.

The cross-sections of the plumes in Figure 21 confirms that matrix diffusion is occurring at the aquifer/aquitard interface, as shown by the kink in the contour lines at the bottom of the model. However, the plots do not provide any additional insight for why back diffusion is so low. Since back diffusion is minimal for the case of 90% source mass removal, this observed upstream tail is a result of the 10% source mass remaining in the subsurface. The contour plots, therefore, suggest that in some cases, plume persistence can be explained by residual source mass that is left behind after remediation.

Additionally, looking back at the No MD models in Figures 17 and 18, a residual source mass produces a model curve that actually resembles the “plume tailing” that is indicative of the back diffusion signal. Further inspection shows that the decrease in the effect from back diffusion seen in cases with partial source zone remediation is mostly due to the residual source mass dominating the overall plume tailing signal, as shown by the tailing observed in the No MD models. This presents the complicated problem when evaluating field data in a monitoring well for a site that has a risk for back diffusion because as shown by the contour plots and the TCE concentration profiles, the plume tailing signal due to residual source mass can look similar to the plume tailing signal due to back diffusion, and the relative contributions to overall plume persistence can vary.

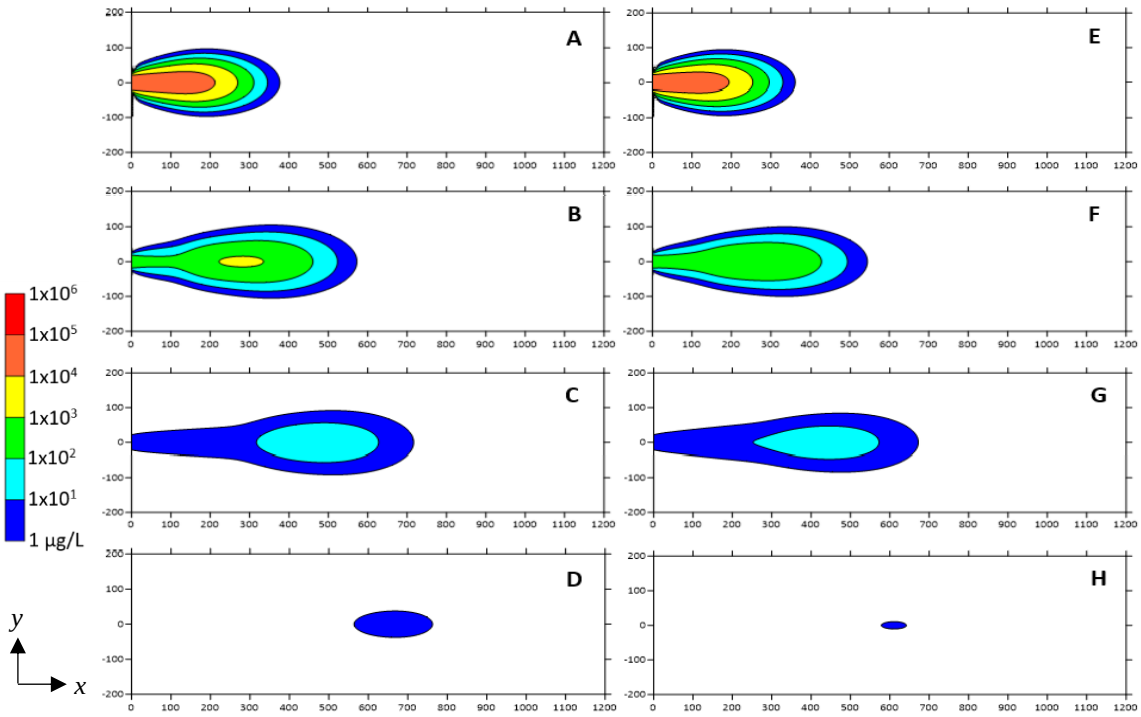

Figure 20: Comparison of REMChlor-MD TCE concentration contours in *xy* plane (at lowest gridblock) for No MD and MD models with a decaying source and 90% source zone remediation. A-D: No MD contour plots. A) t=30 yrs; B) t=60 yrs; C) t=90 yrs; D) t=120 yrs. E-H: MD contour plots. E) t=30 yrs; F) t=60 yrs; G) t=90 yrs; H) t=120 yrs.

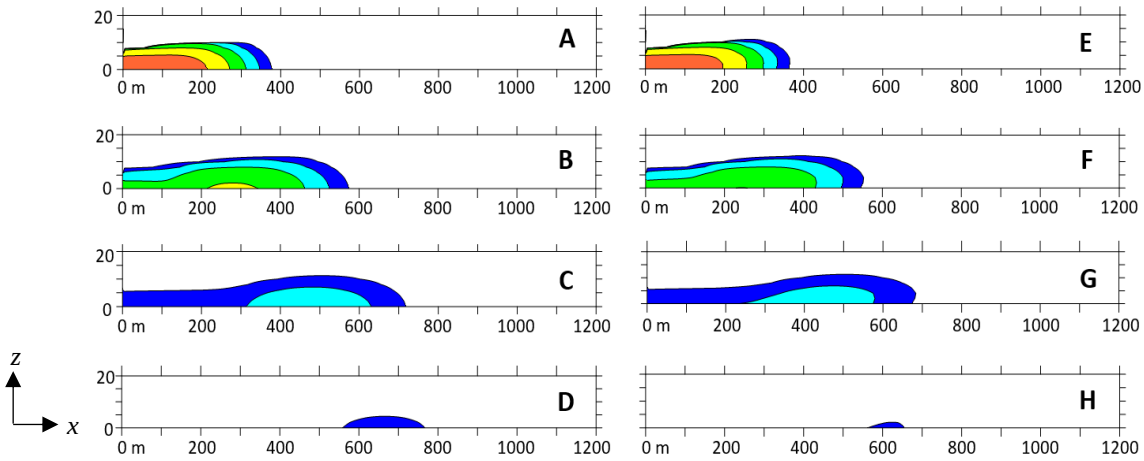

Figure 21: Comparison of REMChlor-MD TCE concentration contours in *xz* plane (at first gridblock from center) for No MD and MD models with a decaying source and 90% source zone remediation. A-D: No MD contour plots. A) t=30 yrs; B) t=60 yrs; C) t=90 yrs; D) t=120 yrs. E-H: MD contour plots. E) t=30 yrs; F) t=60 yrs; G) t=90 yrs; H) t=120 yrs.

4.3 Scenario 2: Heterogenous sand aquifer with an underlying clay aquitard

It has already been shown that the back diffusion signal decreases as Γ increases, and the signal also decreases as the source decay rate increases. Additionally, using theoretical conditions for a homogeneous sand aquifer and an underlying clay aquitard, a remediation effort that results in less than 100% source mass removal was shown to cause only small effects from back diffusion. However, because back diffusion increases with the addition of embedded low permeability layers, it is possible that back diffusion may still result in significant plume tailing for heterogenous sites with less than 100% source mass removal.

In order to investigate the effect of partial source zone remediation on back diffusion for the case of a heterogenous sand aquifer with an underlying clay aquitard, a theoretical site was assessed that used an intermediate geometric parametrization for the embedded low permeability material. A transmissive zone volume fraction of 50% was used with a diffusion length of 0.5 m and diffusion area of 50 m^2. The source strength function was changed from Γ=0 to Γ=1, and the source mass removal was again explored. A source decay rate due to dissolution of 0.12 yr^{-1} (half-life =5.8 years) was used. However, it should be noted that due to a decrease in the average Darcy velocity as a result of the decrease in the transmissive zone volume fraction, the groundwater flowrate is affected. Therefore, the initial mass was adjusted to account for the lower flowrate and to calculate the desired source zone decay rate. For a source decay rate of 0.12 yr^{-1}, a source mass of 3761 kg was used.

4.3.1. Partial Source Zone Remediation

Scaled TCE concentrations in four observation wells for a case with a source mass removal of 99% after a 30 year loading period are shown in Figure 22. Starting at the first observation well at x=2.5 m, it takes 5 additional years for the MD model to decline to concentrations below the MCL. At this location, back diffusion was previously not observed for the homogenous sand aquifer case with source mass removals less than 100%.

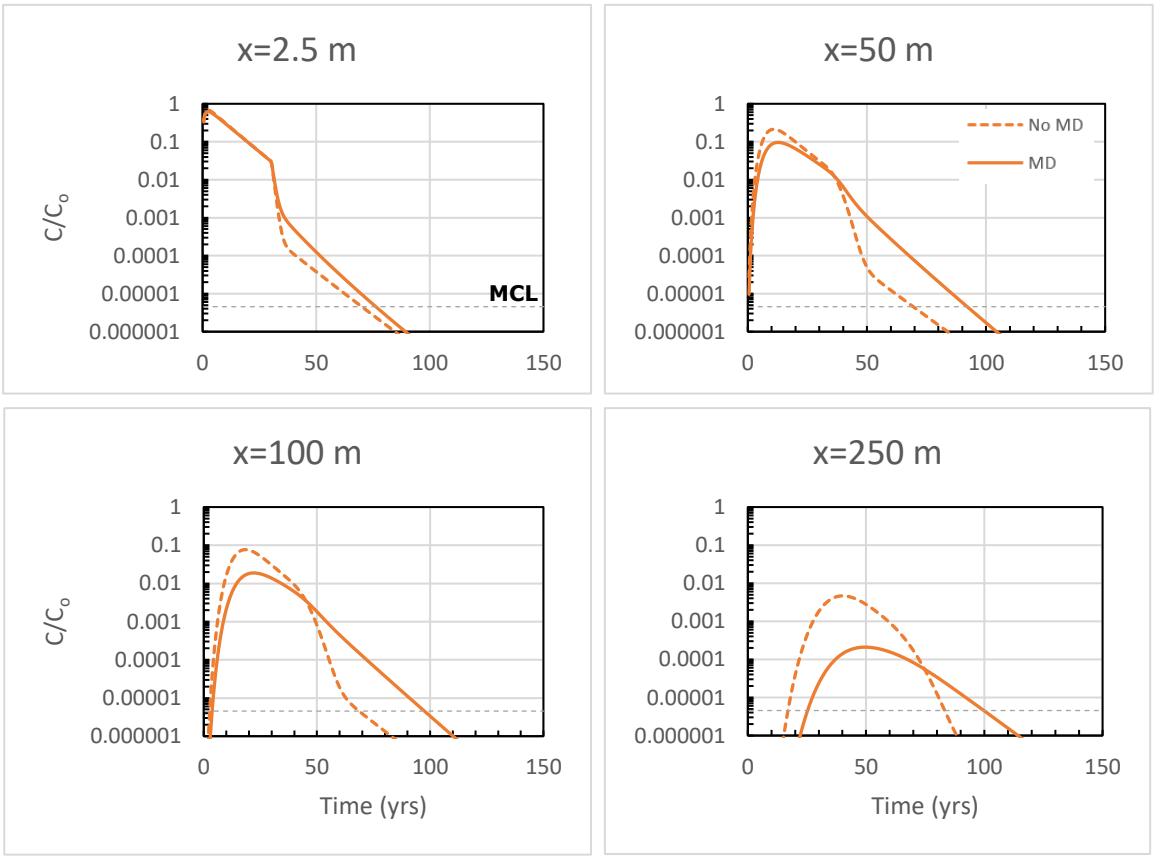

Figure 22: Comparison of scaled TCE concentrations at observation wells from No MD and MD models with 99% source zone remediation.

Moving downgradient, back diffusion results in 21, 20, and 18 additional years of plume tailing for wells at x=50, 100, and 250 m. As expected, the addition of embedded low permeability material results in a larger back diffusion effect. After a remediation effort that results in 99% source mass reduction, aquifer concentrations will be sustained above the MCL for a few decades at some location as a result of back diffusion.

Since 99% source mass removal is often not a feasible remediation goal, the source mass removal was reduced to 90%, and the resulting models are shown in Figure 23. The observation well at x=2.5 m shows no differences between the MD and No MD models. At x=50 m, 6 years of plume tailing is observed that sustains aquifer concentrations above the MCL. At x=100 m, 10 years of plume tailing is observed, and at x=250 m, the MD models shows concentrations above the MCL for 12 more years. When only the aquitard was assessed for back diffusion with a 90% source mass removal, the largest back diffusion effect was observed at x=250 m (Figure 19), which resulted in only 5 years of plume tailing. However, for a 50% volume of embedded low permeability material, a 90% source removal results in plume tailing that causes aquifer concentrations to be sustained above the MCL for about a decade in some locations, with tailing increasing downgradient of the source.

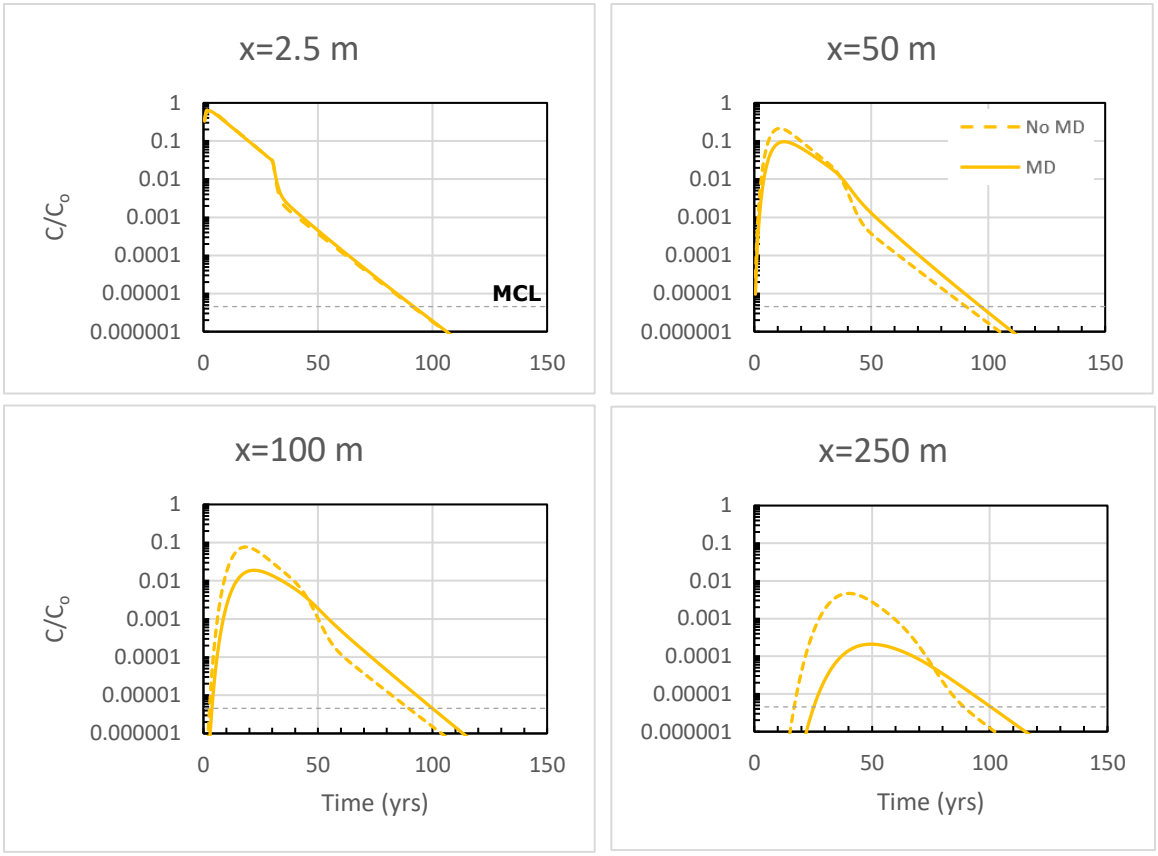

Figure 23: Comparison of scaled TCE concentrations at observation wells from No MD and MD models with 90% source zone remediation.

Lastly, Figure 24 shows observation wells for models with an 80% source removal. As seen before for the case with 90% source mass removal, back diffusion is not observed near the source. At the downgradient wells, back diffusion results in 4, 6 and 7 additional years for concentrations to decline below the MCL at locations x=50, 100, and 250 m, respectively. With 20% of the source mass remaining in the subsurface, back diffusion only impacts the remediation timeline by a few years, and the effect is comparable to the effect of back diffusion in the case of only an aquitard with 90% source mass removal.

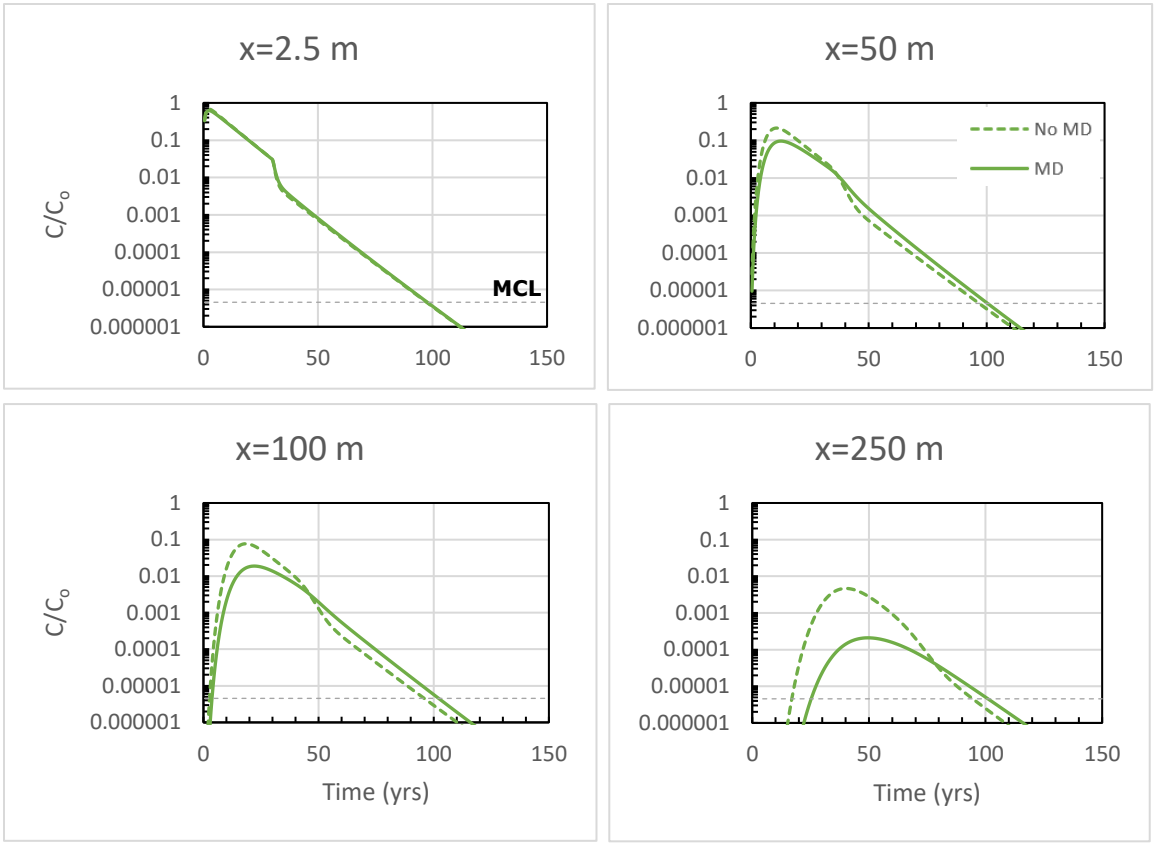

Figure 24: Comparison of scaled TCE concentrations at observation wells from No MD and MD models with 80% source zone remediation.

Therefore, as the source zone remediation results in less and less source mass removal, the plume tailing signal becomes more and more dominated by the residual source mass and less by back diffusion. Seyedabbasi et al. (2012) studied the relative contribution of DNAPL dissolution and matrix diffusion to source zone persistence in more detail and found that a significant portion of source longevity could be attributed to matrix diffusion process; however, this contribution greatly varied based on contaminant solubilities. Another factor to consider is the decay rate in the low *k* zone. As the decay

rate decreases relative to the transmissive zone decay rate, the back diffusion signal would increase as shown previously in this study, and as a result, back diffusion might contribute a greater role to plume persistence. All in all, partial source remediation that leaves a residual source mass in the subsurface is another factor to consider when assessing field sites for potential back diffusion risk.

4.4 Conclusions

In this chapter, the study first confirmed that back diffusion reduces for a decaying source zone, as shown by previous studies (Brown, 2012, Yang et al., 2016), and is primarily caused by the relative decrease in overall aquifer concentrations.

Next, it was demonstrated that for a source zone that is characterized by $\Gamma=1$, the dynamics of source dissolution are more important for observing back diffusion at magnitudes above the MCL than the initial concentration alone, as was the case when $\Gamma=0$. Higher source zone decay rates result in plumes with relatively lower contaminant concentrations, and therefore, back diffusion effects occur at lower magnitudes, while the opposite is true for lower decay rates. Therefore, site conditions, specifically the C_o, M_o, and the groundwater flowrate, govern source zone decay, and in turn, impact the magnitude of back diffusion effects. Because of this, a better picture of the magnitude at which potential back diffusion will occur can be determined by using C_o to delineate the upper limit on aquifer concentrations and λ to determine how long those concentrations will be sustained.

The effect of remediation efforts to remove the source zone was explored for a theoretical case with a homogenous sand aquifer and a heterogenous sand aquifer with a

volume fraction of 50% embedded clay lenses, both with an underlying clay aquitard. For the homogeneous sand aquifer and the parameters used, it was found that a near 100% source mass removal was required for back diffusion to have a significant impact on remediation timelines. A 90% source mass removal resulted in a minimal back diffusion effect of about 5 more years on the remediation timeline, and this is observed only at locations a few hundred meters downgradient from the source. For the heterogenous aquifer and the parameters used, it was found that source mass removals less than 100% still resulted significant back diffusion effects. A remediation effort resulting in 80% source mass removal will, however, only result in back diffusion effects that increase the remediation timelines by about 5 years.

Lastly, partial source zone remediation produces a “plume tailing” effect in the chemical transport models that closely resembles the effect from back diffusion, and as a result, overall plume persistence can be a combination of both back diffusion and a residual source mass. From this study, the relative contributions of each to plume persistence is dependent on the amount of the source mass removed by remediation, the amount of low permeability material in the aquifer system, and the location with respect to the source.

5. SEMI-ANALYTICAL SIMULATION OF MATRIX DIFFUSION IN FRACTURED MEDIA CASES

5.1 Methods

Another scenario that has a risk for back diffusion is a fractured system, where the fractures act as the transmissive conduits and the rock/media is the low permeability material. The semi-analytical method approaches embedded low permeability heterogeneities and fractured systems the same, and for each case, the volume fraction of the high and low permeability material in each gridblock must be specified, and three geometric parameters are required (Muskus and Falta, 2018). Therefore, the fractured system is essentially an embedded low permeability material case with a very low transmissive zone volume fraction, and the semi-analytical method can be applied to simplified fractured rock sites assuming parallel fractures (Muskus and Falta, 2018). The transmissive zone volume fraction is determined by fracture spacing (*a*) and the typical thickness of the fracture aperture (*b*). Unlike in the porous media cases, the REMChlor-MD interface does not allow for the manual specification of transmissive zone volume fraction, the average characteristic diffusion length, and the matrix diffusion surface area. These values are automatically calculated from the specified fracture characteristics. The transmissive zone volume fraction can be obtained from (Farhat et al., 2018):

$$V_f = \frac{b}{a} x\ 100 \qquad (6)$$

The average diffusion length can be obtained from:

$$L = (a - b)/2 \quad (7)$$

The interfacial matrix diffusion area (A_{md}) can be obtained by using Eq. 1 and the known V_f and L.

For the fractured rock scenario, the porous media base model was adjusted to better capture the contaminant plumes in a very low transmissive zone environment. The new base model for the fractured rock cases is 1500 meters long in the x-direction (direction of groundwater flow) with a cell size of 5 m, 300 m in the y-direction with a cell size of 5 m, and 20 m in the z-direction with a cell size of 2 m. The source is 40 m wide, 4 m thick, and located at the bottom of the model. The source, transport, and natural attenuation parameters used in the fractured case base model are shown in Table 2.

The back diffusion signal in the fractured rock scenario was assessed for three rock types: Granite, Sandstone, and Shale. The Toolkit default values in REMChlor-MD were used for the rock porosity, which were found from averages of typical porosity ranges for each rock type (Domenico and Schwartz, 1990; Payne et al., 2008; Farhat et al., 2018). For fractured rock, the tortuosity (τ) was calculated by the Toolkit, which estimates values of τ using the relationship (Farhat et al., 2018):

$$\frac{D_e}{D_o} = \tau \cong \emptyset^p \quad (8)$$

Where D_o is the molecular diffusion coefficient in free water, D_e is the effective diffusion coefficient, $\emptyset$ is the porosity, and *p* is the Apparent Tortuosity Factor Exponent.

Table 4: Input parameters used in base model for fractured rock cases.

Source, Transport, and Natural Attenuation Parameters Used in Base Model				
Parameter	**High K Zone**	**Granite**	**Sandstone**	**Shale**
Initial source concentration, C_0 (mg/L)	1,100	-	-	-
Initial source mass, M_0 (kg)	75,000	-	-	-
Source width, w (m)	40	-	-	-
Source depth, d (m)	4	-	-	-
Source decay rate (yr^{-1})	0	-	-	-
Source decay rate (dissolution) (yr^{-1})	0	-	-	-
Power function exponent, Γ	0	-	-	-
Bulk Darcy velocity, V_d (m/yr)	0.125	-	-	-
Porosity, ϕ	1	0.006	0.1	0.055
Tortuosity, τ	1	0.06	0.1	0.06
Retardation factor, R	3	3	3	3
Longitudinal dispersivity (m)	1	-	-	-
Transverse dispersivity (m)	1	-	-	-
Vertical dispersivity (m)	0.01	-	-	-
TCE plume natural degradation rate, λ (yr^{-1})	0.3	0.3	0.3	0.3
Molecular Diffusion Coefficient (cm^2/s)	$9.10x10^{-6}$	$9.10x10^{-6}$	$9.10x10^{-6}$	$9.10x10^{-6}$
Distance between parallel fractures, a (m)	2	-	-	-
Aperture thickness of fractures, b (m)	$5x10^{-5}$	-	-	-

A fracture spacing of 2 m was used with a fracture aperture of 50 microns, resulting in a transmissive zone volume fraction of 0.0025% and diffusion length of 1 m for a total gridblock volume of 50 m^3. Because the each gridblock is treated as having the same amount of "fractured rock", monitoring well location for the strongest back diffusion signal is dependent only on aquifer concentrations, and therefore, the wells were placed near the source zone depth at the bottom of the aquifer. Well screens remain

2 m long. For an actual field site, however, a monitoring well should be placed near an actual fracture for the highest back diffusion signal. The conceptual model for this scenario is shown in Figure 25.

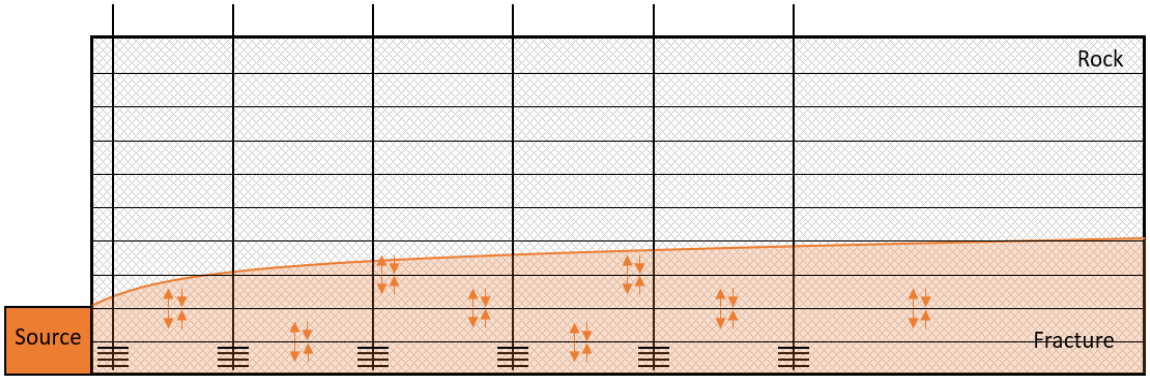

Figure 25: Cross-sectional view of conceptual model for a fractured rock system. Fractures are shown in the *xy* plane, but they can be in any direction assuming they are all parallel.

5.2 Results

The MD and No MD models for three different fractured rocks are shown in Figure 26. Since the fracture spacing and aperture width are the same, the No MD models are the same for each rock type. The source is completely removed after a 30 year loading period. When matrix diffusion is not considered, concentrations in the plume decrease rapidly after source removal, as shown by the No MD models. Plume tailing is initially greatest for the fractured sandstone, as shown in the monitoring well at x=2.5 m. For fractured sandstone, it takes 65 more years for concentrations to decline below the MCL. At x=100 m, plume tailing results in the addition of 84 years to the remediation

timeline, and at x=250 m, it results in 77 years. At x=450, the monitoring well shows that concentrations in the plume never rise above the MCL for the MD case, which is indicative that the contaminant plume does not travel as far as it does in the other fractured rock cases. Fractured granite results in relatively less plume tailing, but MD models still show concentrations sustained above the MCL for about 4-6 decades after source removal, depending on the downgradient location. Fractured shale results in plume tailing that is comparable to fractured sandstone at locations near the source; however, the contaminant plume for shale travels further than the plume in sandstone.

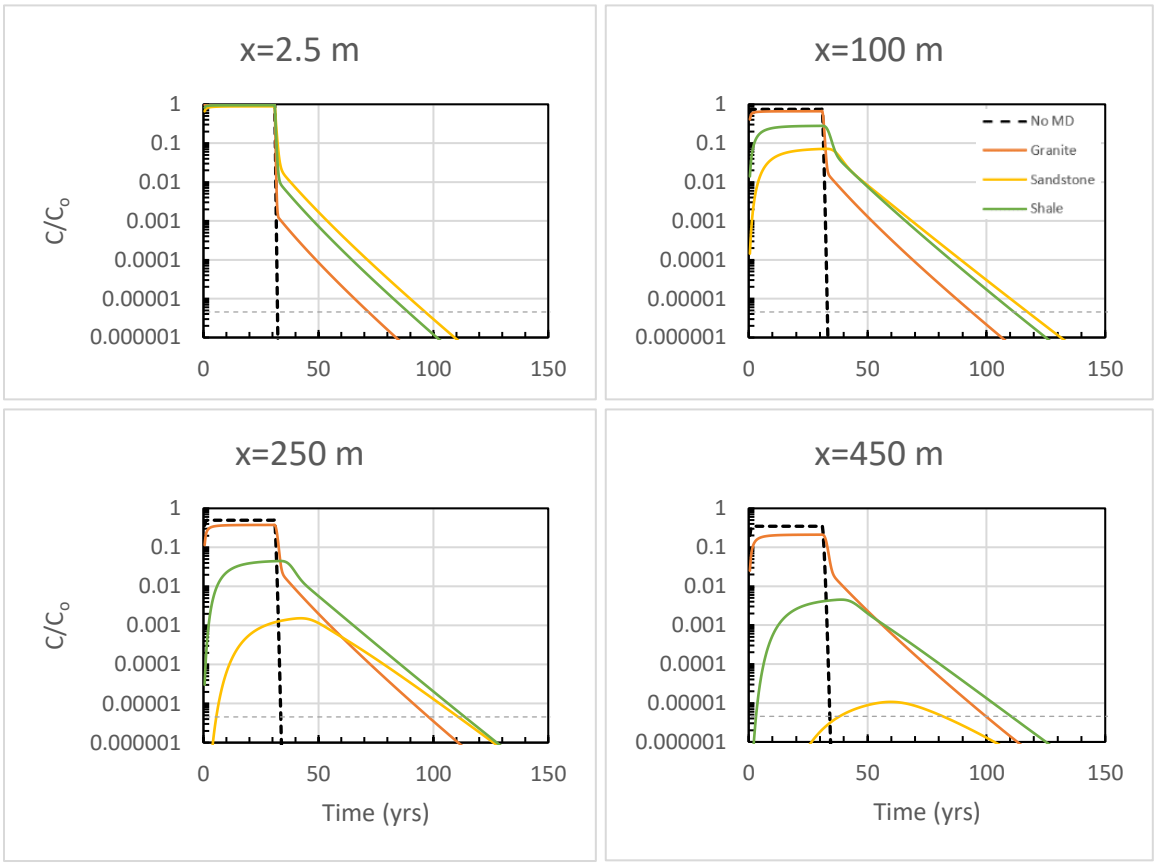

Figure 26: Comparison of scaled TCE concentrations from MD and No MD models at different observation wells for cases with fractured granite, sandstone, and shale that have a constant source.

Relative to the other fractured cases, the largest effect from back diffusion at further downgradient locations is seen in the fractured shale, with about 80 years of plume tailing observed at x=250 m and 77 years of tailing observed at 450 m.

In Figure 27, the MD and No MD models are shown for the different fractured rock systems for a case where Γ=1, the initial source mass is 188 kg, and the resulting source decay rate is 0.12 yr^{-1}. Under these conditions, the effect of back diffusion on plume tailing is reduced by about 2 decades for all three fractured rock cases in comparison to the case with a constant source.

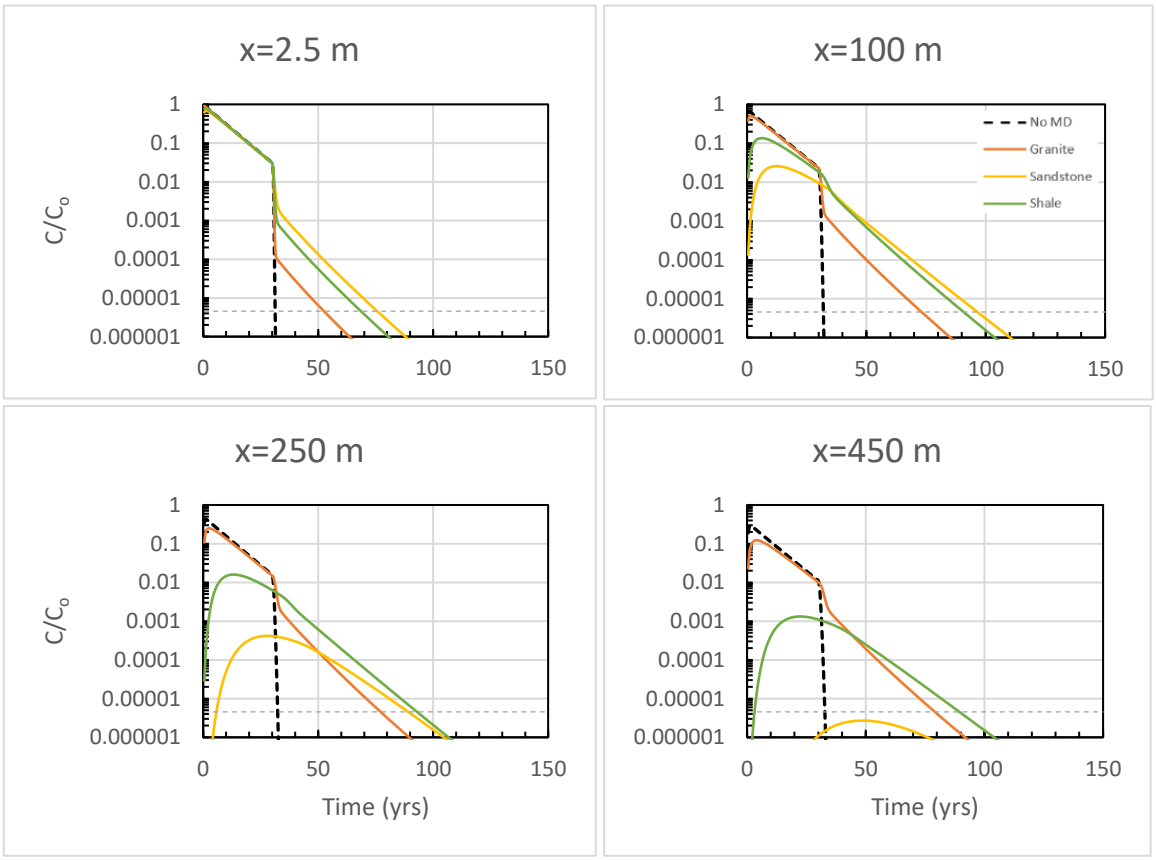

Figure 27: Comparison of scaled TCE concentrations from MD and No MD models at different observation wells for cases with fractured granite, sandstone, and shale that have a decaying source.

For the fractured rock cases, the main intrinsic rock property that determines the effect of back diffusion is porosity. In the models, sandstone has the highest porosity of 0.1. Although this porosity does not result in a material that is very transmissive of groundwater, it allows for a relatively larger diffusive mass flow of solutes out of the open fracture and into the low permeability rock. Because of this larger diffusive mass flow, back diffusion has a large effect at locations near the source; however, the larger mass flow also removes more contaminants from the fractures, resulting in a plume that does not travel as far downgradient.

Granite has the lowest porosity of 0.006, which in many cases, is low enough to consider the crystalline rock impermeable. However, the diffusive process is strong enough to drive the transfer of solutes from the open fracture and into the very low porosity material, albeit at relatively lower diffusive mass flows. Because of the low porosity rock and the resulting lower diffusive mass flow, concentrations within the fractures stay high, resulting in a plume that travels farther downgradient and in back diffusion that remains significant at further downgradient locations. Although the observation wells only extend to 450 m downgradient, the plume for fractured granite extends much further. Shale has an intermediate porosity of 0.055, and as a result, the behavior of matrix diffusion falls in between fractured sandstone and granite.

Therefore, a fractured rock with a higher porosity, such as sandstone, results in the highest risk of back diffusion at locations near the source while a fractured rock with a lower porosity, such as granite, results in the highest risk of back diffusion at distances far from the source.

Another case that should be evaluated is one where the decay rate in the low *k* zone is lower than the decay rate in the fractures. It has already been demonstrated that in unconsolidated porous media, a lower decay rate in the low *k* zone relative to the transmissive zone can result in back diffusion that causes decades to centuries more of plume tailing. In the case of a fractured rock system, it is likely that decay in the unfractured rock will be lower than the decay in the open fractures due to the low porosity of the rock and pore throat exclusion, especially in cases of fractured crystalline rock.

Figure 28 shows a case where the degradation in the low *k* zones is a magnitude lower (λ=0.03 yr^{-1}) than the degradation in the fractures (λ=0.3 yr^{-1}), and the time frame is extended out to 500 years. For this case, the source function is 1 (λ=0.12 yr^{-1}) and the source mass is completely removed after 30 years. For all three rock types, back diffusion results in aquifer concentrations that are sustained above the MCL for centuries. Additionally, plume lengths appear to be longer for this scenario, as shown best by the fractured sandstone case where at x=450, concentrations are still 1-2 magnitudes above the MCL for centuries after source removal. In the previous fractured rock scenarios, the sandstone case showed the extent of the plume to be around 450 m.

Therefore, matrix diffusion is demonstrated to be a primary transport process under these conditions for fractured rock. For these fractured rock cases, the implications of back diffusion are that field sites could remain contaminated for centuries, even after the source zone mass is completely remediated.

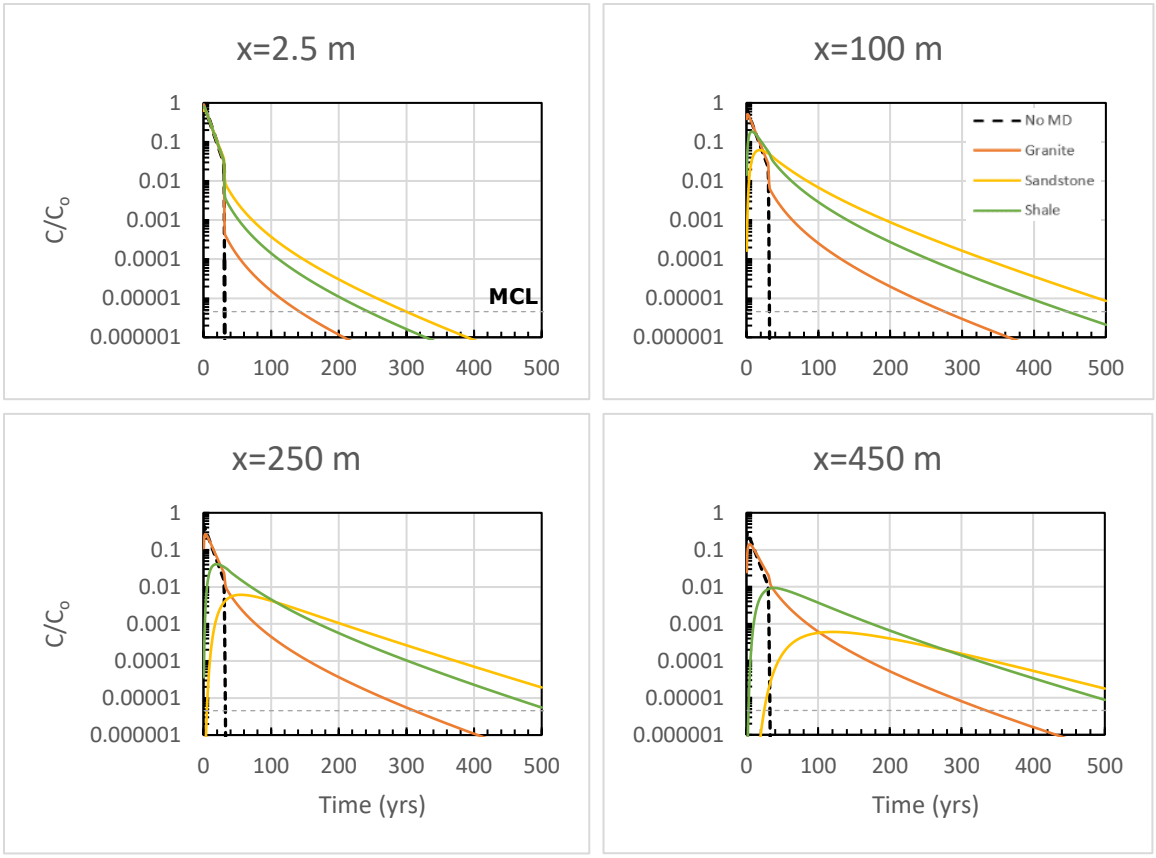

Figure 28: Comparison of scaled TCE concentrations from MD and No MD models at different observation wells for cases with fractured granite, sandstone, and shale that have a decaying source and a low *k* zone decay rate of 0.03 yr^{-1}.

5.2.1. Partial source zone remediation

Next, the effect of partial source zone remediation on back diffusion was explored for the fractured rock cases. All parameters were returned to the base model for the first partial source zone case, which evaluates a source zone remediation of 90% after a 30 year loading period. In Figure 29, no plume tailing is observed for any of the fractured rocks in the first monitoring well. At x=100 m, only 1 year of plume tailing is observed

for granite while about 5 years of tailing is observed for shale and about 10 years is observed for sandstone. As seen before in the previous fractured rock cases, the tailing continues to increase downgradient from the source, and the fractured granite case results in about 5 years of tailing at x=450 m and the fractured shale case shows 10 years. The fractured sandstone case continues to result in a plume that is relatively shorter in length, and concentrations never rise above the MCL in the well at x=450 m.

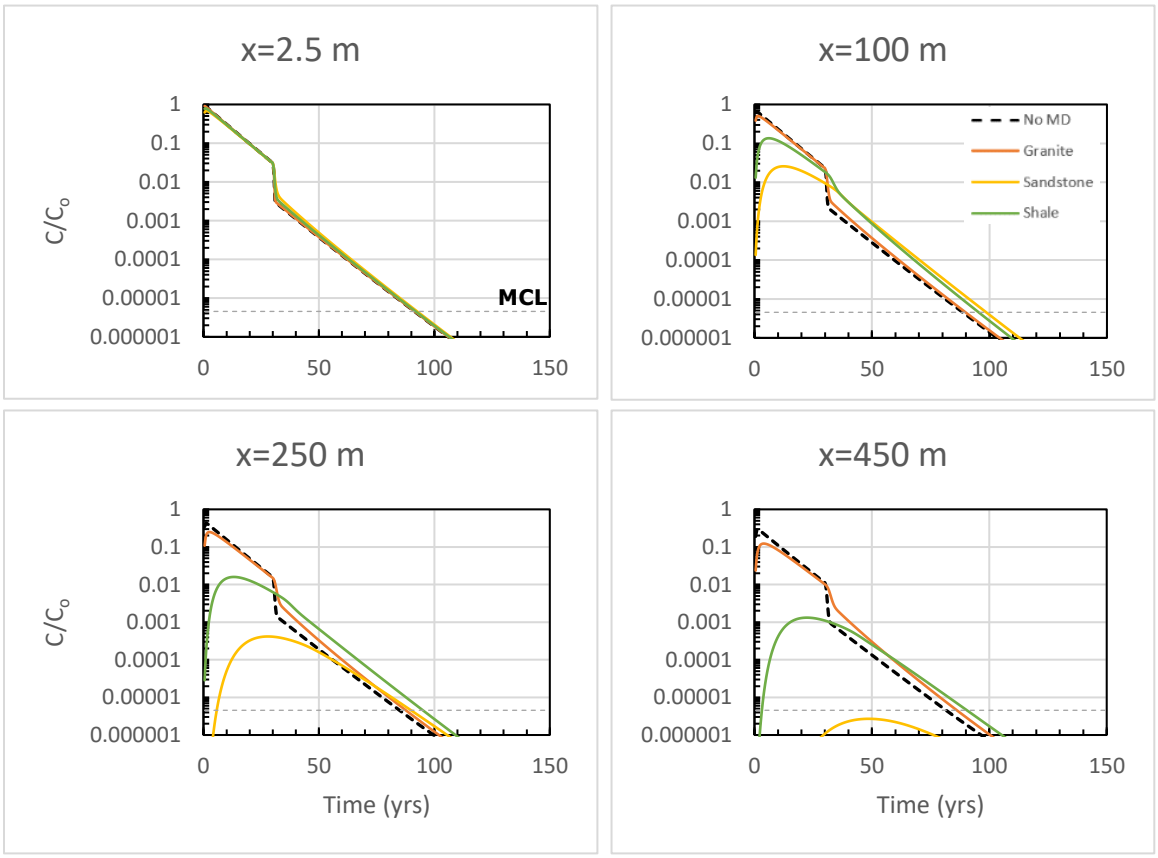

Figure 29: Comparison of scaled TCE concentrations from MD and No MD models at different observation wells for cases with fractured granite, sandstone, and shale that have a 90% source zone remediation.

Overall, a source remediation of 90% will still result in a plume that persists for many decades; however, back diffusion is only responsible for up to a decade. The MD models are not significantly impacted by the remaining 10% source mass. The decrease in plume tailing from back diffusion is mostly due to the changes in the No MD models, where the remaining source mass causes decades of plume tailing. Because the transmissive zone is so small, any mass left in the subsurface could have significant impacts on plume persistence. As seen before, the residual source mass and back diffusion can have a similar effect on the transport model, and for this case, it appears that the residual source mass is likely dominating the plume tailing signal.

Another case shows a 90% source zone remediation after 30 years, but the decay rate in the low *k* zone is 0.03 yr^{-1} instead of the base model value of 0.3 yr^{-1}. In Figure 30, the MD models for each fractured rock show centuries of plume tailing due to back diffusion as a result of the lower decay rate. Using the No MD model as the reference for the amount of plume tailing due to back diffusion, this case shows slightly less plume tailing than in the case when 100% of the source mass was removed (Figure 28). However, the combined plume tailing from the residual source mass and back diffusion result in nearly identical plume persistence to the amount observed in the previous complete source removal case. This suggests that the overall plume tailing signal becomes largely dominated by back diffusion under these conditions, and that over the time frame of multiple centuries, the residual source mass contributes a relatively smaller amount to the plume persistence.

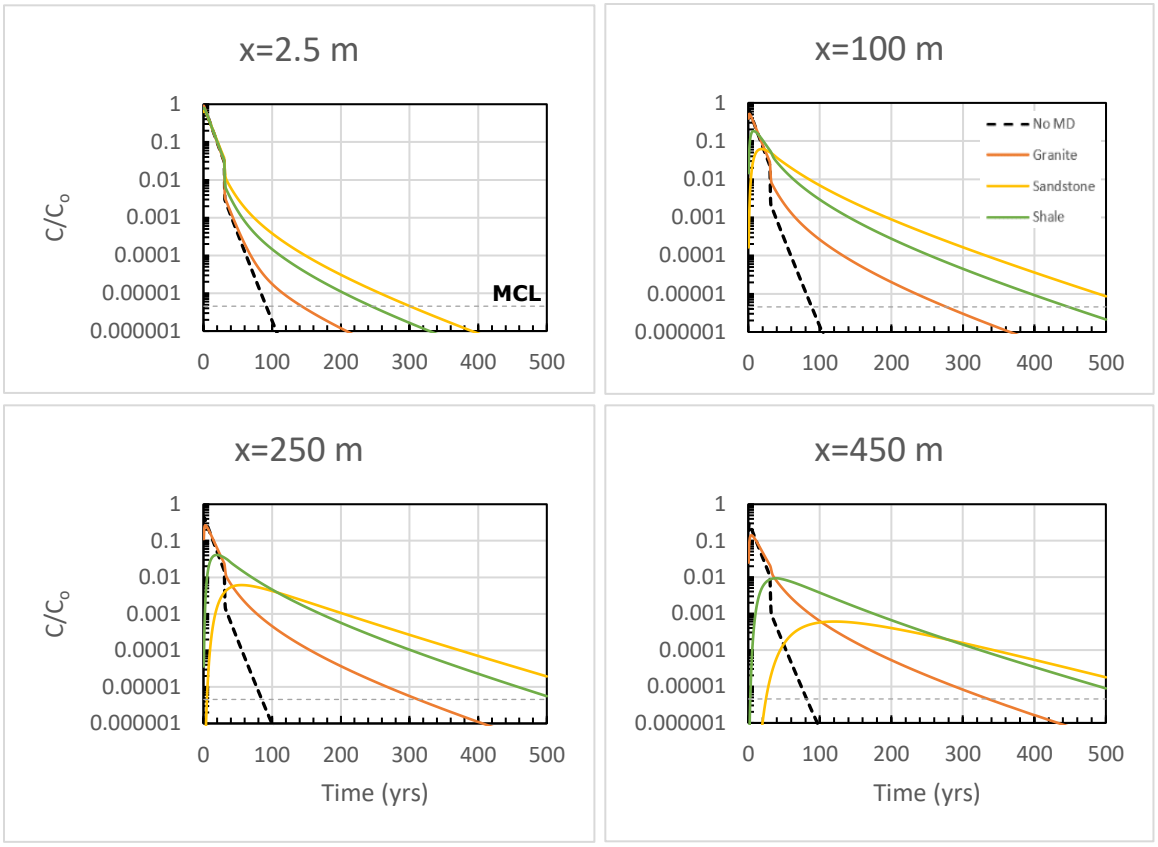

Figure 30: Comparison of scaled TCE concentrations from MD and No MD models at different observation wells for cases with fractured granite, sandstone, and shale that have a 90% source zone remediation and a low *k* zone decay rate of 0.03 yr^{-1}.

It is already intuitive that the increased longevity of contaminants in the low *k* zones contributes to significantly larger back diffusions effects. In Figure 30, the monitoring well at x=2.5 m shows a case with partial source zone remediation where significant plume tailing due to back diffusion occurs in proximity to the source. Previous cases have treated the degradation rates in the low *k* and transmissive zones as the same, and as a result, aquifer and low *k* zone contaminants degrade at the same rate. As a result, any delay to a concentration gradient reversal, e.g., a residual source mass, might have

mitigating effects on back diffusion because contaminants in both the aquifer and the low *k* zone have decayed to very low concentrations before back diffusion begins. In this current fractured rock case, aquifer contaminants degrade faster than the contaminants in the unfractured rock, and as result, the concentration gradient reversal occurs sooner than in the previous cases with equivalent degradation rates in both zones. Despite the residual source mass, significant back diffusion that results in centuries of plume tailing still occurs near the source because concentrations within the unfractured rock remain high.

5.3 Conclusions

In this chapter, the back diffusion signal was evaluated for fractured rock cases, which when using the semi-analytical method, are treated as an extreme case of embedded low *k* material. For a model with no matrix diffusion, 100% source mass removal results in a near instantaneous decline in aquifer concentrations. This makes the contrast between the MD and No MD models sharper, and the back diffusion signal more evident. For all three fractured rocks and the parameters used, back diffusion results in decades of aquifer concentrations being sustained above the MCL. For cases where the decay rate in the low *k* zone is a magnitude lower than the rate in the transmissive zone, back diffusion results in centuries of plume persistence, even after the source zone is completely remediated.

The degree of plume tailing caused by back diffusion is dependent upon the porosity of each rock type. A very low porosity rock will result in relatively lower initial diffusive mass flow into the unfractured rock, but the plume will be sustained longer in the fractures and will travel further distances, resulting in back diffusion risk at locations

very far downgradient from the source. A higher porosity rock will result in relatively higher initial diffusive mass flow, but because more contaminants are removed from the fractures, the plume travels shorter distances, and diffusion risk lowers moving away from the source.

For the parameters used, partial source zone remediation results in significant plume persistence due to a residual source mass, and the effect of back diffusion is comparatively less, although the overall remediation timeline is increased by many decades by both causes. When the low *k* zone decay rate is decreased by an order of magnitude relative to the transmissive zone decay rate, the plume tailing signal becomes dominated by back diffusion, resulting in centuries of tailing due to back diffusion, and the effect of the residual source mass becomes relatively smaller.

6. CASE STUDY

6.1 Site Background and Field Remediation Activities

In order to demonstrate the application of the semi-analytical method for modeling matrix diffusion and to apply the insights gathered from the theoretical portion of this study, a field site was evaluated. For this case study, a DuPont site located in Kinston, NC was assessed. The following site description was taken from Liang et al. (2011). In 1953, the DuPont Kinston Plant began operations and most recently, it manufactures Dacron polyester resin and fibers. In 1989, a site investigation revealed that the surficial aquifer beneath the manufacturing plant was impacted by the release of TCE. The surficial sand aquifer overlies a thick mudstone-confining unit, and the aquifer material is heterogeneous and composed of unconsolidated and interbedded sand, silty sand, clayey silt, and clay, ranging in combined thickness from 2.1 to 7.6 meters. The TCE is mostly confined to the shallow unconsolidated sediments above the mudstone unit and exists mostly in the lower region of the saturated zone above a thin clay layer. The resulting groundwater plume extends approximately 300 m in the downgradient (northwest) direction. A fault trending southwest to northeast is present in the northwestern quadrant of the plant and is found between wells MW-43 and MW-44 and MW-36 and MW-38 (Figure 31).

Remediation efforts started with a pump and treat (PAT) system that operated from 1995 to 2001, but it only extracted 3 lbs of TCE. In 1999, the source area was treated with in-situ zero valent iron (ZVI) treatment using a total of 11 treatment columns and further downgradient, a permeable reactive barrier (PRB) with a thickness of 0.127 m

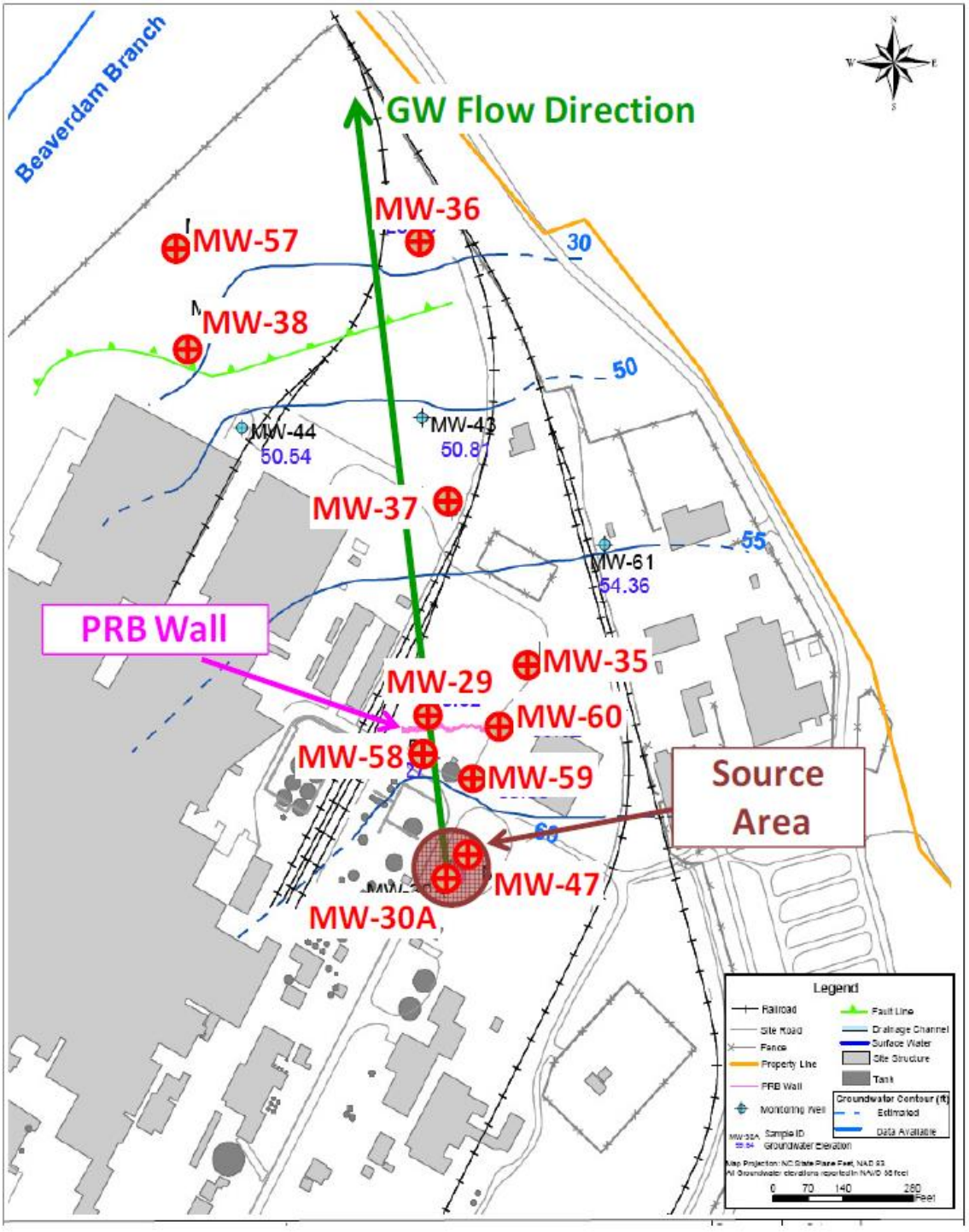

Figure 31: Site map of Kinston plant with monitoring wells (reproduced with permission from Liang, 2009, personal communication, September 26, 2019).

and a length of 122 m was installed 89 m downgradient of the source. It was reported that the source zone mass reduction was 95%; however, there is a large uncertainty associated with this removal percentage (Liang et al., 2011).

Previous work developed a chemical transport model for this site. The work linked the analytical model REMChlor to a Monte Carlo modeling simulation package GoldSim via a FORTRAN Dynamic Link Library application (Liang et al., 2011). This allowed for the simultaneous evaluation of the effectiveness of source and plume remediation considering the inherent uncertainties in all major parameters; however, the version of REMChlor used did not have the capabilities to model matrix diffusion, and therefore, it was not considered. Additionally, the field data in the previous study went only through 2008. Current monitoring well data indicates that the concentrations in the aquifer remain high after remediation, and as a result, the plume persistence at this site has led to the hypothesis that back diffusion might be significant given the existence of low permeability material with the aquifer.

In this case study, the DuPont Kinston site will be evaluated for potential back diffusion risk by assessing the site characteristics that will determine the model parametrization. Using the semi-analytical modeling method via REMChlor-MD, an updated chemical transport model that considers matrix diffusion will be developed to attempt to explain the observed plume persistence.

6.2 Match to Previous Analytical Model

This modeling exercise builds upon the previous work by Liang et al. (2011), and as a result, all source, transport, and natural attenuation parameters for the Kinston site were taken from that study, which are a combination of site reported values, calibrations, and estimations (Table 3). The semi-analytical method was first verified by matching the analytical solution from REMChlor (Falta et al., 2007b) to the numerical solution from REMChlor-MD without any matrix diffusion. A reasonable match between the analytical and numerical models was achieved, as shown in Figure 32; however, a few adjustments to the numerical model were required.

The numerical model developed has a cell size of 1 meter for 500 meters in the x-direction, a cell size of 4 meters for 200 meters in the y-direction, and a cell size of 1.75 meters for 10.5 meters in the z-direction. Ideally, the cell size in the x-direction would be equal to or less than the PRB wall thickness. However, because the PRB is very thin, a cell size of 0.127 m greatly increases computational effort and limits the discretization in the y and z directions. Because of this, the wall width was increased in the numerical model to be equal to the cell size of 1 m.

Liang et al. (2011) related the percent of mass removal across the PRB wall to the degradation rate inside the PRB wall as opposed to only using the bench scale half-life of TCE due to ZVI treatment. The bench scale half-life was reported to be less than 4 hours, which is equivalent to a degradation rate of 1518 yr^{-1} and a mass removal efficiency of 99.9%; however, wall heterogeneity would likely prevent the PRB from achieving this level of efficiency, and this value seems overly optimistic (Liang et al., 2011). The decay

rate was then calculated using Equation 9 by assuming a first-order reaction in aqueous phase, where λ_{PRB} is the TCE degradation rate inside the PRB wall, C_{in} and C_{out} are the aqueous concentrations entering and leaving the PRB wall, V_f is the transmissive zone volume fraction, ϕ is the porosity, v_x is the Darcy velocity, and $X_{removal}$ is the TCE mass removal percentage due to PRB wall treatment.

$$\lambda_{PRB} = -\frac{\ln(C_{out}/C_{in})}{V_f \emptyset / v_x} = -\frac{\ln(1-X_{removal})}{V_f \emptyset / v_x} \quad (9)$$

The degradation rate was treated as an uncertainty parameter in the probabilistic analytical model, but it was determined that the most likely rate in the wall was 436 yr^{-1}, which estimates that the PRB has a mass removal efficiency of 90% (Liang et al., 2011). Using the same method, the degradation in the PRB was adjusted for a wall thickness of 1 m in the numerical model, and a 90% removal efficiency resulted in a rate of 55.3 yr^{-1}. However, when this degradation rate was applied to models in REMChlor-MD, it resulted in a mass removal efficiency that was lower than 90%. Because of this discrepancy, the numerical formulation used in the program was evaluated.

The discretized transport equation with a fully implicit formulation used in REMChlor-MD (Muskus and Falta, 2018) was evaluated for a single gridblock in Equation 10, where conditions are at steady state with no dispersion and upstream weighting for the advective term is assumed.

$$0 = v_x \Delta y \Delta z \, (C_{i-1} - C_i) - V_f \Delta x \Delta y \Delta z \phi \lambda_{PRB} C_i \quad (10)$$

Eq. 10 was then solved for the concentration in the single gridblock, which is shown in Eq. 11:

$$C_i = \frac{v_x C_{i-1}}{v_x + V_f \Delta x \phi \lambda_{PRB}} \quad (11)$$

Where v_x is the Darcy velocity, Δx, Δy, and Δz are the grid spacing, V_f is the transmissive zone volume fraction, ϕ is the porosity, λ_{PRB} is the degradation rate inside the single gridblock, and C_{i-1} and C_i are the aqueous concentrations of the contaminant in the upstream gridblock and in the gridblock of interest. Under these conditions, the numerical approximation in Eq. 11 is the same as the analytical solution for a simple mass balance equation and solving for the concentration leaving the control volume, which is shown in Eq. 12:

$$C_{out} = \frac{v_x C_{in}}{v_x + V_f \Delta x \phi \lambda_{PRB}} \quad (12)$$

Where C_{in} is the concentration entering the control volume and C_{out} in the concentration leaving the volume.

The numerical solution (Eq. 11) was then compared to the concentration output in a single gridblock containing the PRB from the REMChlor-MD program. Both solutions

produced the same results and showed that a degradation rate of 55.3 yr^{-1} for Δx=1 m does not result in 90% mass removal. With the numerical formulation used in REMChlor-MD verified as mathematically correct, the different mass removal across the PRB in the numerical model was hypothesized to be the result of a discretization error. The hypothesis was confirmed when the gridblocks were made smaller and smaller relative to the PRB thickness of 1 m and the two solutions started to match better with the degradation rate for the PRB becoming more accurate. However, as stated before, it would be difficult to make the gridblocks any smaller than 1 meter because it would result in a very large computational effort that would exceed the capabilities of REMChlor-MD. In order to work around the discretization error, the simple steady state formula in Eq. 11 was used to back calculate the decay rate in the wall that would result in the desired mass removal, and rearranged is:

$$\lambda_{PRB} = \frac{v_x(C_{i-1}-C_i)}{V_f \Delta x \phi C_i} \quad (13)$$

For 90% mass removal, the decay rate for a wall of 1 meter in the numerical model with upstream weighting would then be 216.2 yr^{-1}.

The last difference in the parameterization between the analytical and numerical models is in the dispersivity values. Liang et al. (2011) found a better match to plume monitoring well data by calibrating the longitudinal dispersivity to have a value of x/20 and the transverse dispersivity to have a value of x/50, and the vertical dispersivity was

estimated to have a value of x/1000. The transverse and vertical dispersivities were based on the estimated plume length of 300 m, resulting in values of 6 m and 0.3 m, respectively. The longitudinal dispersivity was entered as a *sigmav* value (coefficient of variation for velocity field), where x/20 = 0.31623 (Falta et al., 2007a). When fitting the numerical model to the analytical model, however, the best fit resulted when the longitudinal dispersivity was set equal to zero in the numerical model. The modeling method in REMChlor-MD uses a finite difference upstream weighting method to calculate the advective flux, and the method results in a numerical dispersion equal to the dispersion that would result from a longitudinal dispersivity of (x-direction cell size)/2 (Farhat et al., 2018). Therefore, although the longitudinal dispersivity is set to zero in the model, there is numerical dispersion within the model. With the longitudinal dispersivity calibration and the correction to the decay rate in the PRB, the fit to analytical model was found to be reasonable, as shown in Figure 32.

Table 5: Input parameters used to match the numerical model to the analytical model from Liang et al. (2011).

Source, Transport, and Natural Attenuation Parameters		
Parameter	**REMChlor**	**REMChlor-MD**
Initial Source Concentration, C_0 (mg/L)	**6** *(From site reports)*	**6**
Initial Source Mass, M_0 (kg)	**136** *(From site reports)*	**136**
Source width, w (m)	**8** *(From site reports)*	**8**
Source depth, d (m)	**3.5** *(From site reports)*	**3.5**
Power function exponent, Γ	**1** *(Estimated)*	**1**
Source decay rate (yr^{-1})	**0** *(Estimated)*	**0**
Darcy velocity, V_d (m/yr)	**8** *(Calibrated)*	**8**
Porosity, ϕ	**0.333** *(Estimated)*	**0.333**
Retardation factor, R	**2** *(Estimated)*	**2**
Longitudinal dispersivity (α_x)	**x/20** *(Calibrated)*	**0 m**
Transverse dispersivity (m)	**6** *(Calibrated)*	**6**
Vertical dispersivity (m)	**0.3** *(Estimated)*	**0.3**
TCE plume natural degradation rate, λ (yr^{-1})	**0.125** *(Calibrated)*	**0.125**
PRB degradation rate, λ (yr^{-1})	**436** *(Calibrated)*	**216.2** (Δx=1 m)

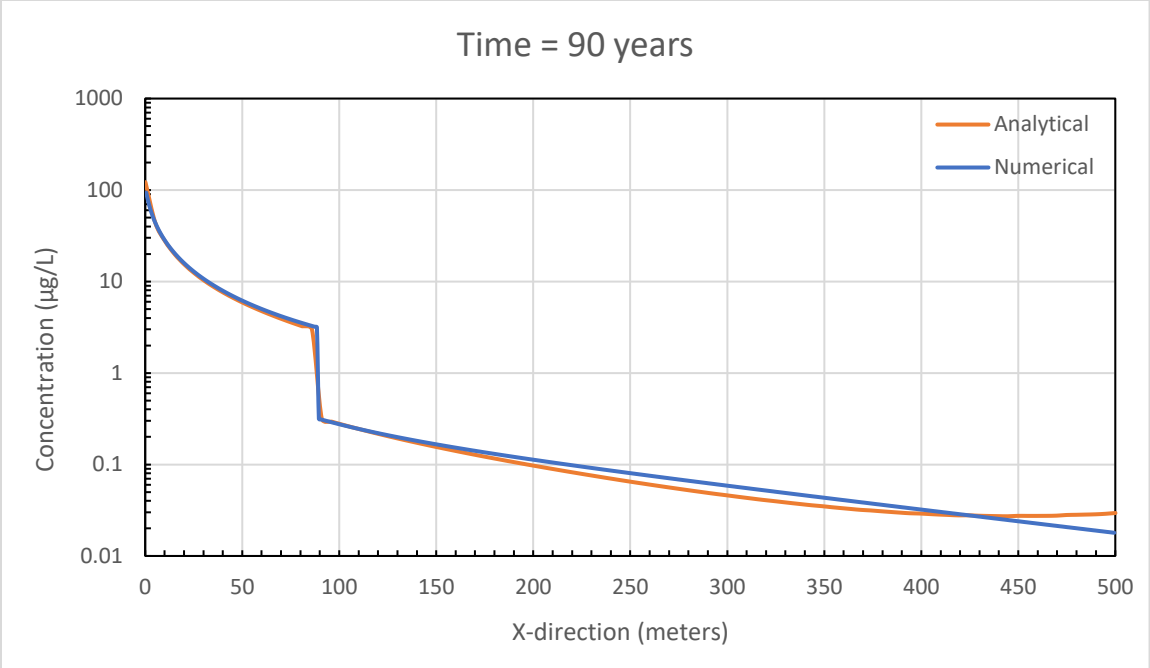

Figure 32: Comparison of the analytical solution from REMChlor and the numerical solution from REMChlor-MD at the plume center line at t=90 years.

6.3 Back Diffusion Risk Assessment

Before attempting to match a chemical transport model to field data, it is important to first determine the potential risk for back diffusion at the site. Some of the key components, as demonstrated throughout this study, that impact back diffusion risk are: amount of low *k* material in the aquifer system and the associated geometric parameterization, source function exponent, initial source concentration, source zone decay rate (dissolution), partial source zone remediation, low *k* zone parameterization, and monitoring well design and location. Additionally, other factors that should be considered are plume remediation and the decay rate in the transmissive zone.

Presence of Low k Material

From the site description from Liang et al. (2011), there are two potential sources for back diffusion at this site: the thick underlying clay confining unit and the interbedded silty sand, clayey silt, and clay. The amount of interbedded low permeability material in the aquifer is unknown and must be estimated. The TCE appears to exist primarily in the lower region of the saturated zone of the sediments above a thin clay layer. An exact thickness for this "thin" layer is not specified, and therefore, the diffusion length will likely need to be calibrated. All in all, the site has a risk for back diffusion due to the presence of low permeability material, and the risk can increase as low *k* heterogeneities increase throughout the site.

Source Function Exponent

The source was assumed to decay over time due dissolution and the function exponent was assumed to be 1, and therefore, back diffusion risk lessens relative to a constant source.

Initial Source Concentration and Source Zone Decay Rate (dissolution)

The initial source concentration was estimated by Liang et al. (2011) to be 6,000 μg/L, which is 1,200 times the MCL for TCE. Therefore, the upper limit for aquifer concentrations will be about 2.5 orders of magnitude above the MCL. Since the source decays over time from dissolution, the source zone decay rate should be evaluated in conjunction to the initial source concentration. Using the relationship between Q, C_o, and M_o in Eq. 5, the source zone decay rate due to dissolution is 0.01 yr^{-1}, which results in a half-life of about 70 years. Because the dissolution rate is low and source zone

remediation takes place a few decades after the estimated initial TCE release, aquifer concentrations will be sustained at or near initial source concentration levels prior to remediation, and this case can be considered comparable to a source with a constant source. From the theoretical models analyzed with a constant source, embedded low *k* material cases will show the effects of back diffusion above the MCL with initial concentrations that are 1,200 times the MCL. Therefore, it is reasonable to assume that back diffusion will likely affect aquifer concentrations above the MCL at some locations.

Source Zone Remediation

The initial TCE release date was estimated to be around 1967 (Liang et al., 2011). In 1999, an in-situ source zone destruction pilot using zero valent iron (ZVI) was used to destroy source zone soil contamination, and source zone mass reduction was reported to be 95%. For a site with embedded low *k* material and an underlying aquitard, this amount of source mass removal will likely result in some effect from back diffusion, although some of the plume persistence may be attributed to the residual source mass, especially at locations closer to the source.

Monitoring Wells

The monitoring wells at this field site were not placed with back diffusion in mind. Nevertheless, six monitoring wells were assessed that are located near the plume centerline, with three wells near or just downgradient of the source zone and three wells downgradient of the PRB. The well screen intervals for these monitoring wells are unknown and need to be estimated.

Low k Zone Parameterization

There is no known reported information about TCE degradation in the low *k* zones at the Kinston Plant site and, and the rate will need to be calibrated. Additionally, the retardation factor in the low *k* zone is unknown and will need to be calibrated as well. The values can be used to increase the back diffusion signal in the model to match any plume tailing observed in the field data.

Other Factors

The theoretical portion of this study did not explore the effect of plume remediation on back diffusion. Nevertheless, the PRB will decrease aquifer concentrations downgradient of the wall, which in turn may provide good conditions for concentration gradients to reverse and back diffusion to occur. The PRB may even mitigate the effects of any residual source mass and lead to an increased back diffusion effect downgradient of the wall. Another important factor to consider is the transmissive zone decay rate. The natural plume degradation was calibrated to be 0.125 yr^{-1} (Liang et al, 2011), which is a relatively low value for TCE (Aziz et al., 2000, Farhat et al., 2018), therefore suggesting that aquifer concentrations will be sustained for longer periods of time.

6.4 Model Parameterization

Wells MW-30A and MW-47 are both located in the source zone, and MW-58 is located 71 m downgradient of the source (Figure 31). MW-29 is the first well on the downgradient side of the PRB while MW-35 and MW-37 are located further downgradient, with MW-37 located the furthest from the plume centerline. No

information on the well screen length or screened interval was found, and therefore, a screen length of 1.75 m (equal to z-direction gridblock size) was estimated and was placed in the bottom gridblock in the model. This well screen location in the model is in proximity to the aquitard and the source depth.

Because there was no access to boring logs, the general description of the aquifer material was used to estimate a transmissive zone volume fraction of 50%. The diffusion length was then calibrated, and it was found that for most monitoring wells, a shorter diffusion length of 0.1 m resulted in the better fit. This correlates with the reported "thin clay layer," however, the lateral extent of this layer is not known, and due to aquifer heterogeneities, diffusion lengths could likely vary spatially. Using the field data in MW-29, the retardation factor in the low *k* was calibrated to be 4, and the degradation rate in the low *k* zone was calibrated to 0.05 yr^{-1}. By increasing the retardation factor and decreasing the decay rate in the low *k* zone, the effect of back diffusion was effectively increased. The matrix diffusion geometric parameters and the low *k* zone parameters are summarized in Table 6.

Table 6: Geometric matrix diffusion parameters and low *k* zone parameters used in the MD model for the Kinston Plant field site.

Parameter	
Total gridblock volume, V_i (m^3)	7
Transmissive zone volume fraction, V_f	50% *(estimated)*
Diffusion Length, *L* (m)	0.1 *(calibrated)*
Matrix Diffusion Area, A_{md} (m^2)	35 *(calibrated)*
Retardation Factor, *R*	4 *(calibrated)*
TCE plume natural degradation rate, λ (yr^{-1})	0.05 *(calibrated)*

6.5 Matrix Diffusion Model Results

The model results and comparison to TCE concentrations over time for the first source zone well is shown in Figure 33. The red dots are the field sampling data. The blue line is the MD model, and the doted black line shows the same model but with matrix diffusion turned off. The vertical dashed green line shows remediation events. In Figure 33, the MD model reasonably captures the early time field data before it drops in concentration due to the source remediation. After source remediation, concentrations in the well spike back up to concentration levels before source removal, which is not explained by the MD models. This "spike" in the data is much sharper than any back diffusion signal previously observed. The MD and No MD models at this location are nearly identical, which has been previously observed at near source locations when the source zone is not completely removed or isolated.

Figure 34 shows MW-47, which is a few meters further downgradient but still located within the source zone. Field data from this well also does not show large concentration reductions after source remediation. Both the MD and No MD models moderately capture the field data, and a "spike" after source remediation is observed at this location as well. MW-58 is located 71 m downgradient from the source and is shown in Figure 35. Field data continues to show concentrations that remain high after source remediation. Concentrations in the well drop to concentrations near the MCL briefly before jumping back up about one order of magnitude. The MD model slightly underestimates the field data and shows a good fit.

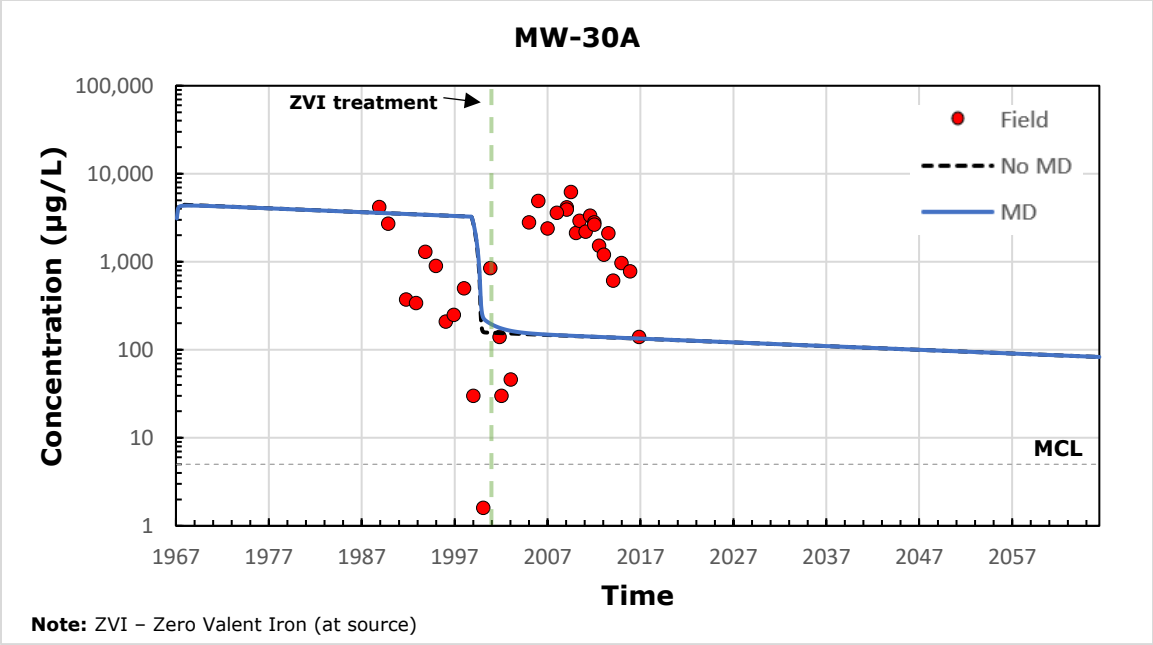

Figure 33: Comparison of TCE concentrations between modeled results and field data for MW-30A (source zone).

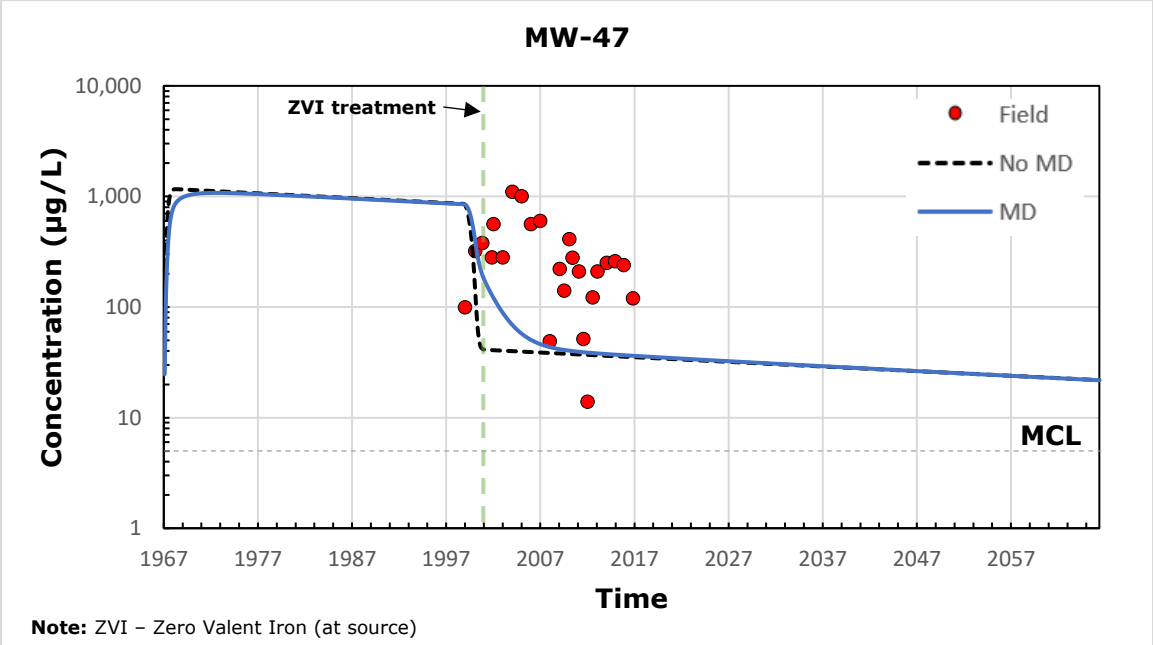

Figure 34: Comparison of TCE concentrations between modeled results and field data for MW-47 (source zone).

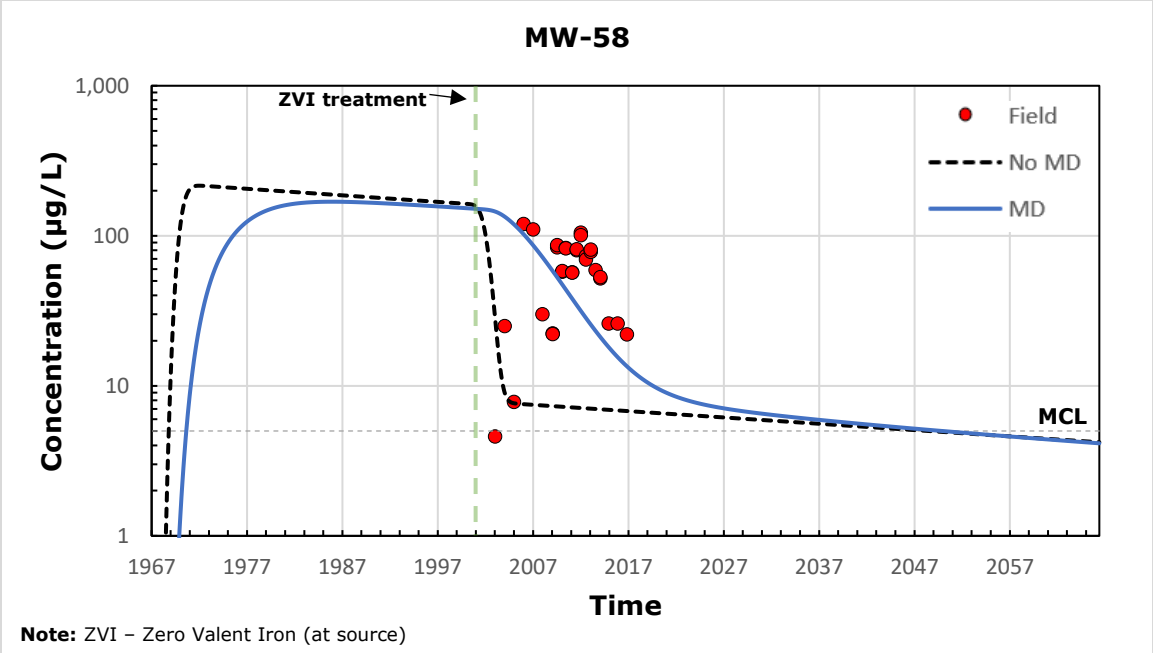

Figure 35: Comparison of TCE concentrations between modeled results and field data for MW-58 (downgradient of source, before PRB).

The model results and comparison to TCE concentrations in the aquifer over time for the plume downgradient of the PRB is shown in Figure 36. The field data shows a plume tailing-like pattern after remediation, and the MD model captures most of the field data with a good fit. The "spike" signal observed at the source zone may be evident in the field data between 2007 and 2013, however, this may only be noise. MW-35, shown in Figure 37, is located about 30 m east of the plume centerline, and as a result, concentrations are lower and hover close to the MCL prior to remediation. The field data shows a response to remediation, but the concentrations bounce back up shortly after remediation, where they then show a more gradual decrease over time. This up-and-down pattern in the data does not reflect the back diffusion signal, and as a result, the MD

model only moderately fits the field data. Additionally, MW-35 is located near the edge eastern edge of the PRB and may be affected by a part of the plume going around the wall and as a result, the sharp "spike" seen in the data at the source zone is also seen in this well.

Lastly, Figure 38 shows the most downgradient monitoring well assessed. The MD model slightly overestimates the concentrations in the aquifer, and the model fit is reasonable. Although the MD model does not exactly match the field data, the shape of the curve resembles the field data closely, and it is very likely that plume tailing is occurring due to back diffusion at this location.

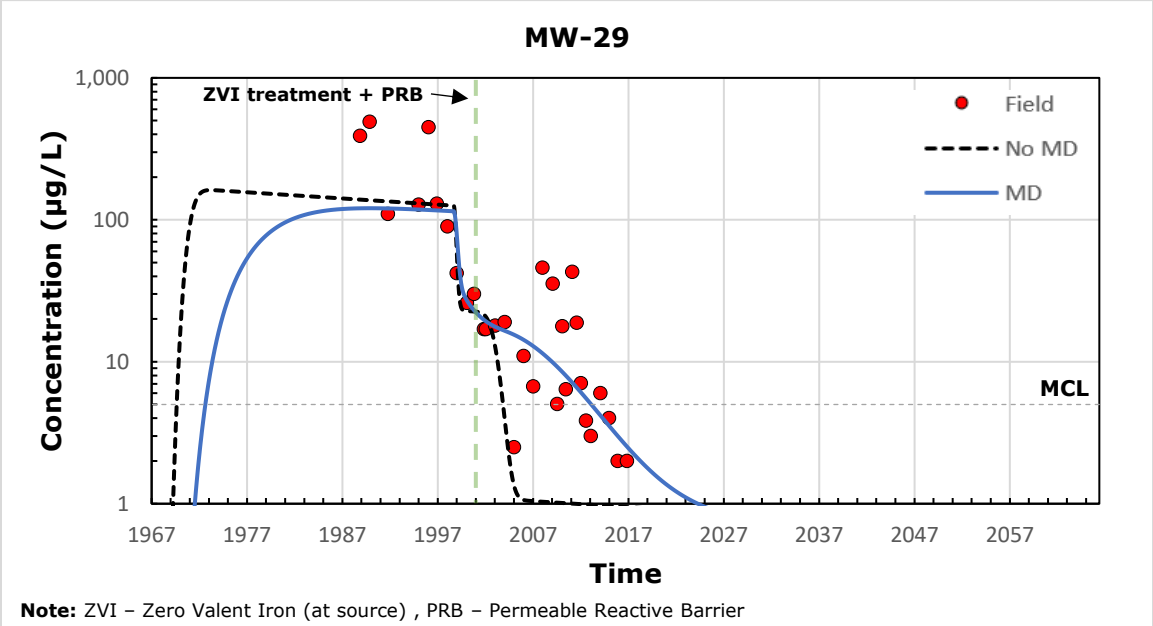

Figure 36: Comparison of TCE concentrations between modeled results and field data for MW-29 (downgradient of PRB).

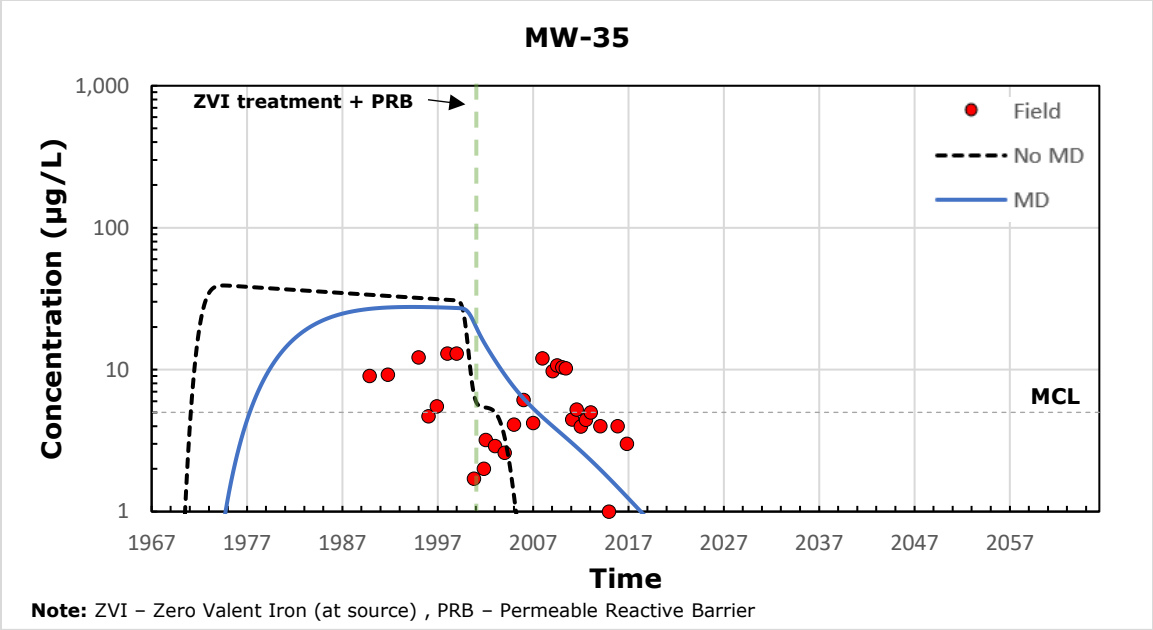

Figure 37: Comparison of TCE concentrations between modeled results and field data for MW-35 (downgradient of PRB).

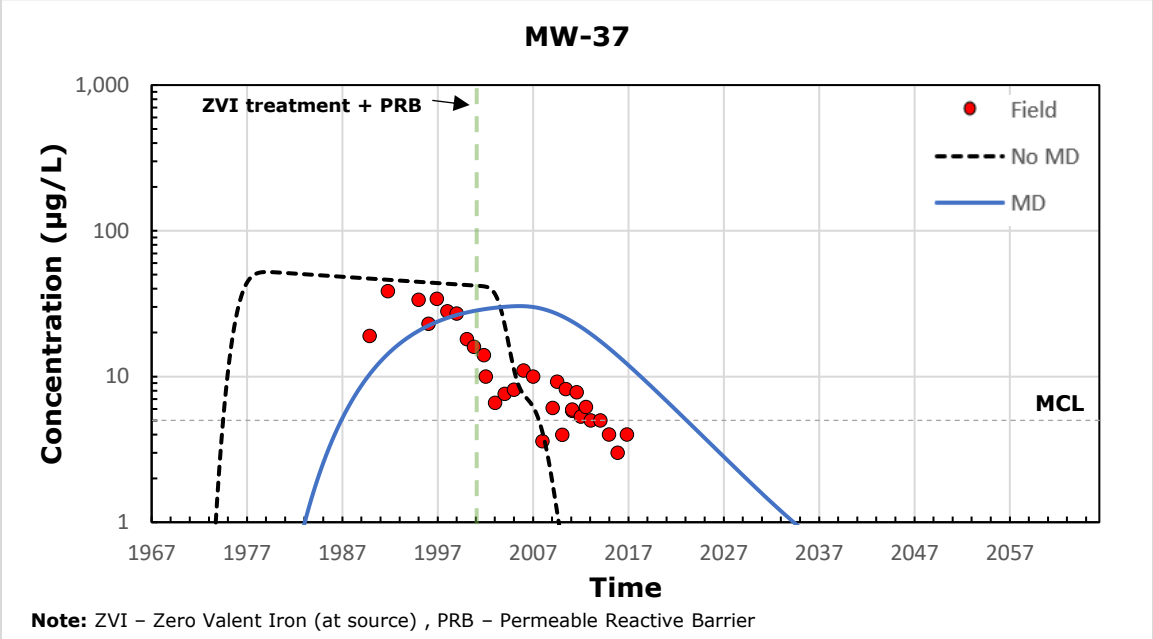

Figure 38: Comparison of TCE concentrations between modeled results and field data for MW-37 (downgradient of PRB).

6.6 Discussion

Overall, the MD models reasonably capture the field data in most of the monitoring wells. Comparatively, the No MD models do not capture the field data as well as the MD models. The MD models near the source show the most inconsistencies with the field data, which could be explained by the uncertainties in the site reported values.

Another reason for the poor model fits near the source is explained by the absence of a clear back diffusion signal. As characterized previously in this study, the back diffusion signal is described as "plume tailing," which occurs when the aquifer concentrations are sustained at higher concentrations that anticipated following remediation. Although aquifer concentrations remain high after remediation at the Kinston site, the signal is different from the plume tailing caused by back diffusion or by a residual source mass. At the site, aquifer concentrations immediately respond to source zone remediation and drop significantly, sometimes by orders of magnitude. However, shortly after, the concentrations rebound to pre-remediation levels. Back diffusion, as demonstrated, is a much more gradual process. Even for large initial diffusive mass flows, back diffusion does not result in sharp changes in the concentrations. If only back diffusion was occurring, aquifer concentrations would not have dropped so rapidly after remediation and would have instead responded by barely changing at all.

According to the Kinston site remediation description in Liang et al. (2011), the source zone remediation method involved high pressure jetting a slurry of ZVI (Zero-valent Iron) and kaolinite clay into a total of 11 treatment columns, which were emplaced on top of the mudstone-confining layer. Therefore, this method aimed to treat the source

zone as opposed to physical removing it. Although there is uncertainty about the amount of embedded low *k* material at the source zone, this remediation method should effectively treat the bulk material, thereby eliminating any interbedded low *k* layers as source zones for back diffusion and leaving only the underlying aquitard as a potential secondary source. After 11 months of installation, it was reported that the source mass was reduced by 95%. This field site analysis cannot determine exactly why concentrations in the source zone rebound to historic levels after remediation. It does not appear to be related to matrix diffusion processes.

The best fit to field data from an MD model was achieved at MW-29. Located just downgradient of the wall, the aquifer concentrations are reduced significantly, and the effect of the persisting source mass appears to be dampened by the PRB. The field data suggests a pattern of plume tailing, and the MD model suggests that back diffusion is responsible for the sustained concentrations above the MCL at that location. Although current concentrations are now below the MCL, the No MD model suggests that without back diffusion, the concentrations in the aquifer would have decreased below the MCL 8 years earlier. The MD model for MW-37 overestimates the concentrations, but the model reflects the shape of the field data and suggests that back diffusion may be a factor at this location as well.

6.7 Conclusions

In summary, the persisting source mass appears to be the primary reason that source zone and aquifer concentrations are remaining at or near historic levels after remediation in the area upgradient of the PRB. Despite the risk for back diffusion at this

field site, the signal from the rebounding source zone concentrations after remediation is inconsistent with a back diffusion signal, and therefore, it is concluded that back diffusion is probably not a key factor at the source location.

Possible back diffusion is observed downgradient of the source in MW-58, but the field data sample size is too to conclude this. The MD model at this location does not predict that back diffusion will be a significant factor in the remediation timeline. Downgradient of the PRB in MW-29, back diffusion is likely occurring; however, current concentrations are now below the MCL, thereby limiting any future back diffusion risk. Moving even further downgradient to MW-37, back diffusion may be occurring, but concentrations are even lower, and the future effect of back diffusion can be considered insignificant.

7. FINAL CONCLUSIONS

This research used a semi-analytical/numerical method to demonstrate the simulation of matrix diffusion in a chemical transport model and to determine the parameters that affect back diffusion and its contribution to plume persistence. From the study, the following conclusions are made:

- The back diffusion signature in a chemical transport model is identified by "plume tailing," where aquifer concentrations are sustained at high levels following remediation, typically above the MCL.
- Observation of the most significant back diffusion effects in any aquifer system is dependent on a monitoring wells location relative to the highest concentrations within the aquifer and the low permeability/high permeability interfaces.
- The initial source concentration determines the magnitude at which back diffusion affects aquifer concentrations, which in some cases, back diffusion can occur below the MCL.
- When a source zone is determined to decay over time from dissolution, the initial source concentration determines the upper limit of aquifer concentrations while the decay rate determines how long those concentrations will be sustained, which will affect the magnitude at which back diffusion affects the aquifer concentrations

- The degradation rate of contaminants within the low *k* zone is a key parameter for determining the magnitude of plume tailing from back diffusion, varying from years to centuries.
- Increasing the retardation factor within the low *k* zone will result in back diffusion effects that increase plume tailing by decades.
- The geometric parameterization used for embedded low *k* material and fractured rock cases affects the diffusive mass flow and as a result, affects back diffusion behavior, plume length, and the magnitude of concentrations at which plume tailing begins
- For fractured rock, the rock porosity governs the diffusive mass flow into the fractures, with low porosity rock resulting in relatively lower initial diffusive mass flows. For this case, the back diffusion risk increases moving downgradient from the source. Relatively higher porous rock results in higher diffusive mass flows, but the risk for back diffusion decreases at more downgradient distances.
- Partial source zone remediation can result in plume tailing that looks similar to the plume tailing caused by back diffusion, and the relative contributions of a residual source mass and back diffusion to overall plume persistence are determined by the amount of source mass removed, the amount of low *k* material or fractures in the aquifer system, the location in the aquifer relative to the source zone, and the low *k* zone parameterization, i.e. the degradation rate.

REFERENCES

Aziz, C.E., C.J. Newell, J.R. Gonzales, P. Hass, T.P. Clement, and Y. Sun, 2000. BIOCHLOR Natural Attenuation Decision Support System User's Manual Version 1.0, *U.S. Environmental Protection Agency*, EPA/600/R-00/008.

Ball, W.P., Liu, C., Xia, G., Young, D.F., 1997. A diffusion-based interpretation of tetrachloroethene and trichloroethene concentration profiles in a groundwater aquitard. Water Resour. Res. 33, 2741-2757.

Bear, J., Nichols, E., Kulshrestha, A., Ziagos, J., 1994. Effect of Contaminant Diffusion into and out of Low-Permeability Zones. Lawrence Livermore National Laboratory Report UCRL-ID-115626.

Brown, G.H., M.C. Brooks, A.L. Wood, M.D. Annable, and J. Huang., 2012. Aquitard contaminant storage and flux resulting from dense nonaqueous phase liquid source zone dissolution and remediation, Water Resour. Res., 48, W06531, doi:10.1029/2011WR011141.

Chapman, S.W., Parker, B.L., 2005. Plume persistence due to aquitard back diffusion following dense nonaqueous phase liquid source removal or isolation. Water Resour. Res. 41.

Chapman, S.W., Parker, B.L., Sale, T.C., Doner, L.A., 2012. Testing high resolution numerical models for analysis of contaminant storage and release from low permeability zones. Journal of Contaminant Hydrology 136–137, 106-116.

Chapman, S.W., Parker, B.L., 2013. Chapter 5.0 Type site Simulations, in: Sale, T., Parker, B.L., Newell, C.J., Devlin, J.F. (Eds.), State-of-the-Science-Review: Management of Contaminants Stored in Low Permeability Zones. SERDP Project ER-1740, pp. 79.

Dieter, C.A., Maupin, M.A., Caldwell, R.R., Harris, M.A., Ivahnenko, T.I., Lovelace, J.K., Barber, N.L., and Linsey, K.S., 2018, Estimated use of water in the United States in 2015: U.S. Geological Survey Circular 1441, 65 p., https://doi.org/10.3133/cir1441. [Supersedes USGS Open-File Report 2017–1131.]

Domenico, P.A. and F.W. Schwartz, 1990. Physical and Chemical Hydrogeology, Wiley, New York, New York.

Falta, R.W., 2005. Dissolved Chemical Discharge from Fractured Clay Aquitards Contaminated by DNAPLS, in: Faybishenko, B., Witherspoon, P.A., Gale, J. (Eds.), Dynamics of Fluids and Transport in Fractured Rock. American Geophysical Union, Washington, D. C., pp. 165-174.

Falta, R.W., P.S.C. Rao and N. Basu., 2005. Assessing the impacts of partial mass depletion in DNAPL source zones: I. Analytical modeling of source strength functions and plume response. Journal of Contaminant Hydrology 78(4), 259-280.

Falta, R.W., M.B. Stacy, A.N.M. Ahsanuzzaman, M. Wang, and R.C. Earle, 2007a. REMChlor Remediation Evaluation Model for Chlorinated Solvents User's Manual Version 1.0, https://www.epa.gov/water-research/remediation-evaluation-model-chlorinated-solvents-remchlor.

Falta, R.W., M.B. Stacy, A.N.M. Ahsanuzzaman, M. Wang, and R.C. Earle, 2007b. REMChlor Version 1.0, https://www.epa.gov/water-research/remediation-evaluation-model-chlorinated-solvents-remchlor.

Falta, R.W., Wang, W., 2017. A semi-analytical method for simulating matrix diffusion in numerical transport models. Journal of Contaminant Hydrology 197, 39-49.

Falta R.W., Farhat, S.K., C.J. Newell, and K. Lynch, 2018. REMChlor-MD, developed for the Environmental Security Technology Certification Program (ESTCP) by Clemson University, Clemson, South Carolina and GSI Environmental Inc., Houston, Texas.

Farhat, S.K., C.J. Newell, R.W. Falta, and K. Lynch, 2018. REMChlor-MD User's Manual, developed for the Environmental Security Technology Certification Program (ESTCP) by GSI Environmental Inc., Houston, Texas and Clemson University, Clemson, South Carolina.

Fetter, C.W., 2014. *Applied Hydrogeology*, 4th edition. Harlow: Pearson Education.

Foster, S.S., 1975. The Chalk groundwater tritium anomaly—a possible explanation. Journal of Hydrology 25, 159-165.

Gillham, R.W., Sudicky, E.A., Cherry, J.A., Frind, E.O., 1984. An Advection-Diffusion Concept for Solute Transport in Heterogeneous Unconsolidated Geological Deposits. Water Resour. Res. 20, 369-378.

Golden Software, 2017. Surfer® Powerful contouring, gridding & surface mapping system. Full User's Guide.

Goodall, D.C., Quigley, R., 1977. Pollutant migration from two sanitary landfill sites near Sarnia, Ontario. Canadian Geotechnical Journal 14, 223-236.

Hadley, P.W., Newell, C., 2014. The New Potential for Understanding Groundwater Contaminant Transport. Groundwater 52, 174-186.

Jing, Z., Jiangtao, H., Xueyan, Q., Kunfeng, Z., Lu, H., 2010. The Influence of Soil Constitution on the Sorption of Trichloroethylene in the Vadose Zone. Acta Petrologica et Mineralogica 29, 4, 439-444.

Krumholz, L. R., McKinley, J. P., Ulrich, G. A., and Suflita, J. M., 1997. Confined subsurface microbial communities in Cretaceous rock. Nature, 386(6620): 64-66.

Liang, Hailian, 2009. Probabilistic Remediation Evaluation Model for Chlorinated Solvents Considering Uncertainty. *All Dissertations*. 462. https://tigerprints.clemson.edu/all_dissertations/462

Liang, H., Falta, R.W., Henderson, J.K., Shoemaker, S., 2011. Probabilistic Simulation of Remediation at a Site Contaminated by Trichloroethylene. Groundwater, 32, 131-141.

Lima, G. P. and Sleep, B. E., 2007. The spatial distribution of eubacteria and archaea in sandclay columns degrading carbon tetrachloride and methanol. Journal of Contaminant Hydrogeology, 94(1-2): 34-48.

Lima, G. P., Parker, B., & Meyer, J., 2012. Dechlorinating microorganisms in a sedimentary rock matrix contaminated with a mixture of VOCs. Environmental Science & Technology, 46: 5756-5763.

Lima, G., Parker, B., Chapman, S., Adamson, G., 2013. Chapter 4.0 Transport in Heterogenous Media, in: Sale, T., Parker, B.L., Newell, C.J., Devlin, J.F. (Eds.), State-of-the-Science-Review: Management of Contaminants Stored in Low Permeability Zones. SERDP Project ER-1740, pp. 66-78.

Liu, C., Ball, W.P., 2002. Back diffusion of chlorinated solvent contaminants from a natural aquitard to a remediated aquifer under well-controlled field conditions: Predictions and measurements. Groundwater 40, 175-184.

Mackay, D.M., Cherry, J.A., 1989. Groundwater contamination: Pump-and-treat remediation. Environ. Sci. Technol. 23, 630-636.

McMahon, P. B., 2001. Aquifer/aquitard interfaces: mixing zones that enhance biogeochemical reactions. Hydrogeology Journal, 9(1): 34-43.

Muskus, N., Falta, R.W., 2018. Semi-analytical method for matrix diffusion in heterogenous and fractured systems with parent-daughter reactions. Journal of Contaminant Hydrology 218, 94–109.

Newell, C.J., J. Gonzales, and R.K. McLeod, 1996. "BIOSCREEN Natural Attenuation Decision Support System", U. S. Environmental Protection Agency, Center for Subsurface Modeling Support, Ada, OK, EPA/600/R-96/087.

Newell, C.J., and D.T. Adamson, 2005. Planning-level source decay models to evaluate impact of source depletion on remediation time frame. *Remediation*, Autumn, 2005, 27-47.

Pankow, J.F., Cherry, J.A., 1996. Dense chlorinated solvents and other DNAPLs in groundwater: History, behavior, and remediation.

Parker, J.C., and E. Park, 2004. Modeling field-scale dense nonaqueous phase liquid dissolution kinetics in heterogeneous aquifers, *Water Resources Research* 40: W05109.

Parker, B.L., Chapman, S.W., Guilbeault, M.A., 2008. Plume persistence caused by back diffusion from thin clay layers in a sand aquifer following TCE source-zone hydraulic isolation. Journal of Contaminant Hydrology 102, 86-104.

Payne F., J. Quinnan J, and S. Potter, 2008. Remediation Hydraulics. CRC Press, Boca Raton, Florida, USA.

Pruess, K., Wu, Y., 1988. A semi-analytical method for heat sweep calculations in fractured reservoirs. LBL-24463.

Pruess, K., Wu, Y., 1993. A New Semi-Analytical Method for Numerical Simulation of Fluid and Heat Flow in Fractured Reservoirs. SPE Advanced Technology Series 1, 63-72.

Rao, P.S.C. and J.W. Jawitz, 2003. Comment on "Steady-state mass transfer from single component dense non-aqueous phase liquids in uniform flow fields" by T.C. Sale & D.B. McWhorter, *Water Resources Research* 39(3): COM 1.

Rasa, E., Chapman, S.W., Bekins, B.A., Fogg, G.E., Scow, K.M., Mackay, D.M., 2011. Role of back diffusion and biodegradation reactions in sustaining an MTBE/TBA plume in alluvial media. Journal of Contaminant Hydrology 126, 235-247.

Reszat, T. N. and Hendry, M. J., 2009. Migration of Colloids through Nonfractured Clay-Rich Aquitards. Environmental Science & Technology, 43(15): 5640-5646.

Sale, T.C., Zimbron, J.A., Dandy, D.S., 2008. Effects of reduced contaminant loading on downgradient water quality in an idealized two-layer granular porous media. Journal of Contaminant Hydrology 102, 72-85.

Scheutz, C., Broholm, M. M., Durant, N. D., Weeth, E. B., Jorgensen, T. H., Dennis, P., Jacobsen, C. S., Cox, E. E., Chambon, J. C., and Bjerg, P. L., 2010. Field Evaluation of Biological Enhanced Reductive Dechlorination of Chloroethenes in Clayey Till. Environmental Science & Technology, 44(13): 5134-5141.

Seyedabbasi, M.A., Newell, C.J., Adamson, D.T., Sale, T.C., 2012. Relative contribution of DNAPL dissolution and matrix diffusion to the long-term persistence of chlorinated solvent source zones. Journal of Contaminant Hydrology 134, 69-81.

Sudicky, E., Frind, E., 1982. Contaminant transport in fractured porous media: Analytical solutions for a system of parallel fractures. Water Resour. Res. 18, 1634-1642.

Sudicky, E.A., Gillham, R.W., Frind, E.O., 1985. Experimental Investigation of Solute Transport in Stratified Porous Media: 1. The Nonreactive Case. Water Resour. Res. 21, 1035-1041.

Takeuchi, M., Kawabe, Y., Watanabe, E., Oiwa, T., Takahashi, M., Nanba, K., Kamagata, Y., Hanada, S., Ohko, Y., and Komai, T., 2011. Comparative study of microbial dechlorination of chlorinated ethenes in an aquifer and a clayey aquitard. Journal of Contaminant Hydrogeology, 124(1-4): 14-24.

Tang, D., Frind, E., Sudicky, E.A., 1981. Contaminant transport in fractured porous media: Analytical solution for a single fracture. Water Resour. Res. 17, 555-564.

Travis, C., Doty, C., 1990. ES&T Views: Can contaminated aquifers at superfund sites be remediated? Environ. Sci. Technol. 24, 1464-1466.

Van Stempvoort, D. R., Millar, K., and Lawrence, J. R., 2009. Accumulation of short-chain fatty acids in an aquitard linked to anaerobic biodegradation of petroleum hydrocarbons. Appl.Geochem., 24(1): 77-85.

Vinsome, P., Westerveld, J., 1980. A simple method for predicting cap and base rock heat losses in thermal reservoir simulators. J. Can. Pet. Technol. 19.

Yang, M., Annable, M.D., Jawitz, J.W., 2015. Back Diffusion from Thin Low Permeability Zones. Environ. Sci. Technol. 49, 415-422.

Yang, M., Annable, M.D., Jawitz, J.W., 2016. Solute source depletion control of forward and back diffusion through low-permeability zones. Journal of Contaminant Hydrology 193, 54–62.

Yang, M., Annable, M.D., Jawitz, J.W., 2017. Field-scale Forward and back diffusion through low-permeability zones. Journal of Contaminant Hydrology 202, 47–58.

Zhu, J., and Sykes J.F., 2004. Simple screening models of NAPL dissolution in the subsurface. Journal of Contaminant Hydrology 72, 245-258.